MODELING, SIMULATION AND VERIFICATION OF IMPACT DYNAMICS

Vol. 4, Three Dimensional Plastic Hinge Frame Simulation Module

By:

I. K. McIvor

A. S. Wineman

W. J. Anderson

H. C. Wang

Date:

August 25, 1973

Report Status:

Final Report

1. Report No.	2. Government Accession No.	3. Recipient's Catalog No.
4. Title and Subtitle Modeling, Simulation and Verification of Impact Dynamics - Vol. 4, Three Dimensional Plastic Hinge Frame Simulation Module		5. Report Date 25 August 1973 6. Performing Organization Code
7. Author(s) I.K. McIvor, A.S. Wineman, W.J. Anderson and H.C. Wang		8. Performing Organization Report No. UM-HSRI-BI-73-4-4
9. Performing Organization Name and Address Highway Safety Research Institute and Department of Applied Mechanics and Engineering Science The University of Michigan Ann Arbor, Michigan 48105		10. Work Unit No. 11. Contract or Grant No. DOT-HS-031-2-481 13. Type of Report and Period Covered
12. Sponsoring Agency Name and Address National Highway Traffic Safety Administration U.S. Department of Transportation Nassif Building, 7th and E Streets, S.W. Washington, D.C. 20590		Final Report June 28, 1972-Aug. 25, 1973 14. Sponsoring Agency Code
15. Supplementary Notes		

16. Abstract

This report describes the development of a computer program for modeling three dimensional large plastic deformation response of general frame structures. It is designed to serve as a preliminary version of a general component module in the overall simulation of vehicle impact. The analysis is based on the extension of the plastic hinge concept to the three dimensional deformation of beams.

The main body of the report covers the theoretical analysis, comparison of theory with basic verification tests, and the qualification study which compares computed results with the results of a crush test of a production vehcile frame. In addition, the Appendix contains a Program User's Guide and a complete listing of the current version of the program.

It was concluded from the study that the development of component modules for advanced simulations is feasible, and recommendations for program improvements are suggested.

17. Key Words	18. Distribution Statement

19. Security Classif.(of this report)	20. Security Classif.(of this page)	21. No. of Pages	22. Price

Form DOT F 1700.7 (8-69)

The opinions, findings, and conclusions expressed in this publication are those of the authors and not necessarily those of the National Highway Traffic Safety Administration.

TABLE OF CONTENTS

TABLE OF CONTENTS

(Continued)

LIST OF FIGURES

LIST OF FIGURES

LIST OF TABLES

CHAPTER 1

INTRODUCTION AND SUMMARY

1.1 MODELING STUDY

As originally conceived in the project goals, a modeling exercise was to be conducted on a vehicle component to provide background information for comparing computer simulation with crash testing. As noted in Volume I of this report, it served this purpose. During the course of the investigation, however, the modeling study took an added significance. The state-of-the-art study concluded that only Level 3 simulation capability[1] is currently available. It became evident that the feasibility of advanced simulations is dependent upon the development of self-contained modules which accurately but efficiently model vehicle components. Thus the goal of the modeling study was expanded to the preliminary development of a major simulation module suitable for a Level 4 simulation.

A Level 4 simulation capability requires modeling three dimensional displacements and rotations under a variety of loading conditions. It must compute absorbed energy, relative displacements of major components and the acceleration environment of the passenger compartment with an accuracy comparable to testing. This is to be accomplished with less than three hundred degrees of freedom. It is clear that a general three dimensional frame module would be essential to such a simulation program. Thus a frame module was choosen as the goal of the modeling study.

To develop a general three dimensional, large plastic deformation frame program with the size restriction imposed by Level 4 simulation is a major challenge. From the state-of-the-art study it is clear that a finite element approach based on continuum mechanics is unrealistic for Level 4 simulation. It is also clear that the concept of generalized resistances successfully used in Level 3 simulation is limited to essentially one dimensional motion. The

---

[1] A simulation spectrum is defined in Volume I of this report. Level 3 simulation models overall response and average rigid body accelerations under limited loading conditions.

most promising approach thus appeared to be the extension of the plastic hinge concept to three dimensional response. In carrying out this extension it is necessary to formulate the problem in a manner suitable for use as a module in an overall vehicle simulation. The required flexibility was accomplished here by formulating the problem in a form analogous to a finite element formulation but in which the governing element equations are derived from the concept of an ideal three dimensional plastic hinge.

The basic theory and derivation of equations is given in Chapter 2. A number of experiments designed to verify the basic concept are discussed in Chapter 3. The computer simulation developed was then used to predict the force-deformation curve for a static crush test conducted by CALSPAN on an actual vehicle frame. A discussion of our modeling of the frame and the comparison of computed with experimental results is given in Chapter 4. A brief user's guide for the computer program is given in Appendix A and a complete listing of the current version of the program is given in Appendix B.

Although we do not consider the current version of the program a final product for use as a component module, it is an operating program with most of the essential features. Moreover the modeling cycle was instructive in identifying problem areas. In the remaining sections of this Chapter we summarize the conclusions and recommendations resulting from the study.

1.2 CONCLUSIONS AND RECOMMENDATIONS

The major conclusions resulting from the modeling study are:

1. The ideal plastic hinge is a valid concept for three dimensional plastic deformation of beam.

   To our knowledge there did not exist at the beginning of the study a general theory of beam deformation based on the plastic hinge concept, earlier work in large deformation being confined to planar frames. The theory derived here is self-consistent once the basic assumptions associated with an ideal hinge are postulated. Moreover the validation experiments[2] verified that the theory adequately models the essential features of actual physical behavior over a large deformation range.

2. The development of vehicle component modules suitable for advanced simulations is technically feasible.

   For use as a vehicle module, a component simulation program must adequately model the component behavior, must be internally general, and must be in a form compatible with interaction with other modules. The two latter conditions are satisfied by formulating the program in terms of arbitrarily specified nodal variables. The qualification study demonstrated that the computer simulation could adequately predict the behavior of an actual vehicle frame. Although the study indicated a number of areas that deserve further attention, the basic feasibility of the approach was clearly demonstrated.

In addition to these conclusions which directly bear on the overall project goals, the study brought out a number of points relevant to component modeling. They are:

1. Torsional and axial forces can have significant effects on the responses and should be included in the analysis.
2. The plastic hinge concept has inherent limitations. Due to its "off-on" character, it cannot model in detail elastic-plastic behavior of a cross section. This has only limited effect on the overall response if the yield function is chosen to give a "good" piecewise

---

[2] The validation experiments reported in Chapter 3 indicated that under certain loading conditions plastic extension of the beam which had originally been neglected in the theory was important. This has subsequently been corrected. The theory and computer program given here include this effect.

linear approximation to the actual elastic-plastic behavior. For planer bending this is easily accomplished by choosing an equivalent yield stress to give a yield moment intermediate between initial yield and the ultimate collapse moment. In the general case, however, we need to choose an equivalent yield function. Since the difference between initial yield and fully plastic cross section is different for different modes of deformation, this cannot be accomplished by simple scaling. The functional form of the initial yield function is sufficiently general to permit different scalings for different deformation modes. At the present time, however, our knowledge of the actual elastic-plastic behavior under general conditions is too limited to prescribe this variable scaling in a rational manner. Therefore in the present study a single yield stress was chosen somewhat arbitrarily. In both the verification and qualification studies, the computed results were in general agreement with experiments. It was clear, however, that the choice was not optimum and this topic deserves further attention.

3. The theory developed here can adequately account for the effect on the force-deformation characteristics of the structure due to changes in geometry. It cannot account for softening due to joint inefficiency or local deformation of the cross section. The verification study demonstrated that such effects could be significant. It was also shown in the study, however, that joint behavior similiar to that observed could be obtained by changing parameters in the yield function. Although at the present time there is no rational basis for our choice, the result strongly suggests the possibility of defining a "failure function" by relating the parameters in the yield function to actual joint behavior.

4. It is also worth noting that our modeling of the vehicle frame in the qualification study required considerable judgment and experience. The choice of the number and location of the plastic

hinges and the choice of structural parameters are not obvious. Thus simulation at this level of approximation requires a background of experimental evidence.

Finally in closing this section we note a number of recommendations for both immediate and long range improvement of the computer simulation program developed here. There are two improvements which can be effected without major effort. They are:

1. Extend the formulation to include dynamic effects by adding mass matrix.

   The frame simulation program developed here is not intended to include the major inertial masses of the vehicle. In the envisaged modular development, such masses will be handled by a rigid body module that can interact with other structural modules at arbitrary nodes. Nevertheless it is desirable to extend the capability of the program to include the frame inertia since it could be significant for advanced simulations. In any case this capability would be useful in quantifying the importance of frame inertia. Since the present program requires incremental solution, the inclusion of inertial effects does not complicate the solution procedure. The only effort required is to develop and program a mass matrix consistent with the present formulation.

2. Develop automatic selection of variable step size based on numerical error control.

   The current version of the program obtains the increment step from an input subroutine which prescribes the external forces and displacement constraints for a particular problem. As presently programmed a constant step size is specified in the input subroutine. It is desirable to develop an automatic selection of step size based on a relative error measure. At the present time, we have not had sufficient experience with the program to correlate relative error with total error. In the interest of economy the actual qualification result reported here was run at a relatively large constant step. The relative error in the yield function at some hinges was as high as ten percent for some steps. Nevertheless the overall force deformation curve correlated well with experiment. On the other hand, this step size was too large for accurate computation of the incremental dissipation and continuous loading was assumed. Thus at the present time it is not clear what error measure is the most desirable or what is the effect of step size on various variables of interest. A systematic numerical error analysis is desirable to optimize exercising the program.

Finally we note the need for a research effort in the simulation of joint behavior. As discussed above both the verification and qualification studies indicated that joint inefficiency and local deformation have a measureable effect on the overall force-deformation characteristics. We believe our preliminary "analytical experiments" are strongly suggestive that these effects can be incorporated into a yield function expressed in terms of structural variables. The development of such functions for typical vehicle joints will require, however, a substantial research effort, both analytical and experimental, on the plastic deformation of joints under general loads.

1.3 COMPUTATION COSTS

The qualification study was sufficiently large to give a good assessment of computation costs for the present program. Our experience with exercising the program has demonstrated that the cost is essentially directly proportional to the number of elements. The major program operations are the updating of the element stiffness matrix at each step and the monitoring of the yield hinge switches for each element; the actual inversion of the equations requires almost negligible time in comparison. Since these major operations must be preformed once each step for each element, the run time varies linearly with the number of elements.

Thus it is convenient to express computation cost on a unit base. The following costs are based on exercising the program on the University of Michigan IBM 360-67 computer using the Michigan Terminal System.

In our experience the average unit cost is eight cents per element for each integration step. For general comparison it is convenient to also express the cost per degree of freedom. For typical frame structures the number of nodes is about 80% the number of elements. (For our qualification study we used 19 elements and 15 nodes.) Each node has six degrees of freedom. Thus in terms of degrees of freedom we have a cost of 1.67 cents per degree of freedom for each integration step.

The total cost data for the qualification study is:

No. of Elements	-	19
No. of Nodes	-	15
Total Degrees of Freedom	-	90
Integration Steps	-	66
Total inches of Crush	-	5.1
Total Cost		$ 100.00

It should be pointed out that the present program has not been optimized from the viewpoint of cost. In particular the program does not make use of file storage but retains all computed data in core storage. The Michigan Terminal System changes a substantial premium for core storage. Since storage costs account for over half of total run costs, the use of file storage will significantly reduce cost. In addition some reorganization of the program variables (sequential use of same storage locations) can be implemented. In this way, we estimate that run costs can be reduced to one cent per degree of freedom for each integration step.

With a unit cost determined, determining the cost of a given simulation requires estimating the number of integration steps to be employed. In general this requires considerable experience with the program to gain an understanding of the step size-error relationship. As indicated above we used 66 steps to simulate five inches of crush in the qualification study. Although reasonable results were obtained for the overall force-deformation curve, the computed results for dissipation indicated that step size was too large for accurate determination of all variables. We anticipate that five-ten times as many steps may be required.

At one cent per degree of freedom for each step the qualification frame study would cost about \$60.00 for five inches of crush. With this an overall Level 4 simulation cost of \$200.00-\$400.00 appears quite reasonable. An increase by a factor of ten, however, would put Level 4 simulation cost into the thousands of dollars range. There are two possibilities for overcoming the need for a large number of steps. The present integration scheme is the simplest possible method, essentially replacing derivatives by first order differentials. It is likely that higher-order integration routines which ultilize data from several previous steps can be developed within the present formulation permitting a considerably larger step size for the same relative error.

The second possibility is more speculative. In the present theory, the plastic structural constitutive equations are essentially expressed in the normality condition. The consequence is that the plastic deformation increments are highly constrained in a manner which may not be compatible with kinematic constraints. This requires elastic readjustment when a new hinge is formed, and we have noted that this is the situation where large relative error is introduced unless a very small step size is employed. It is possible that an alternate formulation of the plastic constitutive equations would relieve this difficulty. Such a reexamination is inherent in any general study of the plastic deformation of joints.

Thus our conclusions with respect to computer costs are somewhat equivocal. The present study has obtained overall force-deformation results comparable to experiment at a cost which makes Level 4 simulation economically feasible. In detail, however, the present results are not completely satisfactory from the viewpoint of accuracy of all variables of interest. There is reasonable expectation that improved integration techniques and better understanding of general structural plasticity can improve this accuracy without significant increase of computation cost.

CHAPTER 2

ANALYSIS

2.1 BASIC ASSUMPTIONS

In this chapter we derive the basic equations for a general beam of arbitrary length which forms the basic element of the frame module. The derivation is directed towards obtaining an "element stiffness matrix". With this the global system of equations for an arbitrary frame can readily be assembled.

The major simplifying assumption in the analysis is that all plastic deformation occurs at ideal hinges. The location of potential hinges must be choosen apriori, and this choice dictates the length of the beam element. Thus plastic deformation occurs only at the nodes of our element. We further assume that the hinge is operative when the appropiate stress resultants lie on a yield surface for the cross section which remains constant as the deformation proceeds.

The physical implications of these assumptions are:

(i) Plastic zones are confined to localized regions,

(ii) Material strain hardening may be neglected,

(iii) Detailed elastic-plastic behavior of the cross section between initial yield and a fully plastic section is not critical to the analysis.

For mild steel, thin walled cross sections, and loading typically experienced by vehicle frames, these appear to be reasonable assumptions. The most questionable is the third approximation. For the case of pure bending this is equivalent to replacing the actual moment-curvature relation by an elastic - perfectly plastic approximation which has been successfully used in many structural applications. In the general case, however, there is less evidence for defining a yield surface for an ideal hinge which approximates the actual elastic - plastic behavior. Here we choose the yield surface as that associated with initial yield. The surface can be scaled, however, to better approximate the actual behavior by choosing an "equivalent yield stress" rather than the actual material yield stress. This point is discussed further in the next chapter.

If we were interested only in overall deformation, the assumptions might be extended to neglecting elastic deformation. As a component module, however, we need to determine as accurately as possible the forces transmitted by the component to other modules of the vehicle at each time step. Particularly during the early stage of motion these forces are probably significantly affected by the elastic deformation. From a numerical viewpoint including elasticity is actually beneficial since it removes indeterminancy associated with rigid plastic theory.

2.2 NOTATION

To derive the element stiffness matrix it is necessary to define the configuration of the beam in a general orientation in space and to relate this orientation to the forces acting on the beam. The motion of the beam may consist of elastic deformation, general rigid body motion of its end points, and rigid body motion of the beam itself due to plastic deformation at the hinges.

The necessary reference frames for a beam element between the i^{th} and j^{th} nodes are shown in Figure 1. The nodes are represented by rigid body masses M_i and M_j. For clarity the beam and masses are shown separated, but the beam end points initially coincide with the center of mass of the nodes.

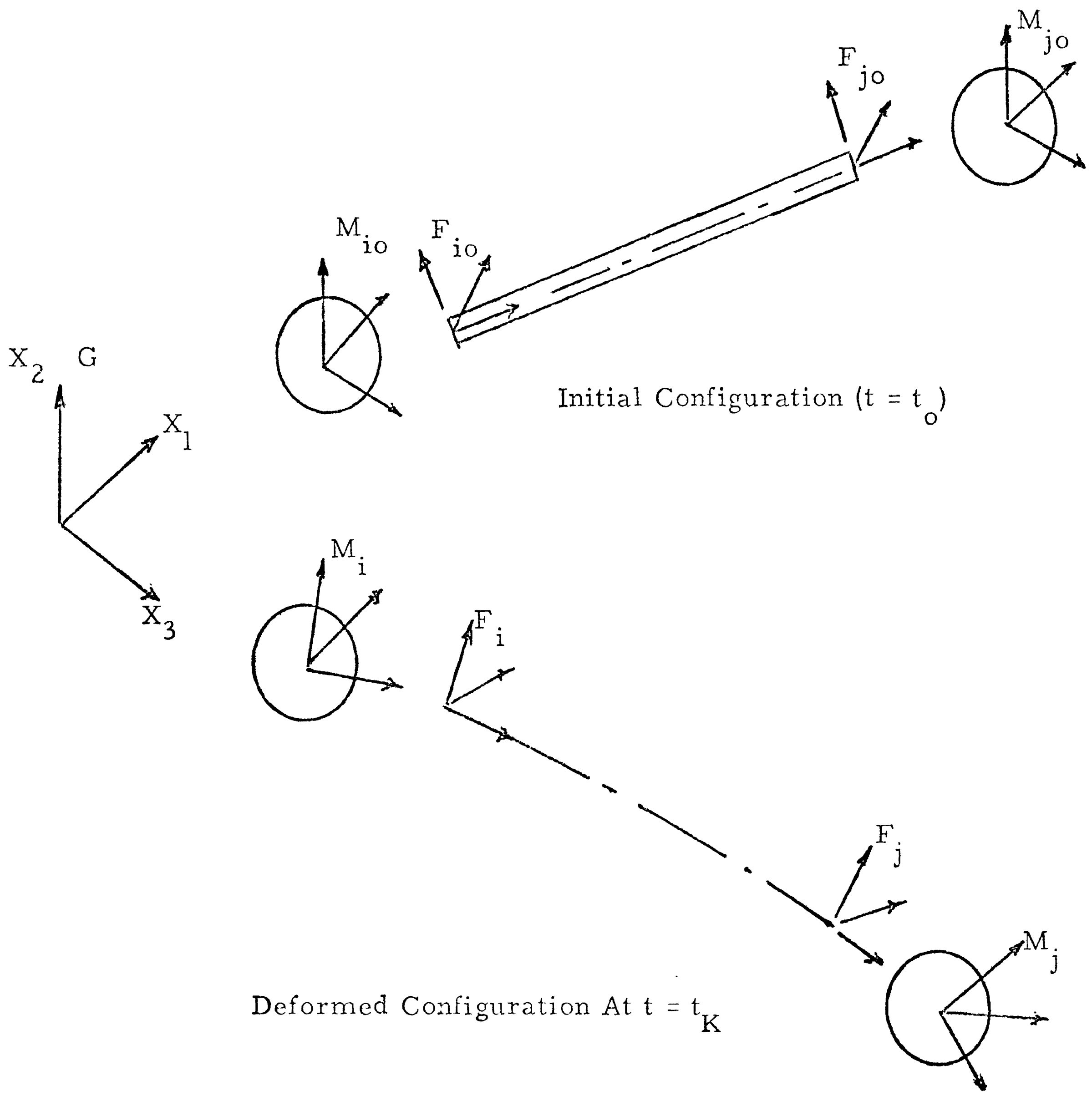

BEAM REFERENCE FRAMES

Figure 1

In Figure 1, G represents the fixed global reference frame, M_i and M_j are frames attached to the nodal masses at a time t_K (denoting the k^{th} forward step in the incremental process), and F_i and F_j are frames attached to the beam end points at time t_K. The origin of the latter frames is at the shear center of the cross section, the x_3 axis is tangent to the beam axis and x_1 and x_2 are along the principal axis of the cross section [1]. The beam is of length ℓ. A subscript "0" denotes the initial position and orientation of the respective frames.

The position of the i^{th} and j^{th} beam frames with respect to the fixed global system is denoted by $\underline{x}^i$ and $\underline{x}^j$ respectively. Likewise the position of the i^{th} and j^{th} mass frames with respect to the global frame is denoted by $\underline{y}^i$ and $\underline{y}^j$ respectively. The orientation of the four frames with respect to the global system is specified by the four direction cosine matrices

$$L^{M_i}, L^{M_j}, L^{F_i}, L^{F_j}$$

in which the components of L^F are

$$\ell^F_{ij} = {}^F\underline{e}_i \cdot \underline{e}_j \tag{1}$$

where $\underline{e}_j$ and ${}^F\underline{e}_i$ are the base vectors in the global system and the frame F respectively.

---

[1] This implies the beam shear center and the nodal center of mass initially coincides. For a physical rigid body mass this, of course, will not be generally true. In our development, however, actual rigid masses will be handled by a separate module which can interact with the frame module at arbitrary "external" nodes. The nodal masses here represent a discretization of the frame mass and a mass matrix appropiate to the postulated reference frames can be derived.

It is convenient to choose the initial orientation of the mass frames to coincide with the global frame, i.e.

$$L^{Mio} = L^{Mjo} = I \tag{2}$$

where I is the identity matrix. Also we have

$$L^{F_{io}} = L^{F_{jo}} \tag{3}$$

In fact we should note that since F_i and F_j are fixed to the beam, differences in their orientation result only from elastic deformation.

In carrying out the derivation we introduce the following vector quantities:

$\underline{U}$ - displacement

$\underline{F}$ - resultant force vector acting at the beam end point

$\underline{M}$ - resultant moment vector acting at the beam end point

$\underline{\omega}$ - rotation rate of beam force

$\underline{\theta}$ - rotation rate of mass frame

We will use the notation ${}^{F}\underline{v}^{i}$, where the superscript i denotes the point or frame associated with the vector and the superscript F denotes the frame in which the vector components are expressed. If F is the global frame the superscript will be suppressed, i.e. $\underline{v}^{i}$ is with respect to the global frame.

The location of a coordinate frame F is specified by the position vector $\underline{x}$ and the direction cosine matrix L^F. Since in general the frame F moves with respect to the fixed global system, we need to define their rate of change with respect to time. We denote the rate of change of the position vector as $\dot{\underline{x}}$. From rigid body dynamics we have

$$\dot{L}^F = \hat{W}L^F \tag{4}$$

where $\hat{W}$ is the 3 x 3 matrix

$$\hat{W} = \begin{bmatrix} 0 & {}^F\omega_3 & -{}^F\omega_2 \\ -{}^F\omega_3 & 0 & {}^F\omega_1 \\ {}^F\omega_2 & -{}^F\omega_1 & 0 \end{bmatrix} \tag{5}$$

Also we note the vector transformation relations

$$\begin{aligned} {}^F\underline{v} &= L^F\,\underline{v} \\ \underline{v} &= (L^F)^T\,{}^F\underline{v} \end{aligned} \tag{6}$$

where the superscript T denotes the transpose.

Finally we introduce generalized displacement rate and force rate vectors associated with the point i as

$$\begin{aligned} \dot{\underline{D}}^i &= \begin{bmatrix} \dot{\underline{U}}^i \\ \dot{\underline{\theta}}^i \end{bmatrix} \\ \dot{\underline{R}}^i &= \begin{bmatrix} \dot{\underline{F}}^i \\ \dot{\underline{M}}^i \end{bmatrix} \end{aligned} \tag{7}$$

From this we introduce the generalized displacement rate and force rate vectors for the beam element as

$$\begin{aligned} \dot{\underline{D}} &= \begin{bmatrix} \dot{\underline{D}}^i \\ \dot{\underline{D}}^j \end{bmatrix} \\ \dot{\underline{R}} &= \begin{bmatrix} \dot{\underline{R}}^i \\ \dot{\underline{R}}^j \end{bmatrix} \end{aligned} \tag{8}$$

Our immediate goal is to relate $\dot{\underline{R}}$ to $\dot{\underline{D}}$.

In the deviation that follows it is convenient to work with the rate variables introduced above. For numerical computation, however, we will work with increments in the variables between the configuration at time t_K and time t_{K+1}. We denote the time increment as Δt, i.e.

$$\Delta t = t_{K+1} - t_K \tag{9}$$

The corresponding increment in the generalized displacement, for example, is

$$\Delta \underline{D} = \dot{\underline{D}}\, \Delta t \tag{10}$$

Since all our equations will be homogenous in time, they may be converted to incremental equations by multiplying through by Δt. In effect this means we may obtain incremental equations by replacing rate quantities, ($\dot{\underline{D}}$ for example) by incremental quantities ($\Delta\underline{D}$).

To complete an incremental formulation we must relate the frame orientation at time t_{K+1} to the orientation at t_K. We have

$$\dot{L}^{F} = \frac{L^{F}(t_{K+1}) - L^{F}(t_K)}{\Delta t} \tag{11}$$

Solving for $L^{F}(t_{K+1})$ and using (4) gives

$$L^{F}(t_{K+1}) = \left[\hat{W}\Delta t + I\right] L^{F}(t_K)$$

Thus

$$L^{F}(t_{K+1}) = W L^{F}(t_K) \tag{12}$$

where

$$W = \begin{bmatrix} 1 & \Delta\omega_3^{F} & -\Delta\omega_2^{F} \\ -\Delta\omega_3^{F} & 1 & \Delta\omega_1^{F} \\ \Delta\omega_2^{F} & -\Delta\omega_1^{F} & 1 \end{bmatrix} \tag{13}$$

where $\Delta\omega_i^{F}$ denotes $\omega_i^{F}\Delta t$ and represents the increment in the frame rotation.

2.3 KINEMATICS OF DEFORMATION

Referring to Figure 1 we can visualize the deformation from the initial state to the configuration at time t_K as a rigid body motion of the beam frames F_i and F_j plus an elastic deformation. The rigid body motion of the beam frames may be due to both overall rigid body motion of the system and to plastic rotation and extension of the hinges at node i and/or node j.

In the initial configuration we have

$$\underline{x}^{io} = \underline{y}^{io}, \ \underline{x}^{jo} = \underline{y}^{j}$$
$$\underline{x}^{jo} = \underline{x}^{io} + (L^{F_{io}})^T \ \underline{r} \tag{14}$$

where $\underline{r}$ is the vector $\underline{r} = \begin{bmatrix} 0 \\ 0 \\ \ell \end{bmatrix}$

At time t_K the mass frames are at $\underline{y}^i$ and $\underline{y}^j$; the beam frames are at $\underline{x}^i$ and $\underline{x}^j$ where

$$\underline{x}^j = \underline{x}^i + (L^{F_i})^T \ \underline{r} + \underline{u}^e \tag{15}$$

in which $\underline{u}^e$ represents the elastic displacement vector of the end j with respect to the end i referenced to the global system.

The origins of the beam and mass frames may differ by plastic displacements occurring at the hinges.

Thus

$$\underline{x}^i = \underline{y}^i + \underline{U}^{ip}$$
$$\underline{x}^j = \underline{y}^j - \underline{U}^{jp} \tag{16}$$

where $\underline{U}^{ip}$ and $\underline{U}^{jp}$ denote the plastic displacements referenced to the global system. With this (15) becomes

$$\underline{y}^j - \underline{y}^i = (L^{F_i})^T \underline{r} + \underline{U}^e + \underline{U}^{ip} + \underline{U}^{jp} \tag{17}$$

The displacements of the mass frames are introduced as

$$\underline{U}^i = \underline{y}^i - \underline{y}^{io}, \ \underline{U}^j = \underline{y}^j - \underline{y}^{jo} \tag{18}$$

Expressing the second equation of (14) in terms of $\underline{y}^{io}$ and $\underline{y}^{jo}$ and subtracting from (18) gives

$$\underline{U}^j - \underline{U}^i = \left[(L^{F_i})^T - (L^{F_{io}})^T\right] \underline{r} + \underline{U}^e + \underline{U}^{ip} + \underline{U}^{jp} \tag{19}$$

We obtain a rate equation by differentiating (19) with respect to time obtaining

$$\underline{\dot{U}}^{j} - \underline{\dot{U}}^{i} = \dot{\overline{(L^{Fi})^T}} \underline{r} + \underline{\dot{U}}^{e} + \underline{\dot{U}}^{ip} + \underline{\dot{U}}^{jp} \tag{20}$$

The plastic displacements are due to plastic extension of the beam. Thus the extension rate is always directed along the current x_3 axis of the beam frame. Thus in the local beam frames we have

$$^{F_i}\underline{\dot{U}}^{ip} = \dot{U}^{ip}\, \underline{i} \tag{21}$$

$$^{F_j}\underline{\dot{U}}^{jp} = \dot{U}^{jp}\, \underline{i}$$

where $\dot{U}^{ip}$ and $\dot{U}^{jp}$ are the scaler axial plastic extensions and $\underline{i}$ is the vector

$$\underline{i} = \begin{bmatrix} 0 \\ 0 \\ 1 \end{bmatrix}$$

Transforming to the global system gives

$$\begin{aligned} \underline{\dot{U}}^{ip} &= (L^{F_i})^T\, \underline{i}\, \dot{U}^{ip} \\ \underline{\dot{U}}^{jp} &= (L^{F_j})^T\, \underline{i}\, \dot{U}^{jp} \end{aligned} \tag{22}$$

It can also be shown that

$$\dot{\overline{(L^{Fi})^T \underline{r}}} = (L^{F_i})^T\, E\, L^{F_i}\, \underline{\omega}^i \tag{23}$$

where

$$E = \begin{bmatrix} 0 & \ell & 0 \\ -\ell & 0 & 0 \\ 0 & 0 & 0 \end{bmatrix} \tag{24}$$

Introducing (22) and (23) into (20) gives

$$\underline{\dot{U}}^{j} - \underline{\dot{U}}^{i} = H_R\, \underline{\omega}^{i} + (L^{F_i})^T\, \underline{i}\, \dot{U}^{ip} + (L^{F_j})^T\, \underline{i}\, \dot{U}^{jp} + \underline{\dot{U}}^{e} \tag{25}$$

where

$$H_R = (L^{F_i})^T\, E\, L^{F_i} \tag{26}$$

A second vector equation is obtained by recognizing that the i and j beam frames differ only due to elastic deformation. Thus the beam rotation rates are related by

$$\underline{\omega}^j = \underline{\omega}^i + \underline{\omega}^e \tag{27}$$

in which $\underline{\omega}^e$ denotes the elastic rotation rate of the F_j frame with respect to the F_i frame referred to the global frame.

Finally we wish to eliminate the beam frame rotation rates from (25) and (27). The difference in orientation of the mass and beam frames is due to plastic rotation at the hinges. Introducing the plastic rotation rates gives

$$\begin{aligned} \underline{\omega}^i &= \theta^i + \underline{\omega}^{ip} \\ \underline{\omega}^j &= \theta^j - \underline{\omega}^{jp} \end{aligned} \tag{28}$$

where the superscript p denotes the hinge rotation rate. Using (28) in (25) and (27) gives

$$\begin{aligned} &\dot{\underline{U}}^j - \dot{\underline{U}}^i - H_R \dot{\underline{\theta}}^i = H_R \underline{\omega}^{ip} + \dot{\underline{U}}^e + ({}^{F}L^{i})^T \, \underline{i} \, \dot{\underline{U}}^{ip} + ({}^{F}L^{j})^T \, \underline{i} \, \dot{\underline{U}}^{jp} \\ &\underline{\theta}^j - \underline{\theta}^i = \underline{\omega}^{ip} + \underline{\omega}^{jp} + \underline{\omega}^e \end{aligned} \tag{29}$$

The left hand side of equations (29) are expressed in terms of the generalized displacement rate $\dot{\underline{D}}$, whereas the right sides involve the elastic deformation of the beam and the plastic deformation occurring at the nodes. It remains to relate these deformation quantities to the generalized forces acting on the beam at the nodes.

2.4 DIFFERENTIAL EQUILIBRIUM OF THE BEAM

The forces and moments acting on the beam in the current state at time t_K are shown in Figure 2. Neglecting elastic deformation the

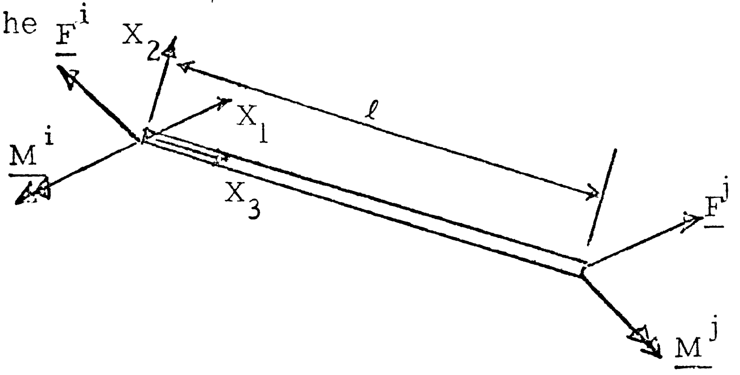

Figure 2

equations of equilibrium can be expressed as

$$ {}^{F_i}\underline{R}^{i} = A \; {}^{F_i}\underline{R}^{j} \tag{30} $$

where

$$ \begin{aligned} {}^{F_i}\underline{R}^{i} &= {}^{F_i}\begin{bmatrix} \underline{F} \\ \underline{M} \end{bmatrix}^{i} \\ {}^{F_i}\underline{R}^{j} &= {}^{F_i}\begin{bmatrix} \underline{F} \\ \underline{M} \end{bmatrix}^{j} \end{aligned} \tag{31} $$

and A is the 6 x 6 constant matrix

$$ A = \begin{bmatrix} I & 0 \\ -E & I \end{bmatrix} \tag{32} $$

We can now obtain a rate equation by differentiating (30) with respect to time. In carrying out this computation we must account for the change in orientation of the F_i frame. This is best done by referencing the generalized force vector to the fixed global system. For this we have the transformation relations

$$ \begin{aligned} {}^{F}\underline{R} &= T^{F}\,\underline{R} \\ \underline{R} &= (T^{F})^{T}\,{}^{F}\underline{R} \end{aligned} \tag{33} $$

where T^F is the 6 x 6 matrix

$$ T^{F} = \begin{bmatrix} L^{F} & 0 \\ 0 & L^{F} \end{bmatrix} \tag{34} $$

It also follows that

$$ \dot{T}^{F} = \overset{\Lambda}{\overline{W}}\, T^{F} \tag{35} $$

where

$$\hat{W} = \begin{bmatrix} \hat{W} & 0 \\ 0 & \hat{W} \end{bmatrix}^{F} \tag{36}$$

Expressing (30) in the global frame gives

$${}^{F}T^{i}\,\underline{R}^{i} = A\;{}^{F}T^{i}\,\underline{R}^{j} \tag{37}$$

Differentiating gives

$${}^{F_i}\dot{T}\,\underline{R}^{i} + {}^{F_i}T\,\dot{\underline{R}}^{i} = A({}^{F_i}\dot{T}\,\underline{R}^{j} + {}^{F_i}T\,\dot{\underline{R}}^{j}) \tag{38}$$

Transforming back to the F_i frame and using (30) and (35) to eliminate ${}^{F_i}\underline{R}^{i}$ and ${}^{F_i}\dot{T}$ gives

$${}^{F_i}\dot{\underline{R}}^{i} = A\;{}^{F_i}\dot{\underline{R}}^{j} + \left[A\hat{W} - \hat{W}A\right]{}^{F_i}\underline{R}^{j} \tag{39}$$

where we have used the fact that ${}^{F_i}T\,({}^{F_i}T)^{T}$ is the 6 x 6 identity matrix. By direct computation it can be shown that

$$\left[A\hat{W} - \hat{W}A\right]{}^{F_i}R^{j} = J\;{}^{F_j}\underline{\omega}^{i} \tag{40}$$

where J is the 6 x 3 matrix

$$J = \begin{bmatrix} 0 \\ \bar{J} \end{bmatrix} \tag{41}$$

in which $\bar{J}$ is the 3 x 3 matrix

$$\bar{J} = \ell\;{}^{F_i}\begin{bmatrix} -R_3 & 0 & 0 \\ 0 & -R_3 & 0 \\ R_1 & R_2 & 0 \end{bmatrix}^{j} \tag{42}$$

Introducing (40) into (39) gives

$${}^{F_i}\dot{\underline{R}}^{i} = A\;{}^{F_i}\dot{\underline{R}}^{j} + J\;{}^{F_i}\underline{\omega}^{i} \tag{43}$$

In what follows we will need (43) expressed in an alternate form. We first transform the variables to the global frame and then eliminate the beam frame rotation through (28). After rearranging, the result is

$$({}^{F_i}T^{i})^{T}\, J\, {}^{F_i}L^{i}\, \underline{\dot\theta}^{i} = \underline{\dot R}^{i} + ({}^{F_i}T^{i})^{T}\, A\, {}^{F_i}T^{i}\, \underline{\dot R}^{j} + ({}^{F_i}T^{i})^{T}\, J\, {}^{F_i}L^{i}\, \underline{\omega}^{ip} \tag{44}$$

2.5 INCREMENTAL YIELD CONDITION

We must relate the plastic deformation rates in (29) and (44) to the generalized forces acting on the beam. The appropiate relations are derived from considering the yield condition for the cross section. A hinge operates at a node permitting plastic deformation at the node when the current stress resultants lie on the yield surface for the section. We assume that the effect of transverse shear on yield can be neglected. Thus the yield condition at node i, for example, is a surface in the four dimensional space associated with the reduced generalized force vector

$${}^{F_i}\underline{R}^{i}_{R} = {}^{F_i}\begin{bmatrix} F_3 \\ M_1 \\ M_2 \\ M_3 \end{bmatrix}^{i} \tag{45}$$

Thus we may denote the yield surface at node i by the scaler function

$$f^{i}\left({}^{F_i}\underline{R}^{i}_{R}\right) = C_i \tag{46}$$

where C_i is a constant.

Since the yield function must remain constant during the plastic deformation process, we have

$$\dot f^{i}\left({}^{F_i}\underline{R}^{i}_{R}\right) = 0 \tag{47}$$

In carrying out the chain rule differentiation, it is convenient to express the argument in terms of the nodal forces at the j node expressed in the global system, i.e.

$$ {}^{F_i}\underline{R}^i_R = A_R \; {}^{F_i}T \; \underline{R}^j \tag{48} $$

where A_R is the 4 x 6 matrix formed from the last four rows of the matrix A.

With this (47) can be expressed as

$$ (\nabla f^i)^T \; (A_R \, {}^{F_i}\dot{T} \; \underline{R}^j + A_R T \; {}^{F_i}\dot{\underline{R}}^j) = 0 \tag{49} $$

in which $\underline{\nabla}$ represents the vector gradient. Using (35) and transforming back to the F_i frame through (33) gives

$$ (\underline{\nabla} f^i)^T \; (A_R \overset{\Lambda}{\overline{W}} \; {}^{F_i}\underline{R}^j + A_R \; {}^{F_i}\dot{\underline{R}}^j) = 0 \tag{50} $$

The matrix $\overset{\Lambda}{\overline{W}}$ involves the beam frame rotation rate ${}^{F_i}\underline{\omega}^i$.

As before this can be expressed in terms of ${}^{F_i}\underline{\omega}^{ip}$ and ${}^{F_i}\theta^i$. Equation (50) can be reduced to an equation for a single scaler by relating the plastic deformation rate to the yield surface. We assume that incremental plastic deformation vector is normal to the yield surface.[2] We introduce the plastic deformation rate vector

$$ \dot{\underline{K}}^i = \begin{bmatrix} U^{ip} \\ {}^{F_i}\dot{\omega}_1^{ip} \\ {}^{F_i}\omega_2^{ip} \\ {}^{F_i}\omega_3^{ip} \end{bmatrix} \tag{51} $$

[2] For a discussion of the normality condition in structural theories see P. G. Hodge, "Limit Analysis of Rotationally Symmetric Shells",

Then the normality condition is

$$\dot{\underline{K}}^{i} = \underline{a}^{i} \lambda \tag{52}$$

where λ is a scaler multiple and $\underline{a}^i$ is the normalized gradient, i.e.

$$\underline{a}^{i} = \frac{\underline{\nabla} f^{i}}{\left| \underline{\nabla} f^{i} \right|} \tag{53}$$

Using (53) to eliminate the components of ${}^{F_i}\underline{\omega}^{ip}$ from (50) gives after some algebric manipulation

$$\lambda \; (\underline{\nabla} f^{i})^{T} \; \Delta A_{R}^{i} \; {}^{F_i}\underline{R}^{j} = -(\nabla f^{i})^{T} \; A_{R} \; {}^{F_{i.j}}\underline{R} \; -(\underline{\nabla} f^{i})^{T} \; B^{i} \; {}^{F_{i.i}}\underline{\theta} \tag{54}$$

where

$$\Delta A_{R}^{i} = \begin{bmatrix} a_3 & -a_2 & 0 & 0 & 0 & 0 \\ \ell a_4 & 0 & -\ell a_2 & 0 & a_4 & a_3 \\ 0 & \ell a_4 & -\ell a_3 & -a_4 & 0 & a_2 \\ 0 & 0 & 0 & a_3 & -a_2 & 0 \end{bmatrix}^{i}$$

$$B^{i} = {}^{F_i}\begin{bmatrix} -R_2 & R_1 & 0 \quad 0 \\ -R_3\ell & -R_6 & (R_1\ell + R_5) \\ R_6 & -R_3\ell & (R_2\ell - R_4) \\ -R_5 & R_4 & 0 \end{bmatrix}^{j} \tag{55}$$

Solving (54) for λ and substituting into (52) gives for the plastic deformation rate

$$\dot{\underline{K}}^{i} = G^{i}\,{}^{F}\underline{R}^{i.j} + \bar{G}^{i}\,{}^{F}\theta^{i.i} \tag{56}$$

where

$$G^{i} = \frac{-1}{(\underline{\nabla} f^{i})^{T}\,\Delta A_{R}^{i}\,{}^{Fi}\underline{R}^{j}}\;\underline{a}^{i}\,(\nabla f^{i})^{T} A_{R}$$

$$\bar{G}^{i} = \frac{-1}{(\underline{\nabla} f^{i})^{T}\,\Delta A_{R}^{i}\,{}^{Fi}\underline{R}^{j}}\;\underline{a}^{i}\,(\underline{\nabla} f^{i})^{T} B^{i}$$

An analogous analysis may be carried out at the node j. The result for the plastic deformation rate at j is

$$\dot{\underline{K}}^{j} = G^{j}\,{}^{Fj.i}\underline{R} + \bar{G}^{j}\,{}^{Fj.j}\theta \tag{57}$$

where

$$G^{j} = \frac{1}{(\underline{\nabla} f^{j})^{T}\,\Delta A_{R}^{j}\,{}^{Fj}\underline{R}^{i}}\;\underline{a}^{j}\,(\underline{\nabla} f^{j})^{T} A_{R}^{-1}$$

$$\bar{G}^{j} = \frac{1}{(\underline{\nabla} f^{j})^{T}\,\Delta A_{R}^{j}\,{}^{Fj}\underline{R}^{i}}\;\underline{a}^{j}\,(\underline{\nabla} f^{j})^{T} B^{j} \tag{58}$$

in which $f^j = C_j$ is the yield function at j and

$$\underline{a}^j = \frac{\underline{\nabla f}^j}{\left|\nabla f^j\right|} \tag{59}$$

$$A_R^{-1} = \begin{bmatrix} 0 & 0 & 1 & 0 & 0 & 0 \\ 0 & \ell & 0 & 1 & 0 & 0 \\ -\ell & 0 & 0 & 0 & 1 & 0 \\ 0 & 0 & 0 & 0 & 0 & 1 \end{bmatrix}$$

$$\Delta A_R^j = \begin{bmatrix} a_3 & -a_2 & 0 & 0 & 0 & 0 \\ -\ell\, a_4 & 0 & \ell\, a_2 & 0 & a_4 & -a_3 \\ 0 & -\ell\, a_4 & \ell\, a_3 & -a_4 & 0 & a_2 \\ 0 & 0 & 0 & a_3 & -a_2 & 0 \end{bmatrix}^j \tag{60}$$

$$B^j = F_j \begin{bmatrix} -R_2 & R_1 & 0 \\ \ell\, R_3 & -R_6 & (-R_1\ell + R_5) \\ R_6 & \ell\, R_3 & (-R_2\ell - R_4) \\ -R_5 & R_4 & 0 \end{bmatrix}^i$$

2.6 ELEMENT STIFFNESS MATRIX

Equations (29) and (44) represent twelve equations which will relate the elements of $\underline{\dot{D}}$ and $\underline{\dot{R}}$ if we can eliminate the elastic and plastic deformation rates. From the previous section we obtain

$$
\begin{aligned}
\dot{U}^{ip} &= G_U^i \; {}^{F_i}\dot{\underline{R}}^j + \bar{G}_U^i \; {}^{F_i}\underline{\theta}^i \\
\underline{\omega}^{ip} &= H^{ip} \; \dot{\underline{R}}^j + \bar{H}^{ip} \; \underline{\theta}^i \\
\dot{U}^{jp} &= G_U^i \; {}^{j}\dot{\underline{R}}^i + \bar{G}_U^j \; {}^{F_j}\underline{\theta}^j \\
\underline{\omega}^{jp} &= H^{jp} \; \dot{\underline{R}}^i + \bar{H}^{jp} \; \underline{\theta}^j
\end{aligned}
\tag{61}
$$

where

$$
\begin{aligned}
H^{ip} &= ({}^{F_i}L)^T \; G_R^i \; {}^{F_i}T \\
\bar{H}^{ip} &= ({}^{F_i}L)^T \; \bar{G}_R^i \; {}^{F_i}L \\
H^{jp} &= ({}^{F_j}L)^T \; G_R^j \; {}^{F_j}T \\
\bar{H}^{jp} &= ({}^{F_j}L)^T \; \bar{G}_R^j \; {}^{F_j}L
\end{aligned}
\tag{62}
$$

in which a subscript "U" on G or $\bar{G}$ denotes the first row of the corresponding matrix and a subscript "R" denotes the bottom three rows.

From elastic beam theory we have relative to the current configuration beam frame F_i

$$
{}^{F_i}\underline{D}^e = K_e^{-1} \; {}^{F_i}\underline{R}^j
\tag{63}
$$

where

$$K_e = \begin{bmatrix} \frac{12EI_2}{\ell^3} & 0 & 0 & 0 & \frac{-6EI_2}{\ell^2} & 0 \\ 0 & \frac{12EI_1}{\ell^3} & 0 & \frac{6EI_1}{\ell^2} & 0 & 0 \\ 0 & 0 & \frac{EA}{\ell} & 0 & 0 & 0 \\ 0 & \frac{6EI_1}{\ell^2} & 0 & \frac{4EI_1}{\ell} & 0 & 0 \\ \frac{-6EI_2}{\ell^2} & 0 & 0 & 0 & \frac{4EI_2}{\ell} & 0 \\ 0 & 0 & 0 & 0 & 0 & \frac{GJ}{\ell} \end{bmatrix} \tag{64}$$

in which E is the elastic modulus, G is the shear modulus, I_1 and I_2 are the principal moments of inertia, A is the cross section area, J is the torsional rigidity, and ℓ is the beam length. In (63) the vector on the left hand side represents

$$F_{i_{\underline{D}}e} = \begin{bmatrix} F_{i_{\underline{U}}e} \\ F_{i_{\underline{\Omega}}e} \end{bmatrix} \tag{65}$$

where $\underline{\Omega}^e$ represents the elastic rotations. We are assuming the elastic deformation is small and hence $\underline{\Omega}^e$ may be considered a vector as well as the elastic rotation rate $\underline{\omega}^e$. We introduce the rate variable

$$\underline{D}^{F_{i.e}} = \begin{bmatrix} F^{i.e}_{\underline{U}} \\ F^{i}_{\underline{\omega}}{}^{e} \end{bmatrix} \tag{66}$$

In calculating this rate from differentiating (63), we must again account for the rotation rate of the beam frame F^i. The procedure is exactly analogous to the differentiation of the equilibrium equation (30). The final result expressed in the global frame is

$$\dot{\underline{D}}^{e} = \left[({}^{F_i}T)^T K_e^{-1}\,{}^{F_i}T + (KRT) \right] \dot{\underline{R}}^{j} + \overline{(KRT)}\ \underline{\theta}^{i} \tag{67}$$

in which

$$\begin{aligned} (KRT) &= ({}^{F_i}T)^T\,(KR)L\ {}^{F_i}H^{ip} \\ \overline{(KRT)} &= ({}^{F_i}T)^T\,(KR)L\ {}^{F_i}(I+\overline{H}^{ip}) \end{aligned} \tag{68}$$

where (KR) is the 6 x 3 matrix

$$(KR) = {}^{F_i}\begin{bmatrix} K_7R_6 & (K_3-K_1)R_3 & (K_1-K_2)R_2-(K_7+K_8)R_4 \\ (K_2-K_3)R_3 & -K_8R_6 & (K_1-K_2)R_1+(K_7+K_8)R_5 \\ (K_2-K_3)R_2+K_8R_4 & (K_3-K_1)R_1-K_7R_5 & 0 \\ K_8R_3 & (K_6-K_4)R_6 & -(K_7+K_8)R_1+(K_4-K_5)R_5 \\ (K_5-K_6)R_6 & -K_7R_3 & (K_7+K_8)R_2+(K_4-K_5)R_4 \\ K_7R_1+(K_5-K_6)R_5 & -K_8R_2+(K_6-K_4)R_4 & 0 \end{bmatrix}^{j}$$

in which K_j represents the nonzero elements of K_e^{-1} and are given by

$$K_1 = \ell^3/3EI_2, \quad K_2 = \ell^3/3EI_1, \quad K_3 = \ell/AE$$

$$K_4 = \ell/EI_1, \quad K_5 = \ell/EI_2, \quad K_6 = \ell/GJ \tag{70}$$

$$K_7 = \ell^2/2EI_2, \quad K_8 = -\ell^2/2EI_1$$

We now partition equation (67) to give

$$\begin{aligned} \dot{\underline{U}}^{e} &= \left[K_u + (KRT)_u\right] \dot{\underline{R}}^{j} + \overline{(KRT)}_u \underline{\theta}^{i} \\ \underline{\omega}^{e} &= \left[K_\ell + (KRT)_\ell\right] \dot{\underline{R}}^{j} + \overline{(KRT)}_\ell \underline{\theta}^{i} \end{aligned} \tag{71}$$

where the subscripts u and ℓ denote the upper three rows and lower three rows respectively of the corresponding matrices in (67).

Finally we write

$$\begin{aligned} ({}^{F}L^{i})^{T}\,{}_{\underline{i}}\dot{U}^{ip} &= \overset{\Lambda}{E}_i \dot{\underline{R}}^{j} + \overset{\Lambda}{\overline{E}}_i \underline{\theta}^{i} \\ ({}^{F}L^{j})^{T}\,{}_{\underline{i}}\dot{U}^{jp} &= \overset{\Lambda}{E}_j \dot{\underline{R}}^{i} + \overset{\Lambda}{\overline{E}}_j \underline{\theta}^{j} \end{aligned} \tag{72}$$

where from (61), (6) and (33) we have

$$\begin{aligned} \overset{\Lambda}{E}_i &= ({}^{F}L^{i})^{T}\,{}_{\underline{i}}G^{i}_{U}\,{}^{F}T^{i} \\ \overset{\Lambda}{\overline{E}}_i &= ({}^{F}L^{i})^{T}\,{}_{\underline{i}}\overline{G}^{i}_{U}\,{}^{F}L^{i} \\ \overset{\Lambda}{E}_j &= ({}^{F}L^{j})^{T}\,{}_{\underline{i}}G^{j}_{U}\,{}^{F}T^{j} \\ \overset{\Lambda}{\overline{E}}_j &= ({}^{F}L^{j})\,{}_{\underline{i}}\overline{G}^{j}_{U}\,{}^{F}L^{j} \end{aligned} \tag{73}$$

We now use (61), (71) and (72) to eliminate the elastic and plastic deformation rates from (29) and (44). The resulting system of equations may be expressed in matrix form

$$B\,\dot{\underline{D}} = H\,\dot{\underline{R}} \tag{74}$$

where the 12 x 12 matrices B and H are

$$B = \left[\begin{array}{c|c|c|c} 0 & 0 & 0 & 0 \\ \hline 0 & (L^{F_i})^T \bar{J}(I + \bar{G}_R^i)\, L^{F_i} & 0 & 0 \\ \hline -I & \begin{array}{c} -(H_R + H_R \bar{H}^{ip} + \hat{\bar{E}}_i) \\ + \overline{(KRT)}_U \end{array} & I & -\hat{\bar{E}}_j \\ \hline 0 & \begin{array}{c} -(I + \bar{H}^{ip}) \\ + \overline{(KRT)}_\ell \end{array} & 0 & (I - \bar{H}^{jp}) \end{array}\right] \tag{75}$$

$$H = \left[\begin{array}{cc|cc} I & 0 & -I & 0 \\ \hline 0 & I & (L^{F_i})^T (E - \bar{J}\, G_1)\, L^{F_i} & -I + (L^{F_i})^T \bar{J}\, G_2 L^{F_i} \\ \hline \multicolumn{2}{c|}{\hat{E}_j} & \multicolumn{2}{c}{K_U + H_R H^{ip} + \hat{E}_i + (KRT)_U} \\ \hline \multicolumn{2}{c|}{H^{jp}} & \multicolumn{2}{c}{K_\ell + H^{ip} + (KRT)_\ell} \end{array}\right] \tag{76}$$

in which G_1 and G_2 denote the first three and and second three columns of G^i_R respectively.

Thus we have the desired result

$$\ddot{\underline{R}} = K\ \dot{\underline{D}} \tag{77}$$

where the element stiffness matrix K is

$$K = H^{-1}\ B \tag{78}$$

2.7 TEST CONDITIONS FOR PLASTIC DEFORMATION AND ELASTIC UNLOADING

In the previous section we derived the stiffness matrix for an elastic-plastically deforming beam element. This general expression is valid, however, only if the plastic hinges at the beam nodes are operating. If the hinge is not operating, the plastic contribution to (78) can be eliminated simply by setting the G and $\overline{G}$ matrices associated with the node to zero.

This implies, however, that in addition to the stiffness matrix we must develop a procedure for monitoring the operation of the hinge, Implementing this procedure is basically a programming problem, but we briefly outline here the general considerations involved. For each node we introduce a hinge switch

$$S^i = \begin{matrix} 0 \text{ No Plastic Deformation} \\ 1 \text{ Plastic Deformation} \end{matrix} \tag{79}$$

Initially S^i is zero. At the end of each forward integration step the value of the yield function f^i is computed. If it is less than C_i, the computation proceeds to the next step with the G and $\overline{G}$ matrices set to zero. If it exceeds C_i, we introduce a scale factor λ such that

$$f^i\,(\lambda\ {}^{F}{}^{i}\underline{R}^{i}_{R}) = C_i \tag{80}$$

Since the generalized force and generalized displacement vectors are linearly related, scaling the last step size by λ gives a deformation state which just satisfies the yield condition. The switch S^i is then set to unity for the next step and the G and $\overline{G}$ matrices are included in the calculations.

Finally we must introduce a condition to monitor elastic unloading. During plastic deformation the rate of energy dissipation must be positive. At node i the dissipation rate is

$$\dot{d} = ({}^{F}{}^{i}\underline{R}^{i}_{R})^{T}\ \underline{\dot{K}}^{i} \tag{81}$$

The dissipation increment for each time step is computed from (81) whenever S^i is equal to unity. If

$$\dot{d} > 0,$$

the computation proceeds to the next step. If

$$\dot{d} \leq 0,$$

the switch S^i is set to zero which eliminates the G and $\bar{G}$ matrices from the computation. Once S^i is zero, of course, it is checked for reloading as discussed above.

2.8 GLOBAL STIFFNESS MATRIX

The global stiffness matrix is obtained by considering the equilibrium of each node. The process of assembling the global matrix is standard and basically a bookeeping operation. Here we briefly outline the basis for the assembly proceedure. Figure 2A shows the beam element LB which connects the nodes i and j. The generalized forces shown are now considered

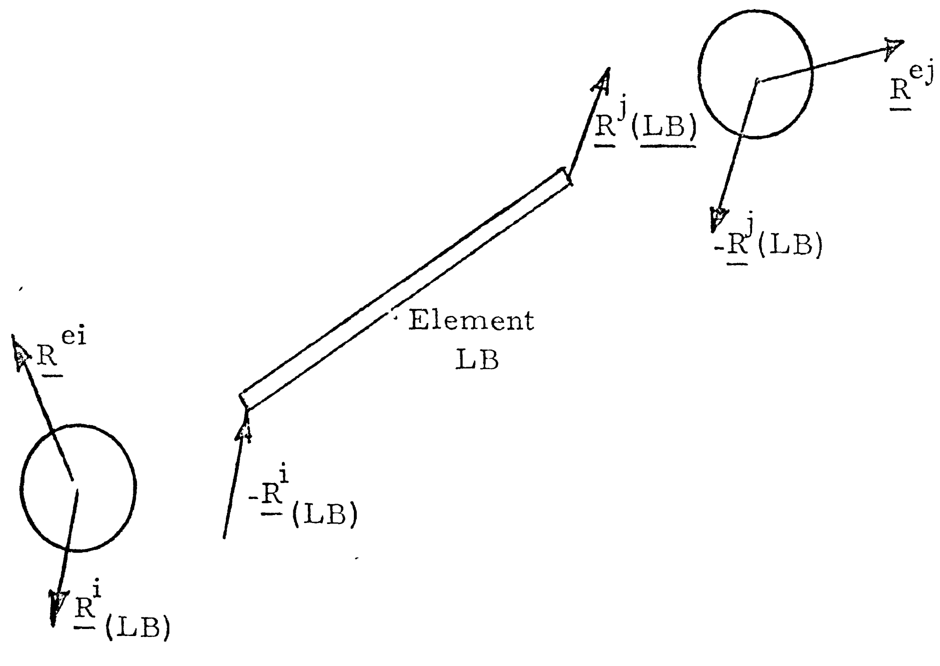

GLOBAL EQUILIBRIUM

Figure 2A

As vectors in the global system. The minus sign is required at the i end of the beam since the elements of $\underline{R}^{i}$ were defined using the usual beam theory sign convention. Equilibrium of the i and j nodes in rate form gives

$$\begin{aligned} \dot{\underline{R}}^{i}(LB) &= -\dot{\underline{R}}^{ei} \\ -\dot{\underline{R}}^{j}(LB) &= -\dot{\underline{R}}^{ej} \end{aligned} \tag{82}$$

where $\underline{R}^{ei}$ denotes the external force acting on the ith node. We partition the element stiffness matrix

$$K(LB) = \begin{bmatrix} SK^{II} & SK^{IJ} \\ SK^{JI} & SK^{JJ} \end{bmatrix}^{LB} \tag{83}$$

where the elements SK are 6 x 6 matrices. Thus we have

$$\begin{bmatrix} \dot{\underline{R}}^{i} \\ \dot{\underline{R}}^{j} \end{bmatrix}^{LB} = \begin{bmatrix} SK^{II} & SK^{IJ} \\ SK^{JI} & SK^{JJ} \end{bmatrix} \begin{bmatrix} \dot{\underline{D}}^{i} \\ \dot{\underline{D}}^{j} \end{bmatrix} \tag{84}$$

Introducing into (82) gives

$$\begin{aligned} SK^{II}\,\dot{\underline{D}}^{i} + SK^{IJ}\,\dot{\underline{D}}^{j} &= -\dot{\underline{R}}^{ej} \\ -SK^{JI}\,\dot{\underline{D}}^{i} - SK^{JJ}\,\dot{\underline{D}}^{j} &= -\dot{\underline{R}}^{ej} \end{aligned} \tag{85}$$

Considering equilibrium of all nodes i = 1, 2...N gives a system of equation

$$TK\,\dot{\underline{D}}^{G} = -\dot{\underline{R}}^{G} \tag{86}$$

where

$$\dot{\underline{D}}^{G} = \begin{bmatrix} \dot{\underline{D}}^{1} \\ \dot{\underline{D}}^{2} \\ \vdots \\ \dot{\underline{D}}^{N} \end{bmatrix} \qquad \dot{\underline{R}}^{G} = \begin{bmatrix} \dot{\underline{R}}^{e1} \\ \dot{\underline{R}}^{e2} \\ \vdots \\ \dot{\underline{R}}^{eN} \end{bmatrix} \tag{87}$$

The global stiffness matrix TK has dimension $6\cdot N \times 6\cdot N$. It may be considered as consisting of $N \times N$ elements, each element being a 6×6 matrix. In this sense we introduce the $N \times N$ matrix element matrix

$$TK(LB) = \begin{array}{cc} \begin{array}{ccccc} \quad & I & \quad & J & \quad \end{array} & \\ \left[\begin{array}{ccccc} \cdots & SK^{II} & \cdots & SK^{IJ} & \cdots \\ \cdots & SK^{JI} & \cdots & SK^{JJ} & \cdots \end{array}\right] & \begin{array}{c} I \\ J \end{array} \end{array} \tag{88}$$

in which all other elements are zero. From (85) it is clear that TK(LB) represents the contribution of the LB beam element to the system of equations (86). Thus we have

$$TK = \sum_{LB=1}^{M} TK(LB) \tag{89}$$

when M is the total number of elements.

2.9 BOUNDARY CONDITIONS

Our problem has been reduced to the solution of the system of equations (86) where the right hand side represents the increments in external force applied to the structure. In general this represents the known loading. In addition, however, boundary conditions may be specified on the displacements such as at supports or imposed displacements of certain nodes. Boundary conditions are handled in the present analysis by contraction of the K matrix.

We let TK_{ij} represent the elements of the TK matrix. Then an alternate form for expressing (86) is

$$\sum_{j=1}^{6\cdot N} TK_{ij} \, \dot{D}_j^G = -\dot{R}_i^e \qquad i = 1, 2 \ldots 6\cdot N \tag{90}$$

We consider a displacement condition

$$\dot{D}_K^G = \Delta \tag{91}$$

The corresponding external generalized force rate $\dot{R}_K^e$ is now an unknown constraint. Introducint (91) into (90) we have

$$\sum_{j \neq K} TK_{ij} \; \dot{D}^G_j + TK_{iK}\Delta = -\dot{R}^G_i \qquad i \neq K \tag{92}$$

$$\sum_{j \neq K} TK_{Kj} \; \dot{D}^G_j + TK_{KK}\Delta = -\dot{R}^G_K \tag{93}$$

Equations (92) have the form

$$\overline{TK} \; \bar{\dot{\underline{D}}}^G = -\bar{\dot{\underline{R}}}^G \tag{94}$$

where $\overline{TK}$ is the matrix obtained by eliminating the Kth row and Kth column from TK, $\bar{\dot{\underline{D}}}^G$ is the vector obtained by eliminating $\dot{D}^G_K$ from $\dot{\underline{D}}^G$ and the N-1 elements of $\bar{\dot{\underline{R}}}^G$ are

$$\bar{\dot{R}}^G_i = \dot{R}^G_i + TK_{KK}\,\Delta, \qquad i \neq K \tag{95}$$

When the reduced system (94) is solved, the unknown constraint force can then be computed from (93). With this the vectors $\dot{\underline{D}}^G$ and $\dot{\underline{R}}^G$ are completely known from which all other variables in the problem can be computed. (For example, the generalized force rate acting on a beam element can be computed from (84)).

2.10 SOLUTION PROCEDURE

The above analysis has been formulated in terms of rate equations and represent a complex set of differential equations. To solve the system numerically we must introduce approximations. Our final set of equations has the form.

$$T\,\dot{\underline{U}} = \dot{\underline{f}} \tag{96}$$

when the right hand side is known and T is a complicated implicit function of $\underline{U}$. We now approximate $\dot{\underline{U}}$ (and similarly $\dot{\underline{f}}$) by

$$\dot{\underline{U}}(t_K) = \frac{\underline{U}(t_{K+1}) - \underline{U}(t_K)}{dt} \tag{97}$$

Thus

$$\underline{U}(t_{K+1}) - \underline{U}(t_K) = \Delta\underline{U}_{K+1} = \dot{\underline{U}}(t_K)dt \tag{98}$$

Introducing into (96) now gives

$$T(t_K)\ \Delta\underline{U}_{K+1} = \Delta\underline{f}_{K+1} \tag{99}$$

Thus the forward integration is actually accomplished by specifying the next increment in the prescribed vector $\underline{f}$. The corresponding increment in $\underline{U}$ is then obtained by solving equations (99) using the current value of the matrix T_K. With $\Delta\underline{U}$ known the increment in all variables can be computed, the variables updated to time t_{K+1}, and the matrix T_K updated after carrying out the check procedures outlined in section 2.7. The details of the numerical computation and the corresponding computer program are discussed in the User's Guide contained in the Appendix.

CHAPTER 3

VERIFICATION OF BEAM-COLUMN ELEMENT

3.1 INTRODUCTION

The computer model for the beam-column with hinge must be verified by comparison with experiment. The specific case chosen is the static deflection of a thin-walled, cantilevered beam. A plastic hinge will form at the root of the beam when tip loads become large. Both qualitative and quantitative comparisons are to be made. The behavior of the hinge at large deformation is of greatest interest.

3.2 EXPERIMENTAL GOALS

The experiment is intended to provide information not only to verify the current element model, but also to serve as a standard for future theories. It is hoped to provide a well-defined and simple experiment.

A beam-column is to be subjected to loads acting initially in axial and in lateral directions (Figures 3 and 4).

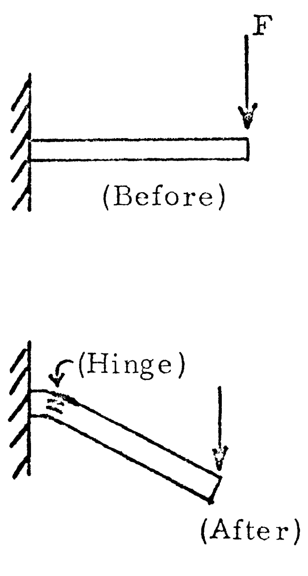

Figure 3. Lateral Loading

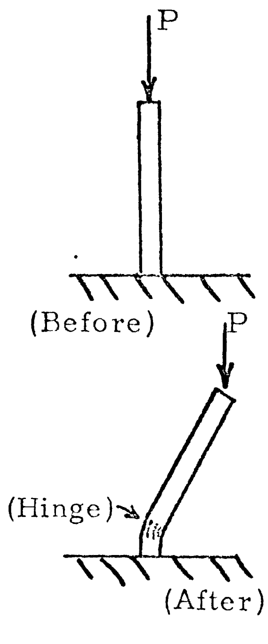

Figure 4. Axial Loading

Criteria for planning the test include:

1) The loads are to be applied in a manner easy to interpret in a global coordinate system, i.e., the verticality of the load must be maintained at very large deflections.
2) The geometry of the cross section must be maintained in the regions where external forces act--at the tip and root. This provides reproducible boundary conditions.
3) The large deflection, plastic flow region is of more interest than the elastic region.
4) Displacements must be controlled so that catastrophic collapse does not occur in softening portions of the load-deflection cycle.

3.3 BEAM SPECIMENS

The test specimens were integrally milled in pairs from cold-rolled 1018 steel bar (Figure 5).

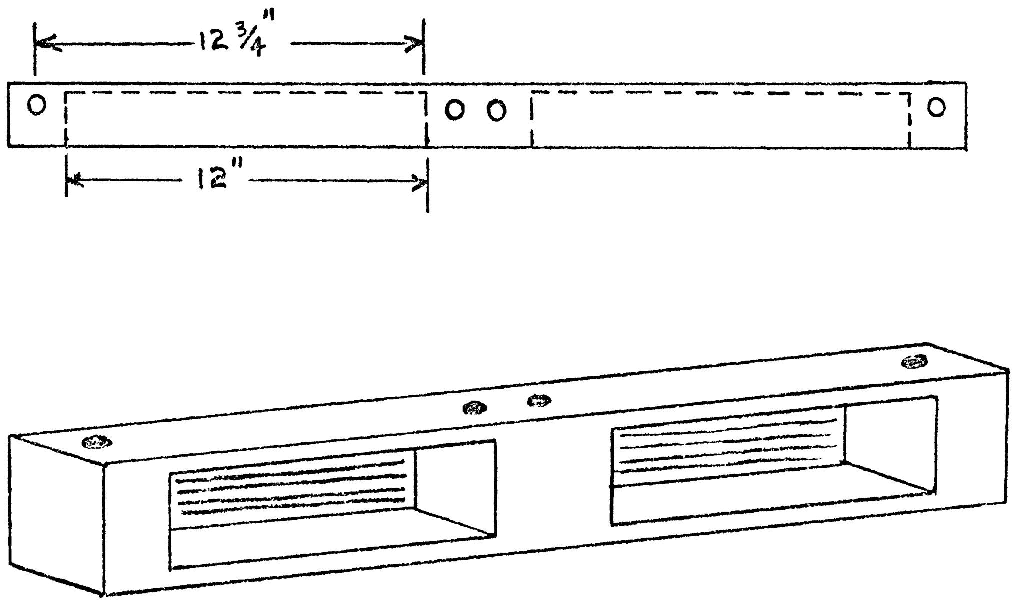

Figure 5. Two-Element Beam Specimen

Two such specimens (a total of 4 beam elements) were tested at the same time in order to maintain symmetry and verticality of loading in the test machine. This same type of specimen can be used for both the dominantly axial and dominantly lateral loadings.

The beam cross section was an open channel with nominal dimensions of h = 1", b = 1-1/2" and t = 0.100".

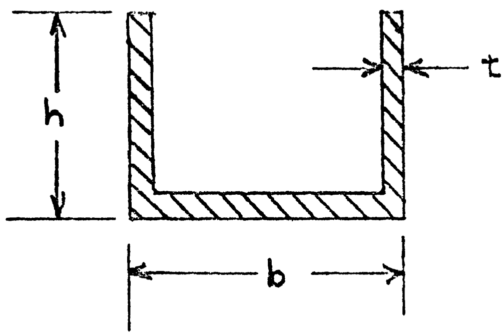

Figure 6. Cross-Section

Average cross-sectional properties for the lateral test were h = 0.998", b = 1.498" and t = 0.102". For the axial test, h = 1.001", b = 1.502", and t = 0.101". The specimens were accurately machined; the integral machining process is viewed as a success. Each two-element beam specimen required 1-1/2 man days to machine.

Material properties for the 1018 steel were found by a standard tensile test. A 0.5" diameter cylinder was tested with the use of a mechanical extensometer of two inch gage length. The important portion of the stress-strain curve is shown in Figure 7. Modulus of elasticity E is found to be 30.35 x 10^6 psi and yield stress based on .002 permanent set is 75,000 psi. The stress-strain law can be approximated as elastic-perfectly plastic, with a yield stress of 78,700 psi; this characterization will be used in later comparisons.

3.4 LOADING CONFIGURATIONS

The specimens can be arranged so that the loading is either dominantly lateral or dominantly axial. It has been historically difficult to maintain a rigid boundary at the root of a cantilever. This was accomplished by milling the specimens in pairs with the root at the center so that symmetric loading yields a zero slope condition at the root. Another, more

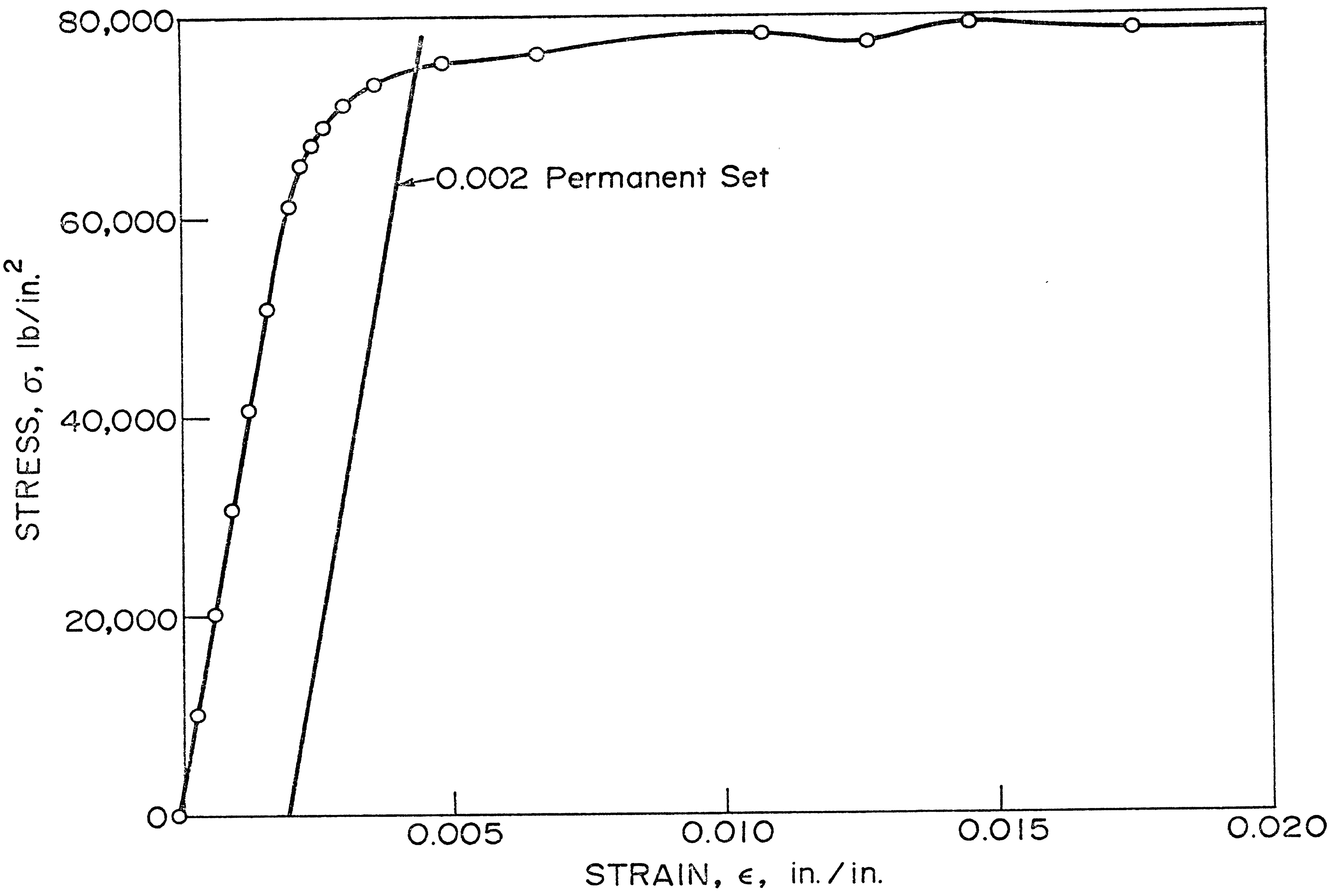

Fig. 7 Tensile test for 1018 steel. (Middle strain range.)

specialized, requirement for the present test is that the direction of loading remain unchanged even to large rotations of the specimen. This is more difficult than one might imagine, but can be satisfied by using two pairs of specimens in a mirror image type of loading.

For lateral loading, links were used to join the tips of the beams (Figure 8). Four hinges formed as large deformation proceded. The links

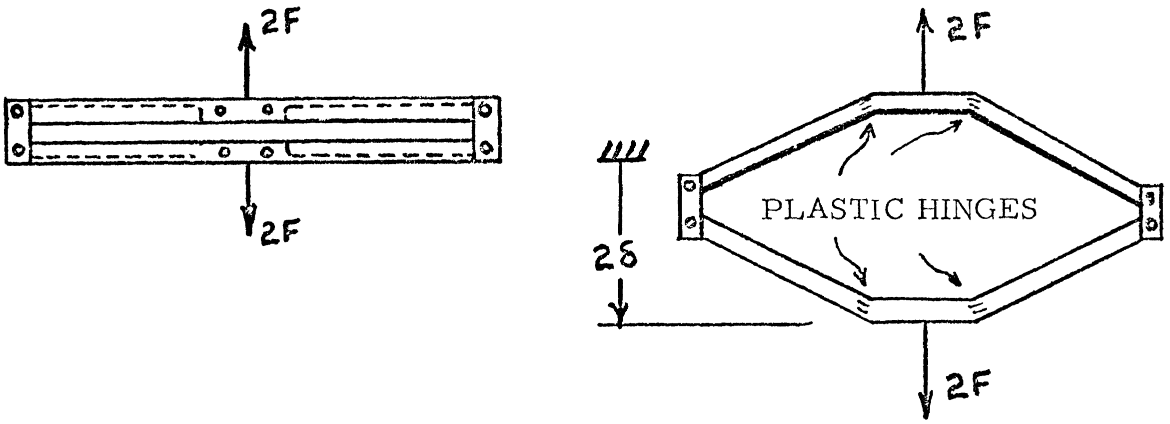

Figure 8. Lateral Loading Geometry

were made as short as possible so that the 4 hinges are forced to maintain the same angle. This approach was successful over most of the test range.

For axial loading (Fig. 9), the specimens were constrained at both the root and tip location. The cover plates at the center enforced equality of hinge angles during the entire test. In order to prevent a catastrophic buckling typical of perfect specimens, an imperfection δ_o was introduced. The small value of imperfection provided, $\delta_o = 0.039''$, allowed a more gradual collapse under load.

In each type of loading, the beam elements act in parallel as well as in series to oppose the load. The notation has been chosen to yield F, P, δ, and β as the appropriate quantities for a single element.

A Tinius Olsen 120,000 lb tensile test machine was used. For each type of loading, special fixtures had to be made to mount the assembly and to prevent slippage. These end fixtures introduced some unwanted flexibility into the system in each case, but this had little effect on the large displacement

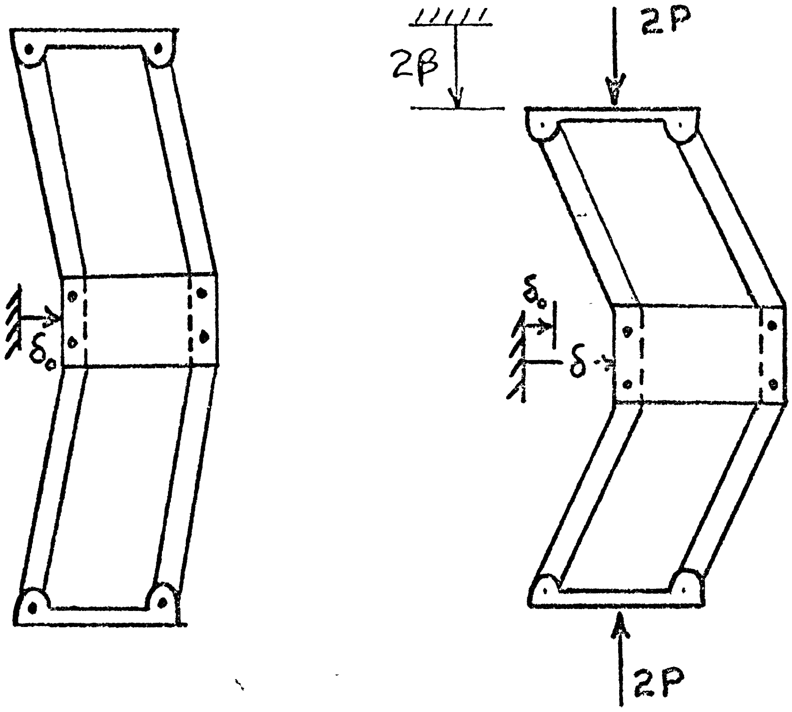

Figure 9. Axial Loading Geometry

readings desired. (See results). Loads were read on the large dial of the Olsen machine, calibrated to within 1%. Displacements of the machine's loading surfaces and of the lateral deflection of the beams were read with mechanical dial gages with least count of 0.001". Angular rotations at the center of each beam element were measured with a protractor with least count of $1/2^{\circ}$. Accuracy of these angular readings was approximately $\pm 1/2^{\circ}$ with error due to parallax and difficult alignment at times.

The tests were displacement-controlled. The loading surfaces were moved in increments of displacement, and then load, lateral displacement, axial displacement and specimen angles were read. In the softening region of loading, a relaxation phenomenon occurred (see Section 3.7). In all load-deflection curves presented, the loads are for long time, i.e., the "static" case. This often meant waiting 5 minutes before reading the load value. The Olsen machine was rigid enough that displacements did not creep to any extent.

3.5 TEST RESULTS FOR LATERAL LOAD

The results given here will in all cases be presented in terms of loads and deflections for a single beam element. This means that system characteristics such as stiffnesses acting in parallel or series, must be appropriately accounted for. In the lateral loading case, the loads applied to the system are actually 2F, and the displacements read are actually 2δ, but results are always given in terms of F and δ.

As initial reduction and plotting of data progressed, it became clear that certain other system properties, such as support flexibilities, might at times be removed before presenting data for the element. These corrections are small and important only in the elastic range. They will be discussed when they arise.

Load-deflection results for the lateral load case are given in Figures 10-12. The beam was at first loaded in increments of 50 lb (Figure 10. The stiffness of the specimen was found to be 1,083 lb/in, as compared to a theoretical value for an Euler beam of 1,450 lb/in. The difference is attributed to flexibility in the integrally milled center section of the specimen bar and to flexibility of supports. Yielding of the cross section occurred between 250 and 300 lb, whereas the theoretical value for yield at the outer fiber is 321 lb. The limit load for the beam was 500 lb. This provides an experimental shape factor of approximately 1.8 in excellent agreement with the theoretical value of 1.81.

After ultimate load has been reached, the beam unloads as seen in Figure 11. Disregarding the strange ripple in the curve between 2 and 4 inches of tip displacement, one can see that the beam softens to approximately 1/2 its ultimate load carrying capacity. It then becomes more rigid at very large deflections because the load is carried in axial tension.

The ripple occurring in the softening portion of the curve has a rational explanation. It is kinematically possible, because of the way the beams are linked together, to have one pair of hinges operating at a different angle from the other pair. In a softening situation, one pair of hinges will freeze while the other pair operates. This can best be

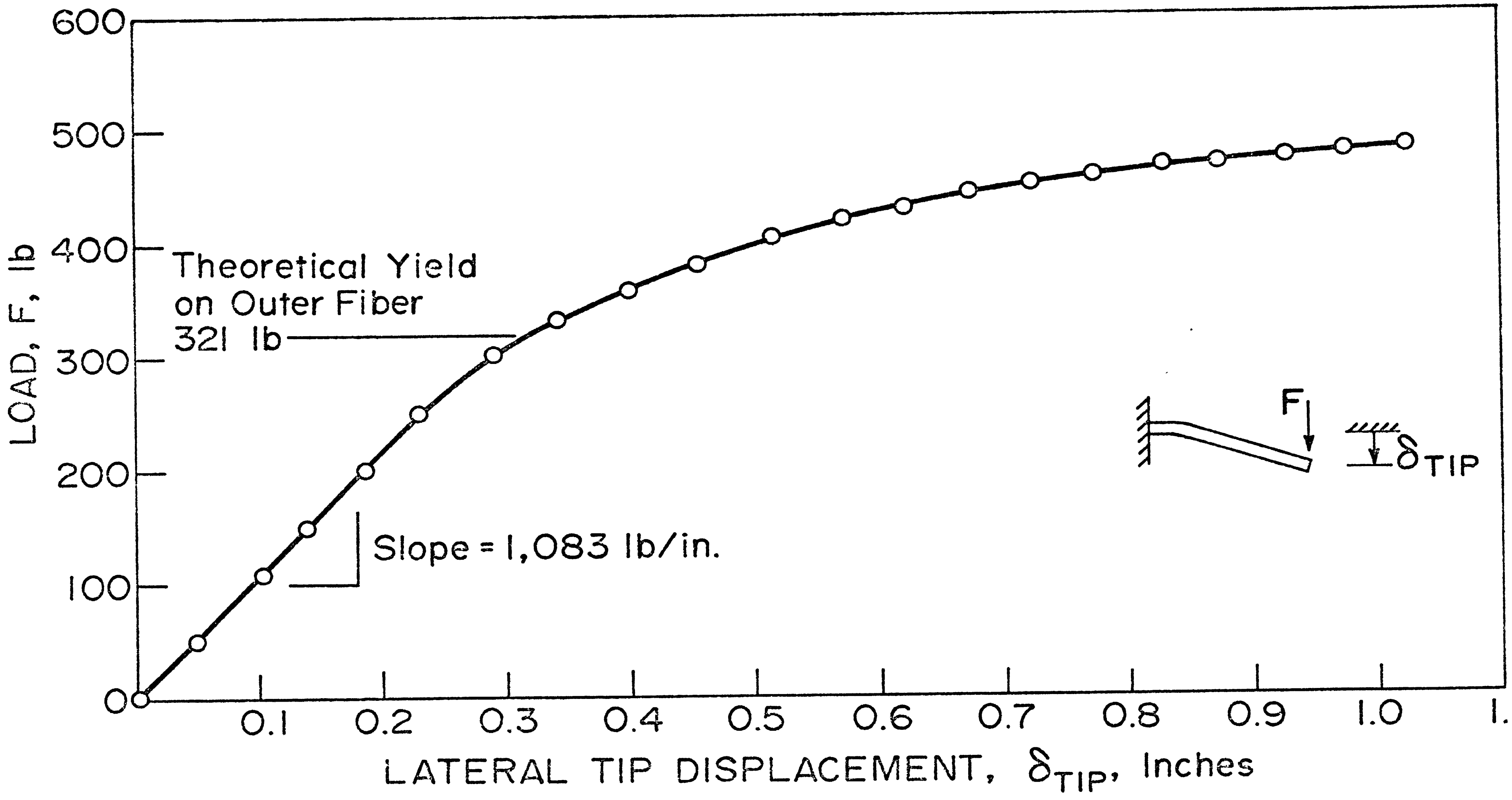

Fig. 10 Formation of Plastic Hinge Under Lateral Load

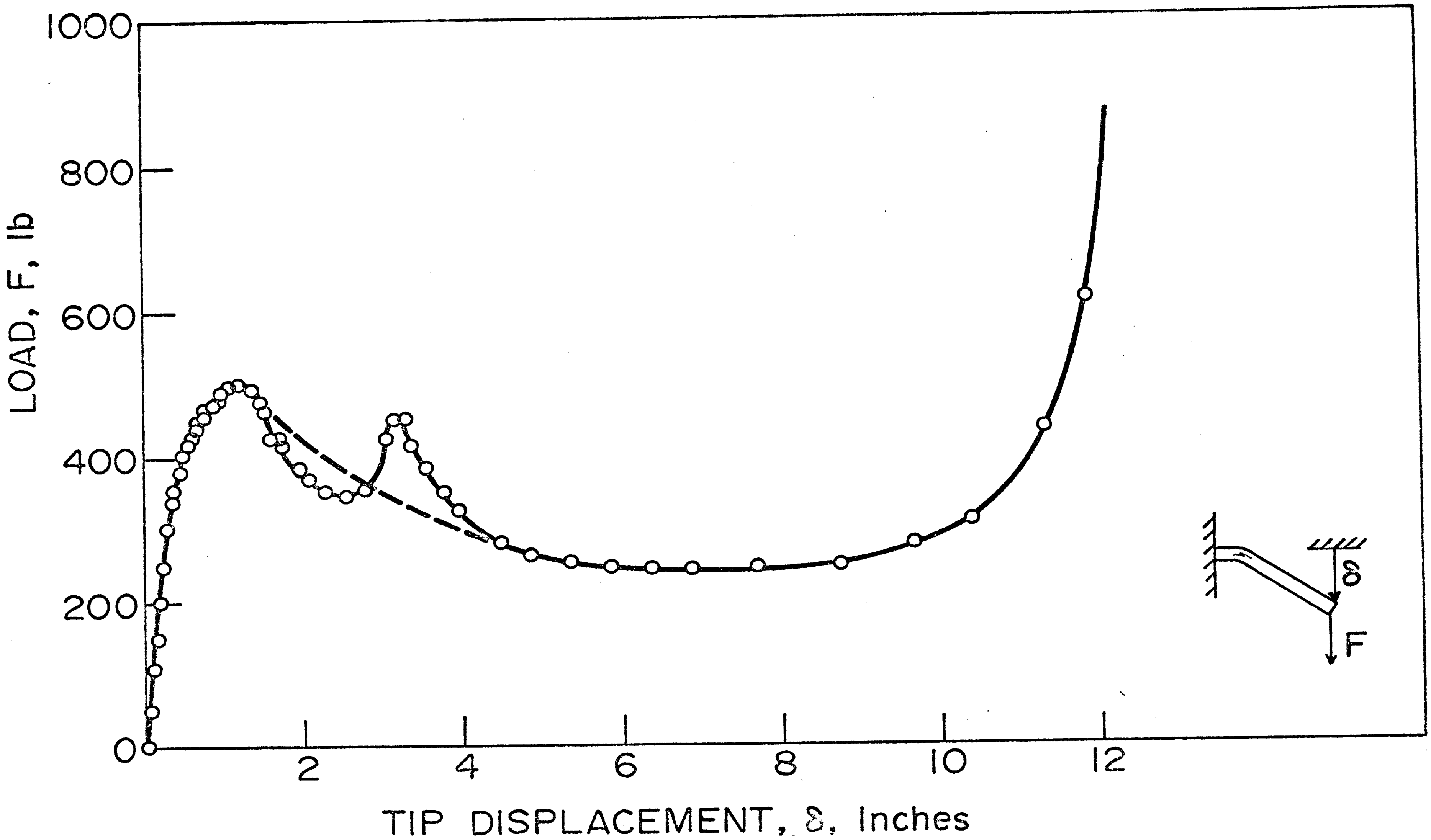

Fig. 11 Large Deflection Under Lateral Load

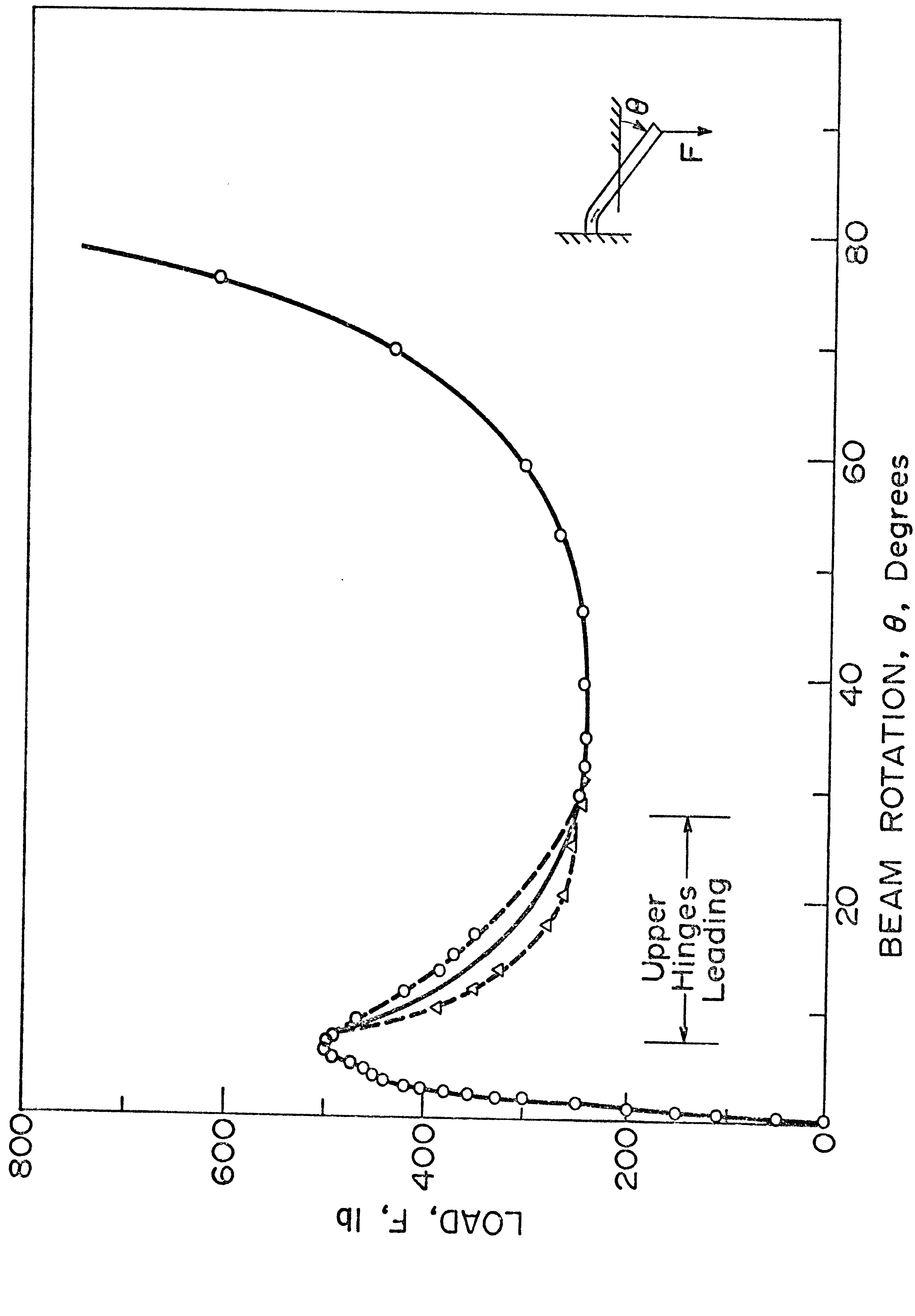

Fig. 12 Rotations Under Lateral Load.

discussed in terms of angular rotations in the next paragraphs. One can propose, however, that the dashed line in Figure 11 represents the true curve for a single beam. The energy absorption should be approximately the same regardless of the order of hinge rotation, and so the area under the solid and dashed lines should be equal. Also, the slope of the dashed line should be one half of that of the experimental value when only half of the hinges were operating in the experiment.

Rotation of each beam was measured at the center of the span of the beam. In the elastic region, this angle is not of much interest, but in the plastic region it is approximately the hinge angle. This is particularly true at low values of load where the outboard portion of the beam became essentially straight. Figure 12 has the same general character as the plot of tip deflection except for the softening range.

It was found that the onset of plastic hinge flow was at 7° of beam rotation. The upper two hinges operated first, until their rotations were 27°. At this time, the system was mildly distorted as in Figure 13. This apparently increased the load needed to operate the upper hinges because of the favorable eccentricity shown in Figure 14. At this point, the lower

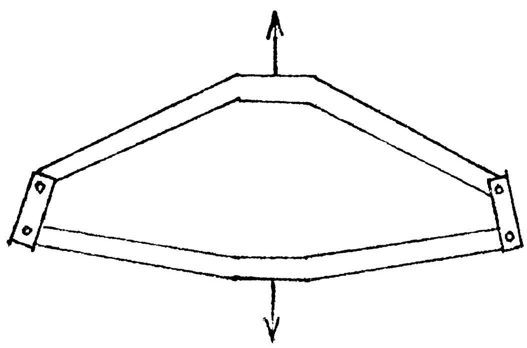

Figure 13. Upper Hinges Leading

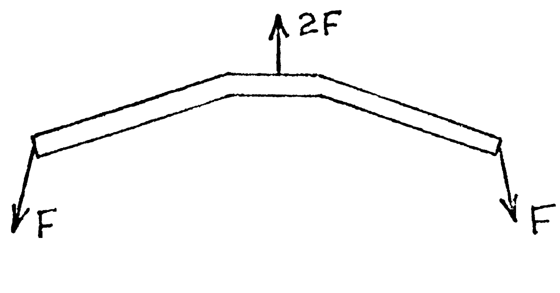

Figure 14. Extreme Position with Upper Hinges Leading

two hinges started to flow and the upper hinges froze. The lower beams rotated from 7° to 27° and all was well again! The loads required to operate the lower hinges were reduced somewhat, apparently due to adverse eccentricity, as in Figure 15.

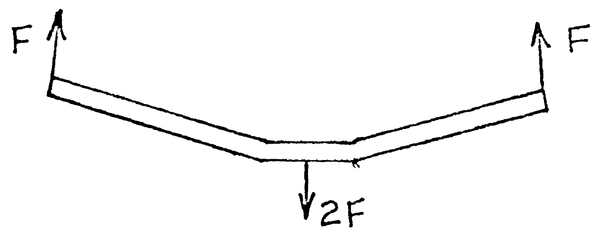

Figure 15. Lower Hinges "Catching Up"

Details of the locus of the loading cycle are shown in Figure 16. The mean value shown is the suggested true curve for a single beam. The effect of this unusual loading cycle seemed confined to the region of 7° to 27°. At higher rotations, all four hinges acted at the same angles. It is felt, therefore, that the results are rather accurate in spite of this phenomenon.

The flexibility of the integrally milled center section can be accounted for in the data reduction. This flexibility in the experiment causes an apparent reduction of lateral stiffness of the beam specimen in the elastic range. Accounting for displacements and rotations at the root of the cantilever specimen, one has

$$\delta_{true} = \delta_{exp} - (2.96 \times 10^{-6} + 68.05 \times 10^{-6} \cos \theta) F$$

This correction yields a lateral stiffness for the beam in the elastic region of 1,179 lb/in, an increase of 10%. This still falls short of the theoretical value of 1450 lb/in and the remaining difference is due to support flexibility. These extraneous sources of flexibility will not be removed from the data because they are not important in the large deflection region.

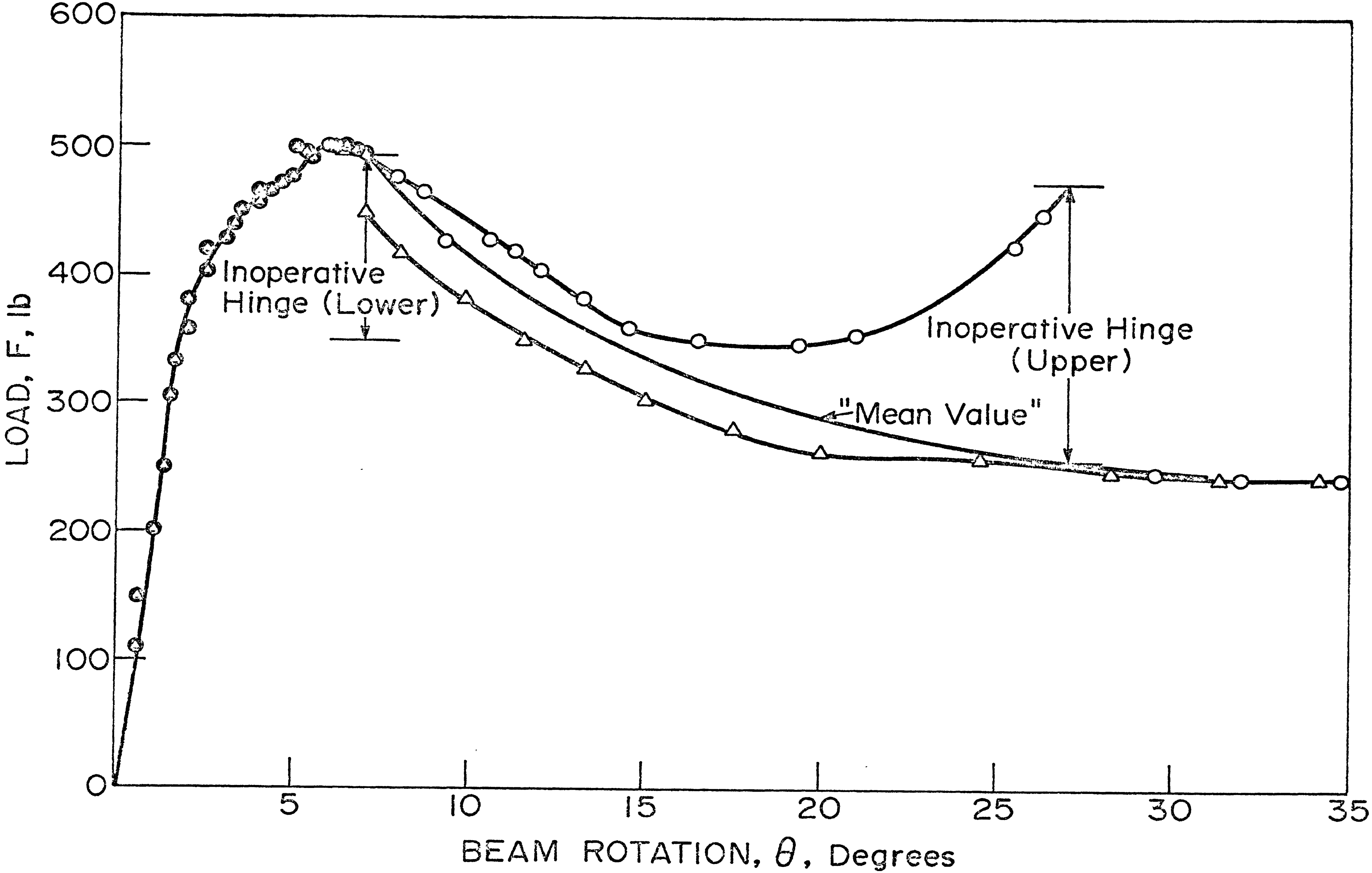

Fig. 16 Locus of Loading Cycle

The hinge, which forms approximately 3/4" from the root of the beam, is characterized by large distortion of the cross section. The specimens have been arranged so that the free edge of the channel is in compression. At the hinge, these free edges buckle outward as plastic flow progresses (Fig. 17). Detailed data of the progressing cross-sectional distortion were not taken. This geometrical effect severely weakens the beam and is responsible for the marked softening of the beam at large deflections.

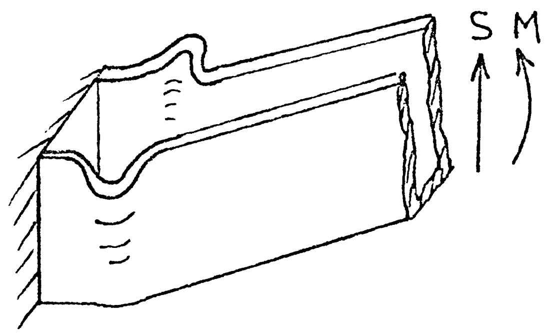

Fig. 17. Plastic Hinge in Thin-Walled Channel.

3.6 TEST RESULTS FOR AXIAL LOAD

The experimental quantities measured in the axial loading case (Figure 9) were applied load P, lateral displacement δ, axial displacement β and beam rotation θ. Again, no detailed measurements of cross-sectional changes at the hinge were made.

The initial "bow" in the specimens, δ_0, was 0.039". This permanent set resulted from the machining process. It was smaller than desired but did prove sufficient to reduce the buckling load substantially from the predicted Euler value and made the buckling phenomena a more gradual process.

The test was carried out without incident. Figures 18 and 19 show, at different scales, the load-axial displacement relation. The assembly had some slack initially until all bolts were well seated, and then behaved elastically up to 9,000 lbs. The ultimate load of 9,440 lb. will be referred to as the buckling load. As this load was reached, increasingly large lateral displacements resulted, with simultaneous formation of plastic hinges. It is not possible to tell from the experiment alone what proportion of the softening exhibited by the system near the buckling load is due to geometrical effects and what part is due to material softening. Both apparently play a role. The system shows softening character at all loads above the buckling load.

The axial stiffness of the system in this linearly elastic range (best seen in Figure 18) was 387,000 lb./in. A simple calculation (neglecting the small effect of the bow on axial stiffness) shows an expected speciment stiffness of 832,000 lb./in. This means that the end fixtures, bolts, etc., were responsible for 53 percent of the elastic axial flexibility, and indicates how difficult it is to obtain a perfectly rigid axial support. If desired, this support flexibility can be removed from the β measurement by:

$$\beta_{true} = \beta_{measured} - 1.382 \times 10^{-6} P$$

where β is in inches and P is in pounds. This correction will be made later in comparing theory and experiment in the elastic range. The correction is very small and never exceeds 0.013".

Lateral displacement is given in Figures 20 and 21. These figures confirm the axial displacement observations and indicate the softening character of the structure.

The angle of rotation of the specimens is studied in Figure 22. Because of the constraining effect of the cover plates, all four hinges operated at the same angle, $\pm 1/2^{\circ}$. The experiment was terminated at 78° because of mechanical interference. Up to this angle no hardening of the system had occurred; however, this would be expected near 90° as the beam column flattens against loading surfaces.

The present axial loading test can be compared with the previous lateral loading test at one point. When the hinge angle θ is 45°, the two cases have the same bending moment at the root and differ only in the axial force. If the axial force is small, then the loads P required to rotate the hinge should be

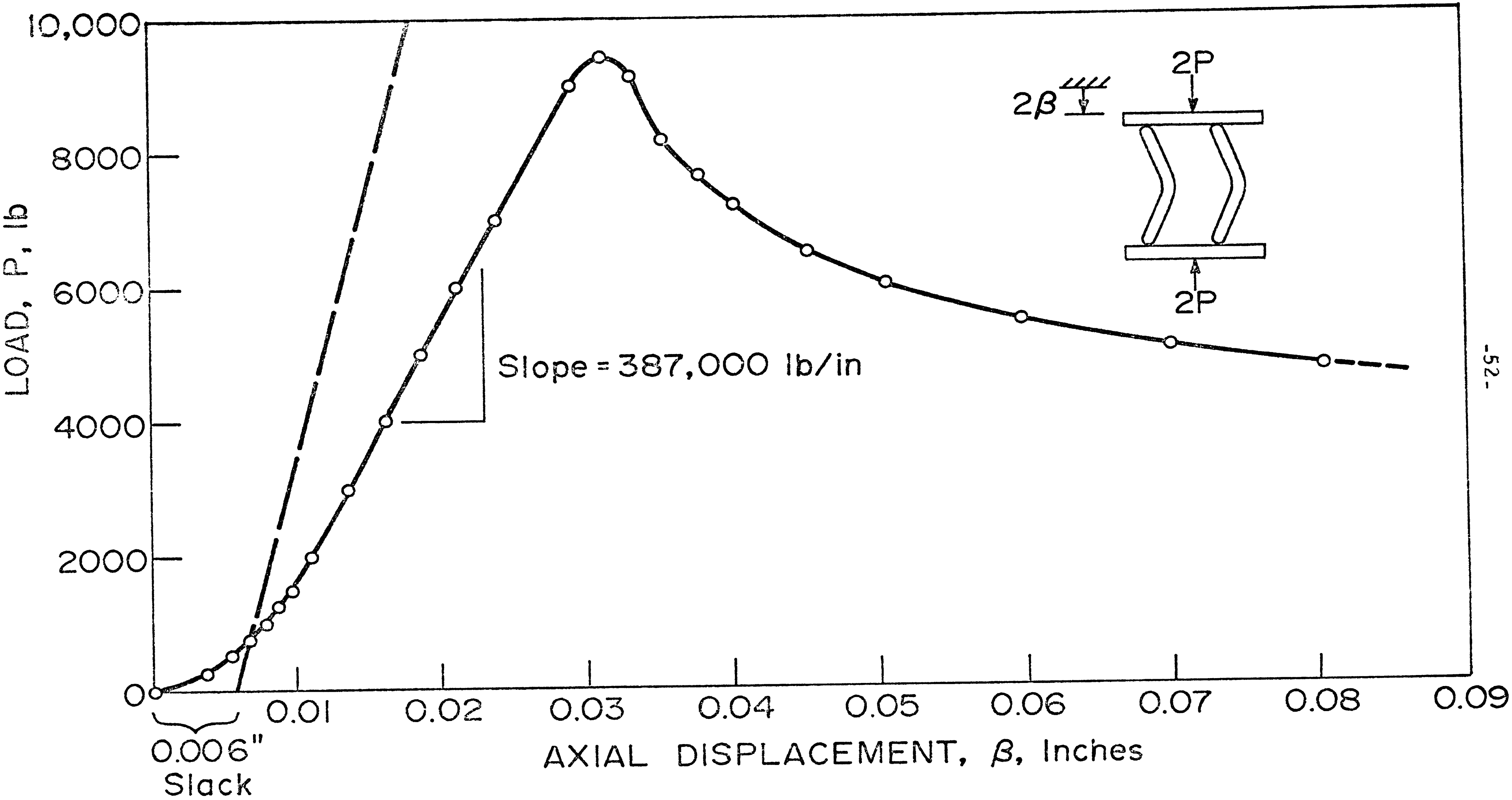

Fig. 18 Axial Loading Test - Small Axial Displacement

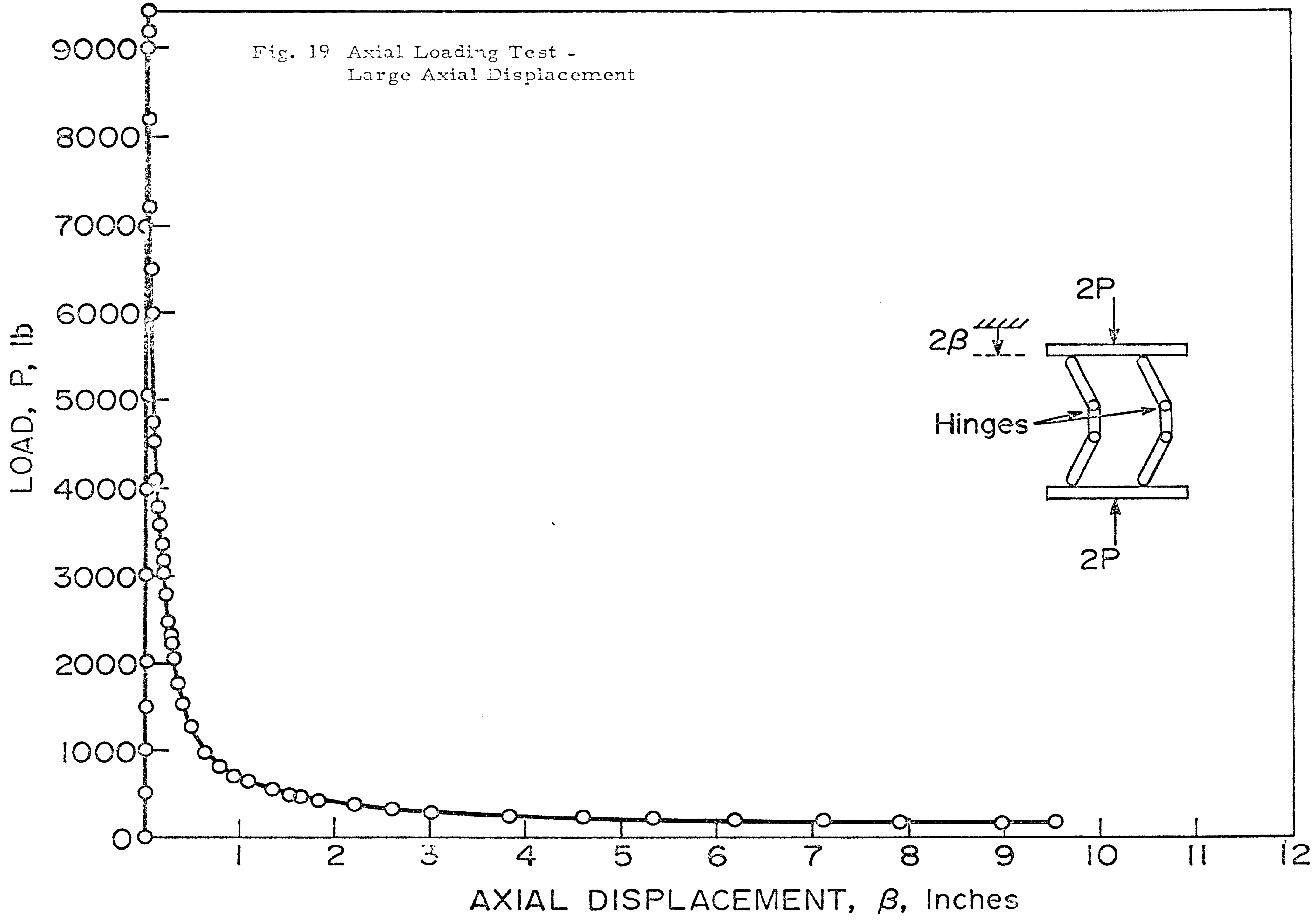

Fig. 19 Axial Loading Test - Large Axial Displacement

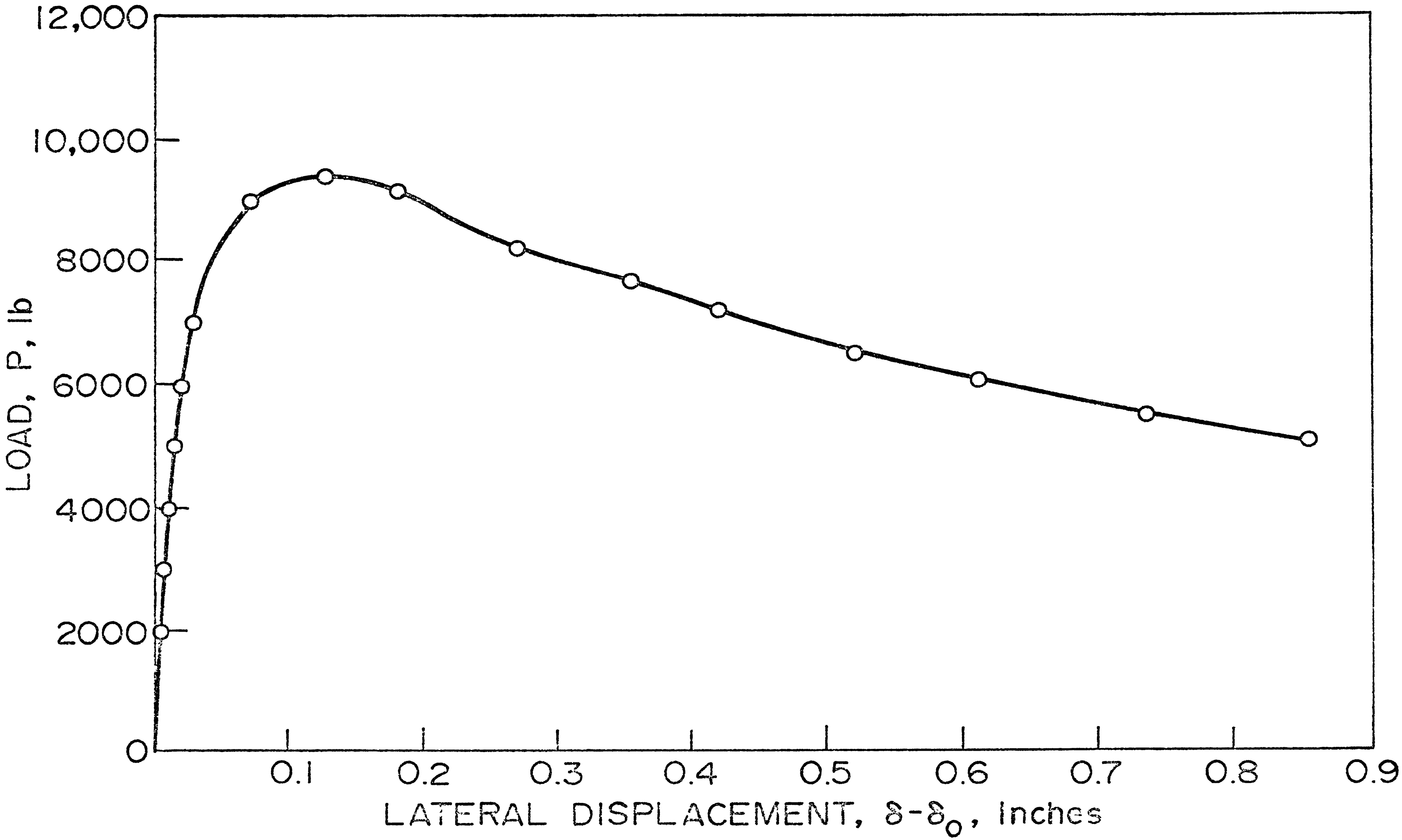

Fig. 20 Axial Loading Test - Small Lateral Displacement
(Measured from Unloaded State)

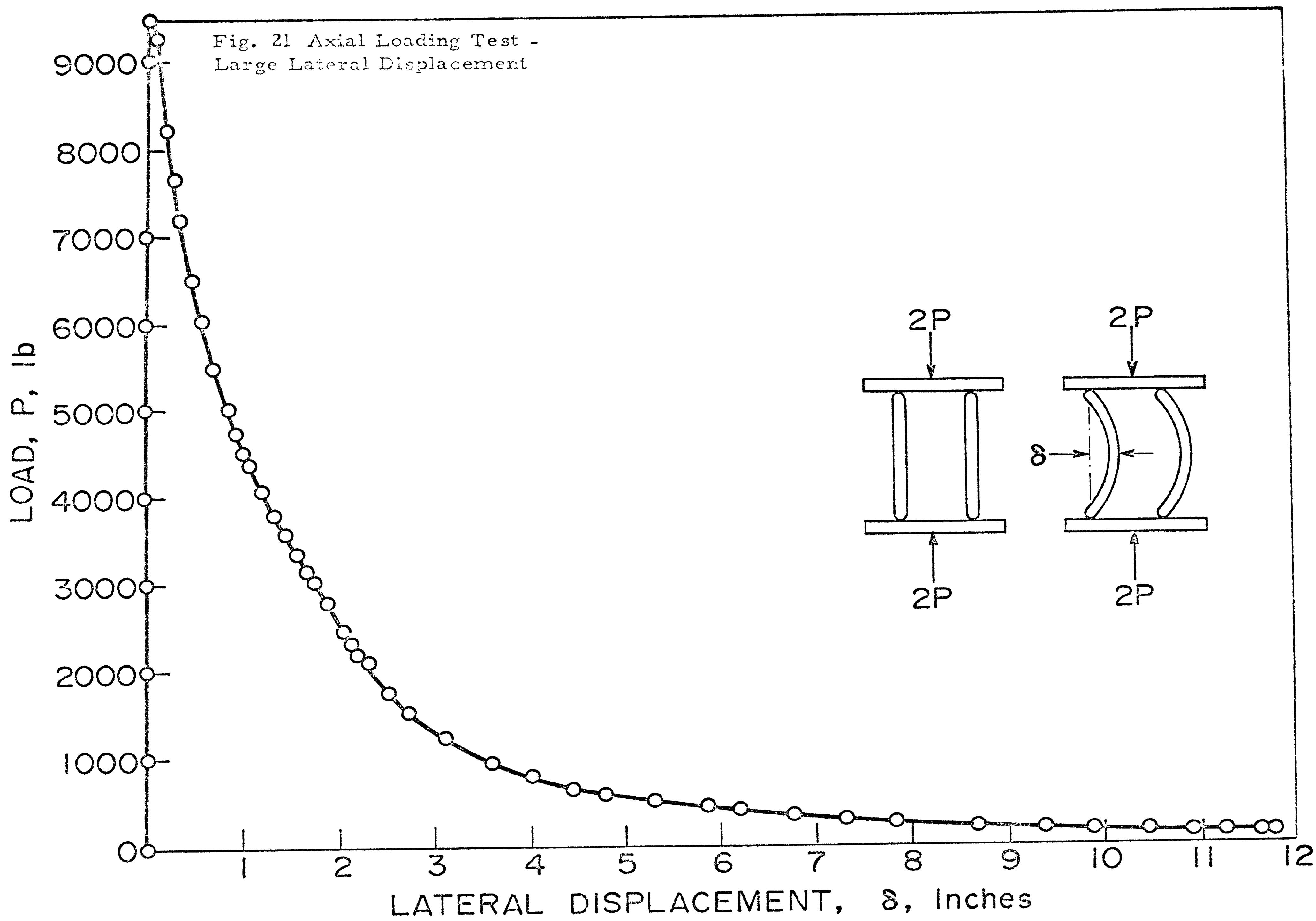

Fig. 21 Axial Loading Test - Large Lateral Displacement

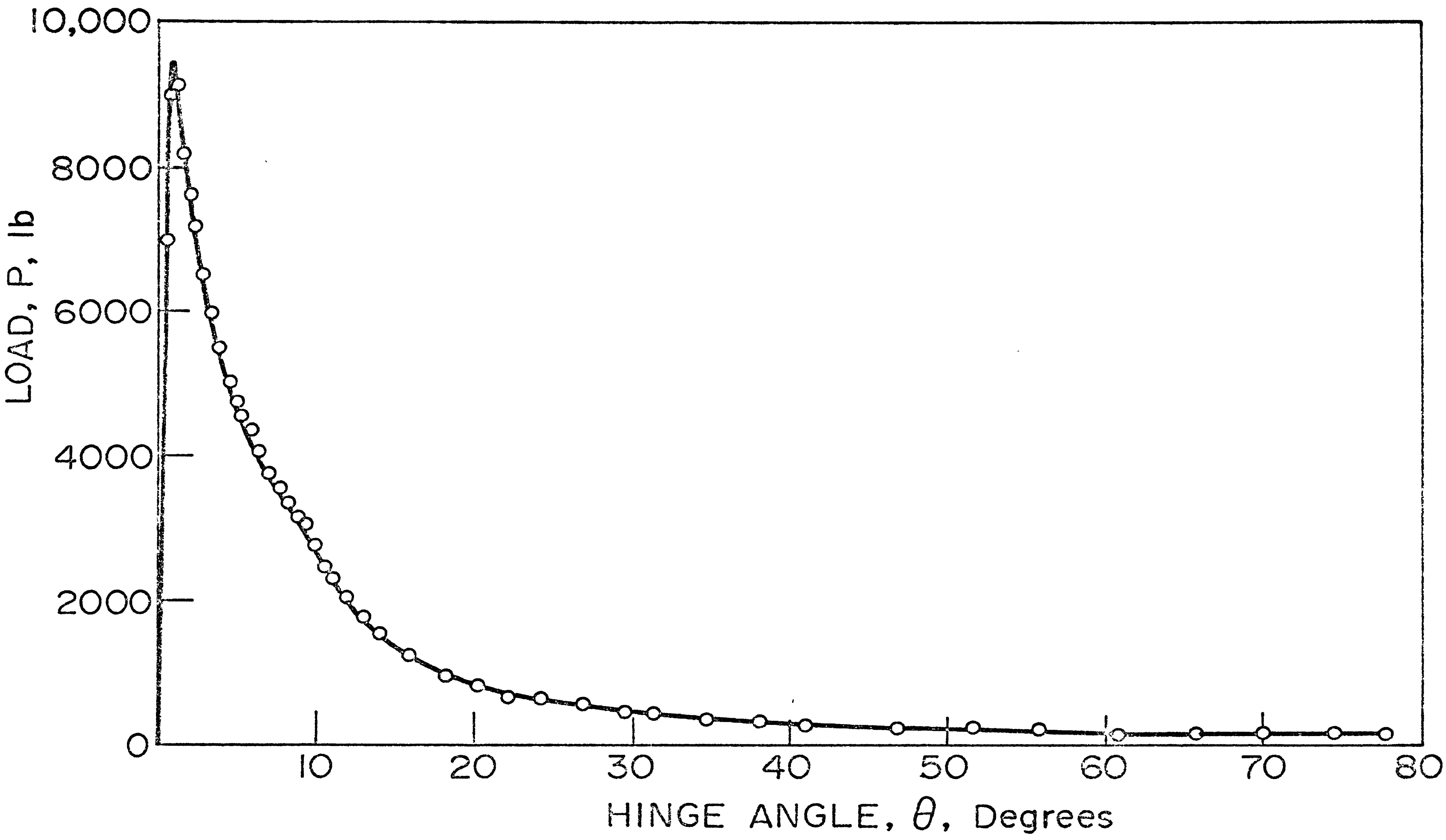

Fig. 22 Axial Loading Test - Hinge Angle

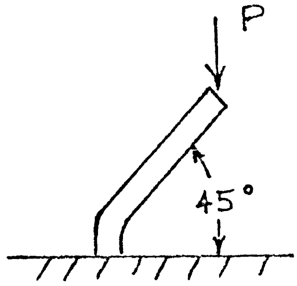

Axial Test

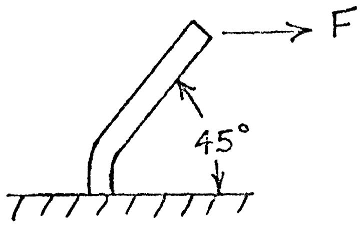

Lateral Test

Fig. 23.

about the same. Figure 24 shows that the loads P and F are equal at an angle of 46° and the difference in P and F at 45° is only 10 lb. This furnishes a remarkable check on the consistency of load and angle measurement.

3.7 LOAD RELAXATION DATA

A load-relaxation phenomena was found in the softening region of hinge rotation. This was noted in both tests, but data were taken only for the axial load case where it seemed more severe. As an increment in compressive axial displacement was made, the load incremented to a new value. For several minutes thereafter, however, the load would creep down to even lower values. This relaxation occurred with no additional axial displacement (demonstrating the rigidity of the test machine) and with zero or very slight lateral displacements.

Figure 25 shows several observations. A straight-line relationship on semi-log paper was found for all eight cases measured. Readings were taken up to eight minutes after the displacement increment. The data presented represents behavior at moderate times after the increment in axial displacement was made. Very short time data were impossible to record from dial gages and would tend to follow some other law. Long time data would surely show the load leveling off because of fixed end displacement (the process cannot extend indefinitely or negative loads result).

The slopes of the lines in Figure 25 represent the rapidity of the relaxation. This slope depends on the initial load on the column at the tir the increment in axial displacement was made. At higher stresses, the relaxation proceeds more quickly. Figure 26 shows the dependence of the relaxation on initial load P_0. For loads up to 5, 500 lb., this is of a straight-line character. Combining results of Figures 24 and 26, one obtains an empirically derived equation

$$P - P_0 = \text{const.} - 0.0172\, P_0 \log(t-t_0)$$

where P_0 and t_0 are the conditions at the start of the observation, and were read as quickly as possible after the displacement increment. The constant changes from case to case and its dependence on P_0 and t_0 are not known.

The full significance of the load relaxation is not apparent at this time. It occurs at a slow enough time scale to affect measurements which are normally considered static. It is believed that the experimentalist must be aware of this phenomena and carefully record the rates of loading when plastic hinge formation is in progress. This will allow later interpretation of the procedure.

3.8 COMPARISON OF BEAM-COLUMN ELEMENT WITH EXPERIMENT

The computer model of the beam-column element will now be compared with the results from the lateral and axial tests. In general, the results demonstrate the validity of the plastic hinge concept, but suggest a number of refinements to incorporate in a second generation simulation.

Figure 27 shows a comparison of computed results with the lateral test. The lowest computed curve is based on a yield stress of 78,700 psi, which was determined in the uniaxial material test. The model predicts elastic behavior up to 381 lbs. at which time a hinge forms. As deformation proceeds, a gradual hardening occurs due to geometric changes in configuration. For large deformation this hardening becomes marked.

Given the limitations of the plastic hinge concept, the agreement is reasonable. There are two considerations in making the comparison. The first is an inherent feature of plastic hinge theory; the hinge is either operative and fully plastic or no plastic deformati·n occurs. Thus, a plastic hinge

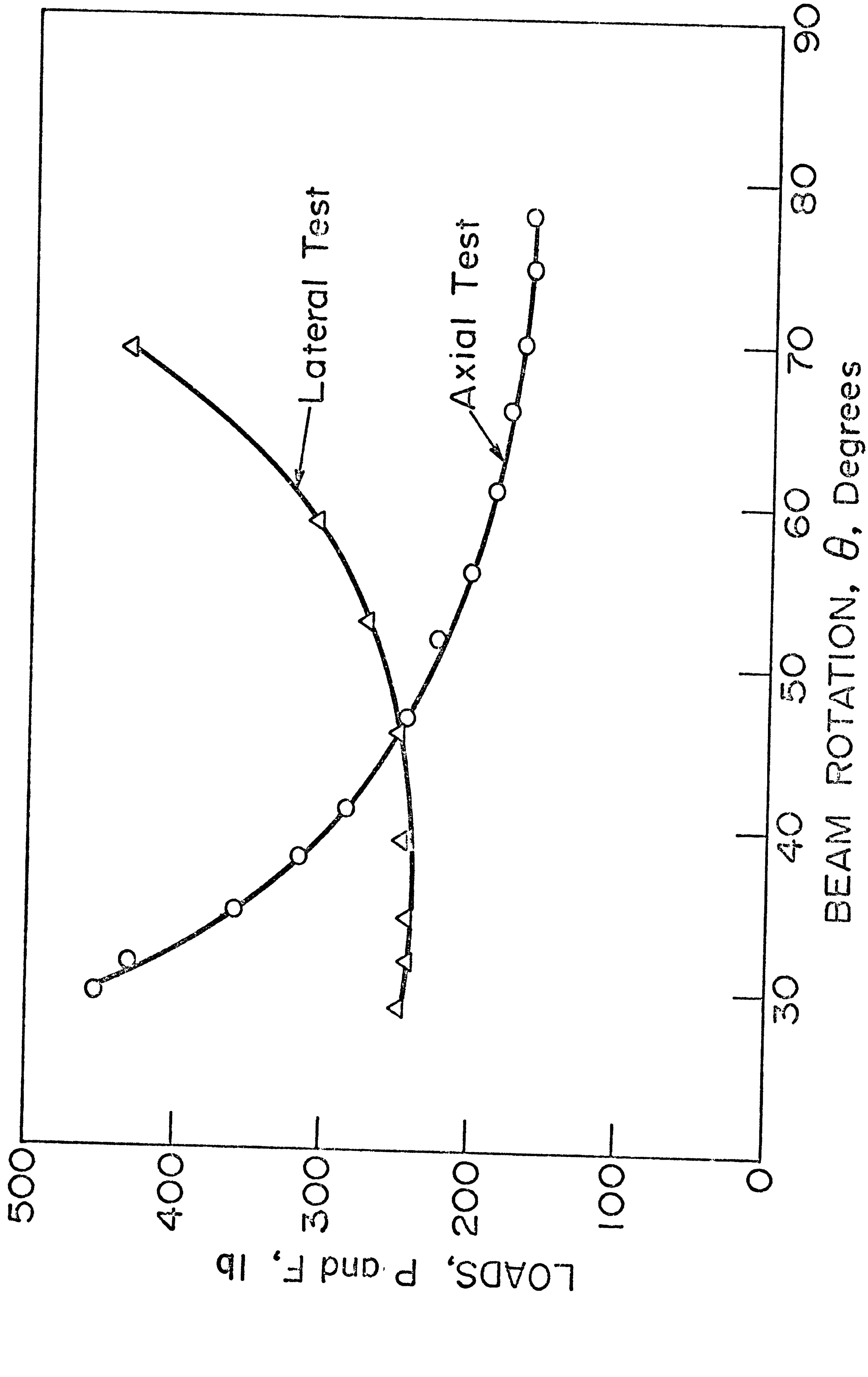

Fig. 24 Comparison of Lateral and Axial Tests for Consistency

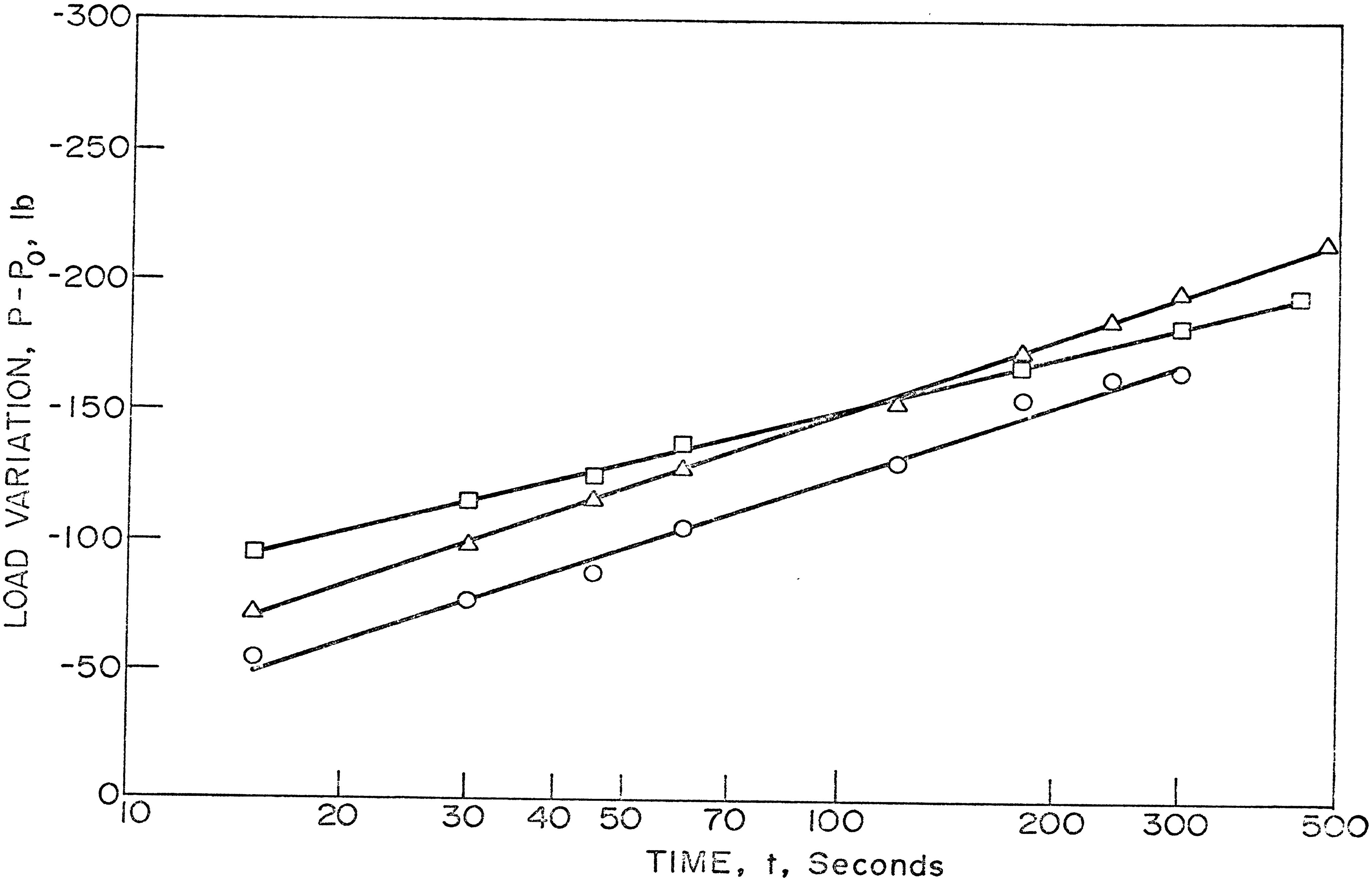

Fig. 25 Load Relaxation

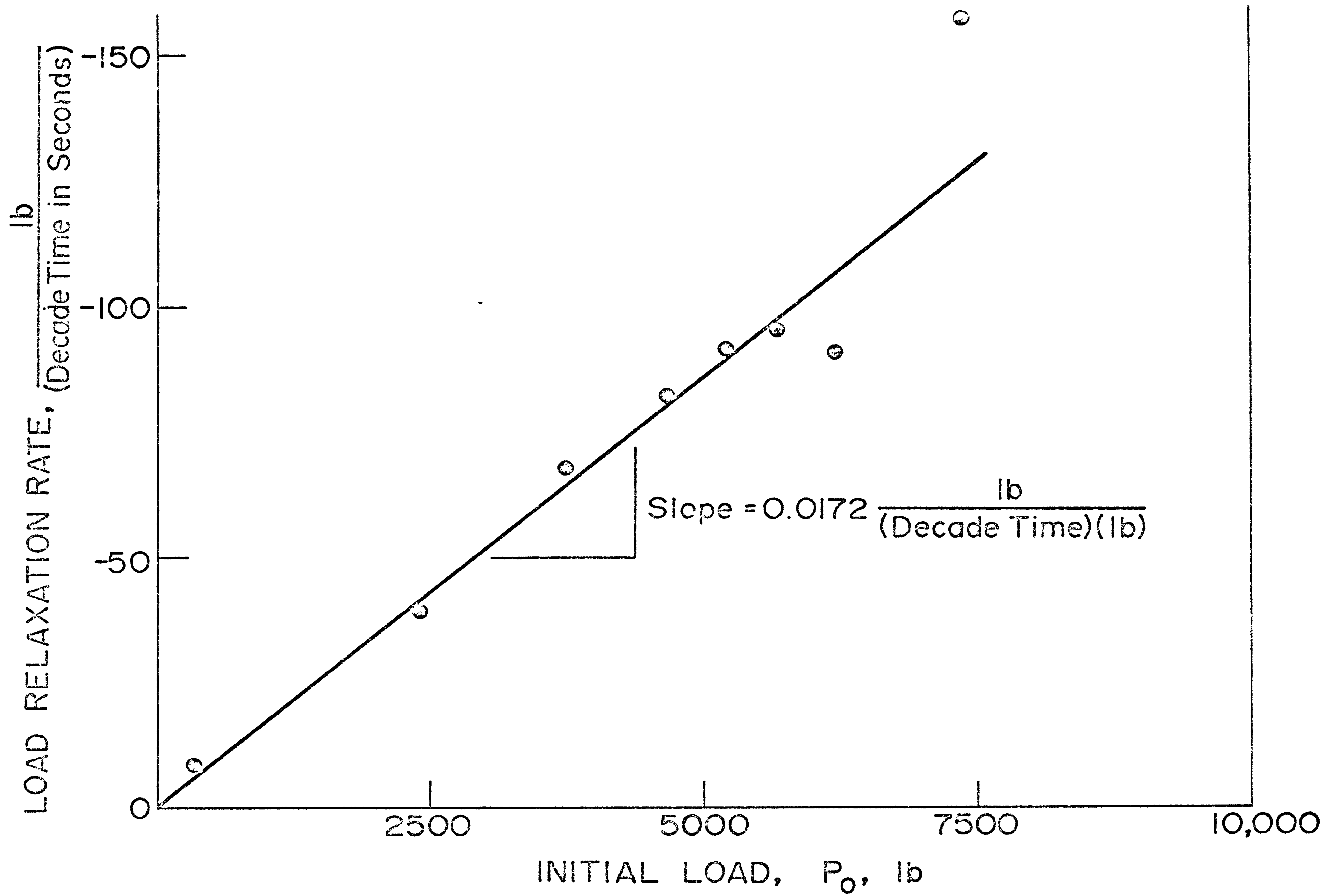

Fig. 26 Rate of Load Relaxation in Axial Test

cannot model elastic-plastic behavior at a cross-section. In the model, the yield condition for hinge operation is based on initial yield. Actually, agreement with the experiment is excellent. The hinge forms at the load for which the experimental result begins to deviate from linearity. The increase in load from 275 lbs. to 500 lbs. in the test is due to elastic-plastic behavior of the cross-section. (For this section the ratio of ultimate moment to moment at initial yield in pure bending can be calculated as 1.81 and was measured as 1.8.)

To account for this elastic-plastic effect, an inflated yield stress may be employed in the yield function. This is demonstrated by the second computed curve which used a yield stress of 90,000 psi. This delays the formation of the hinge until an intermediate load value between actual initial yield and full plasticity of the cross-section.

The second consideration is the marked softening of the structure after the ultimate load is reached. This softening is not predicted by the model. This result demonstrates the importance of local deformation of the cross-section for real structures. In the experiment, changes in cross-section shape were visually observable around the ultimate load. This local deformation became increasingly marked as deformation proceeded. It is clear that if exact detail of the force-deformation curve is required over a broad range of deformation, local deformation must be taken into account.

Within plastic hinge theory there is no rigorous analytical method to incorporate this effect. It is worth noting, however, that the theoretical yield surface can be modified to give a variety of effects. This is illustrated in Figure 28 which again shows the experimental curve and two computed curves. The results are rather dramatic, the model now showing a softening effect very similar to the test. This was achieved by using a yield stress to initiate the hinge at the ultimate load and changing by an order of magnitude one of the parameters in the theoretical yield function. The hardening in the second computed result was achieved by returning this parameter to its original value at an arbitrary point in the computation. It must be emphasized that there is no rational basis for this procedure. Nevertheless, it is interesting to speculate that it might be possible to define a "failure function" which would incorporate in an approximate way both plastic and local deformation effects. This possibility merits further study.

The comparison for the axial test is complicated by the fact that the current computer model is limited to slope imperfections θ_0 greater than .02 radians. The experimental imperfection was .003 radians, which is an order of magnitude less than the simulated results. The approach used will be to view θ_0 as a parameter and show families of curves.

Results for axial load vs. lateral deflection are shown in Figure 29. In the initial elastic range the slope of the curve is theoretically inversely proportional to the initial imperfection. This is evident in the figure. The experimental data have not been corrected for support flexibility because this correction is small and important only in the elastic range. Behavior of experiment and model in the plastic range is very similar in character. The model, of course, demonstrates a discontinuity associated with the off-on nature of a plastic hinge, whereas the experiment has a gradual transition due to elastic-plastic action of the cross-section. Nevertheless, the model appears to adequately predict the softening character of the column in the plastic range.

In Figure 30 the results for axial load vs. axial deflection are given. For a perfectly straight column the elastic slope of this curve should be the axial stiffness of the rod. This slope, however, is also affected by initial imperfections since axial displacement is induced by bending as well as contraction of the column. As the initial imperfection tends to zero, the slope should approach the axial stiffness of 832,000 lb./in. The experimental results in this case have been corrected to this value of 832,000 lb./in., eliminating the flexibility of supports (as well as the very small imperfection) entirely.

In other respects, Figure 30 confirms our conclusions from the previous figure. There is a marked resemblance between the experimental and computed nature of the softening in the force-deformation curve. Thus, we conclude that the basic theory on which the model is based is adequate for representing force-deformation curves in the large deformation plastic range.

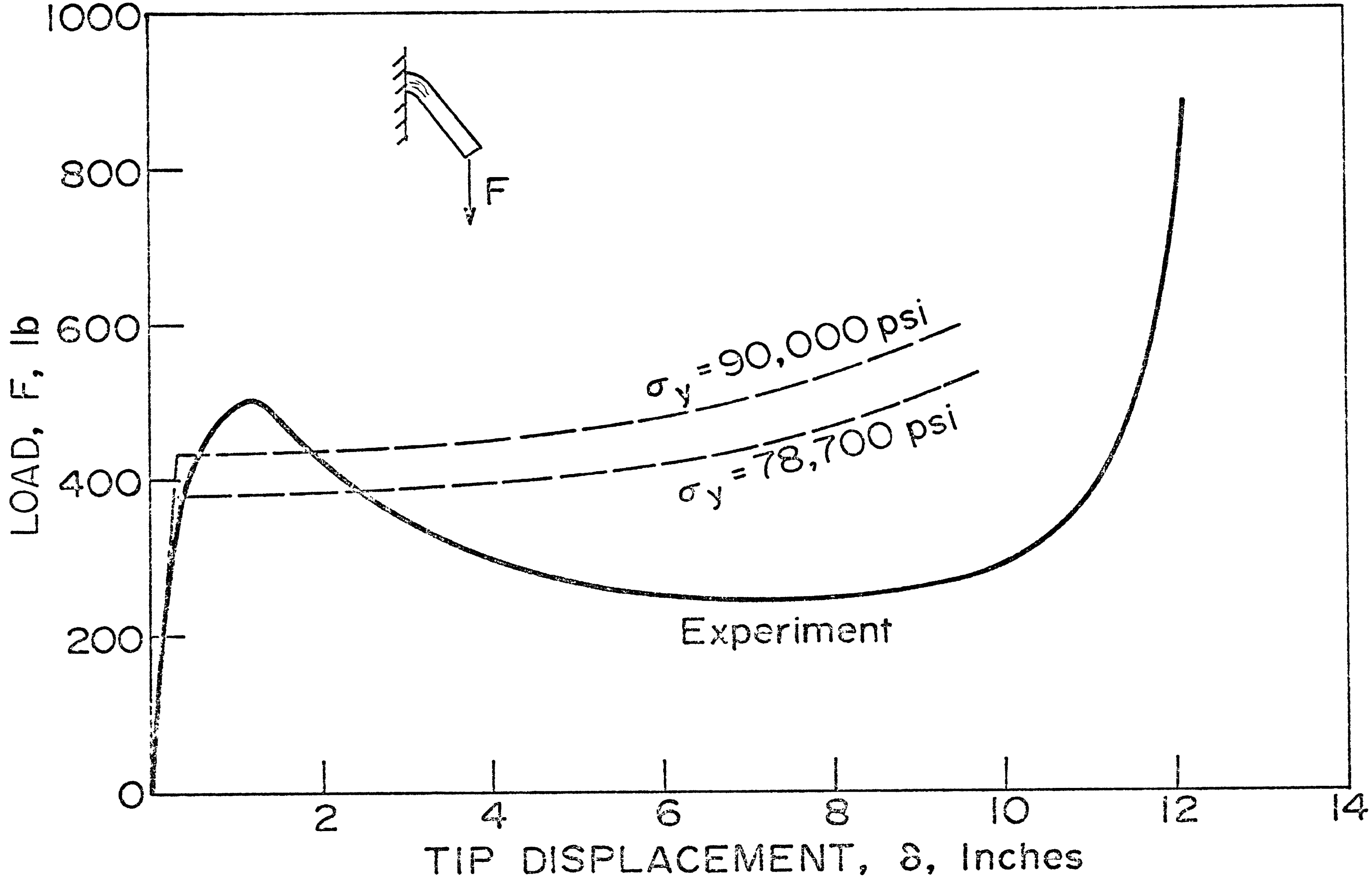

Fig. 27 Beam-Column Element Under Lateral Load

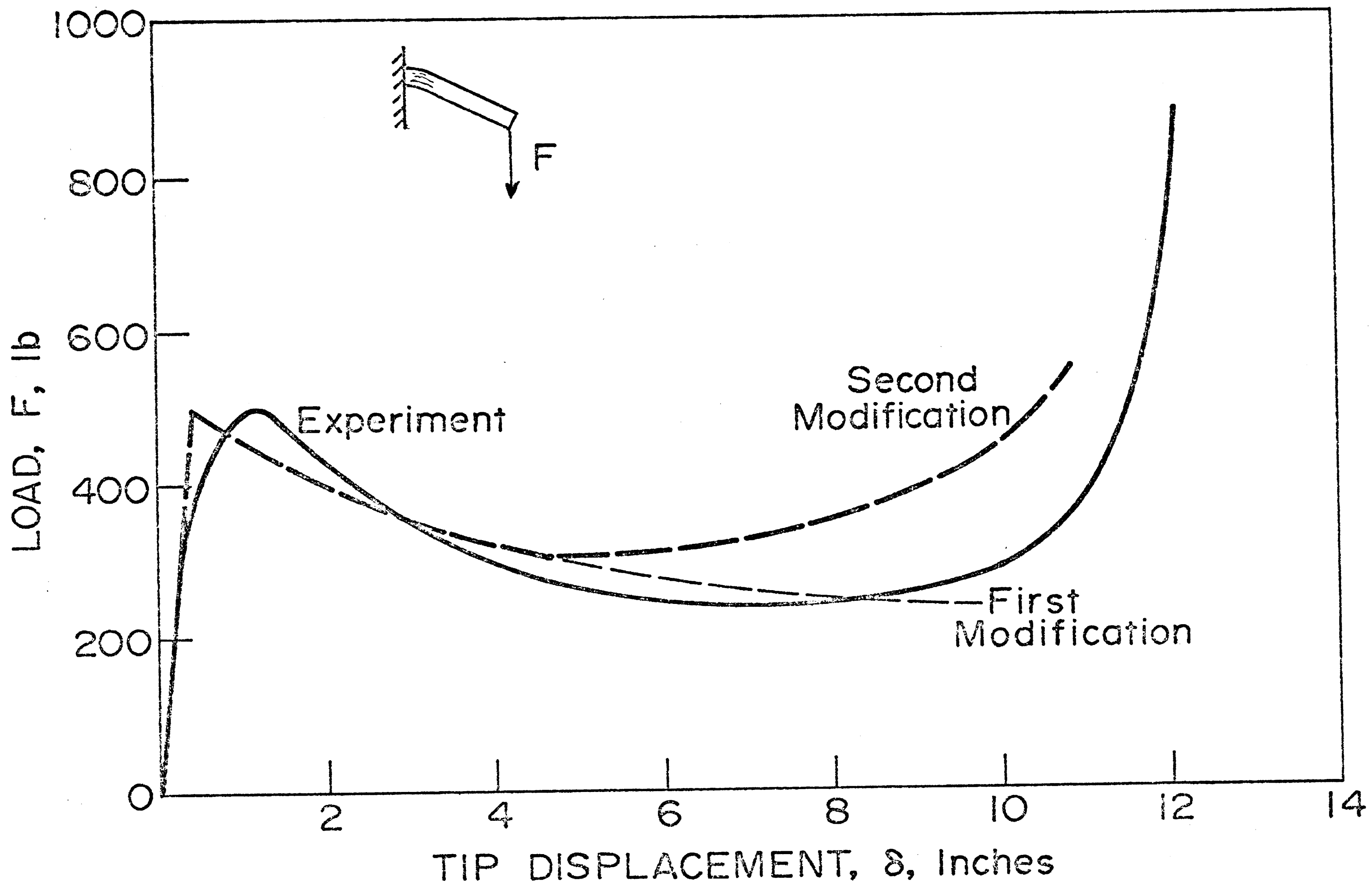

Fig. 28 Modified Models of Beam Under Lateral Load

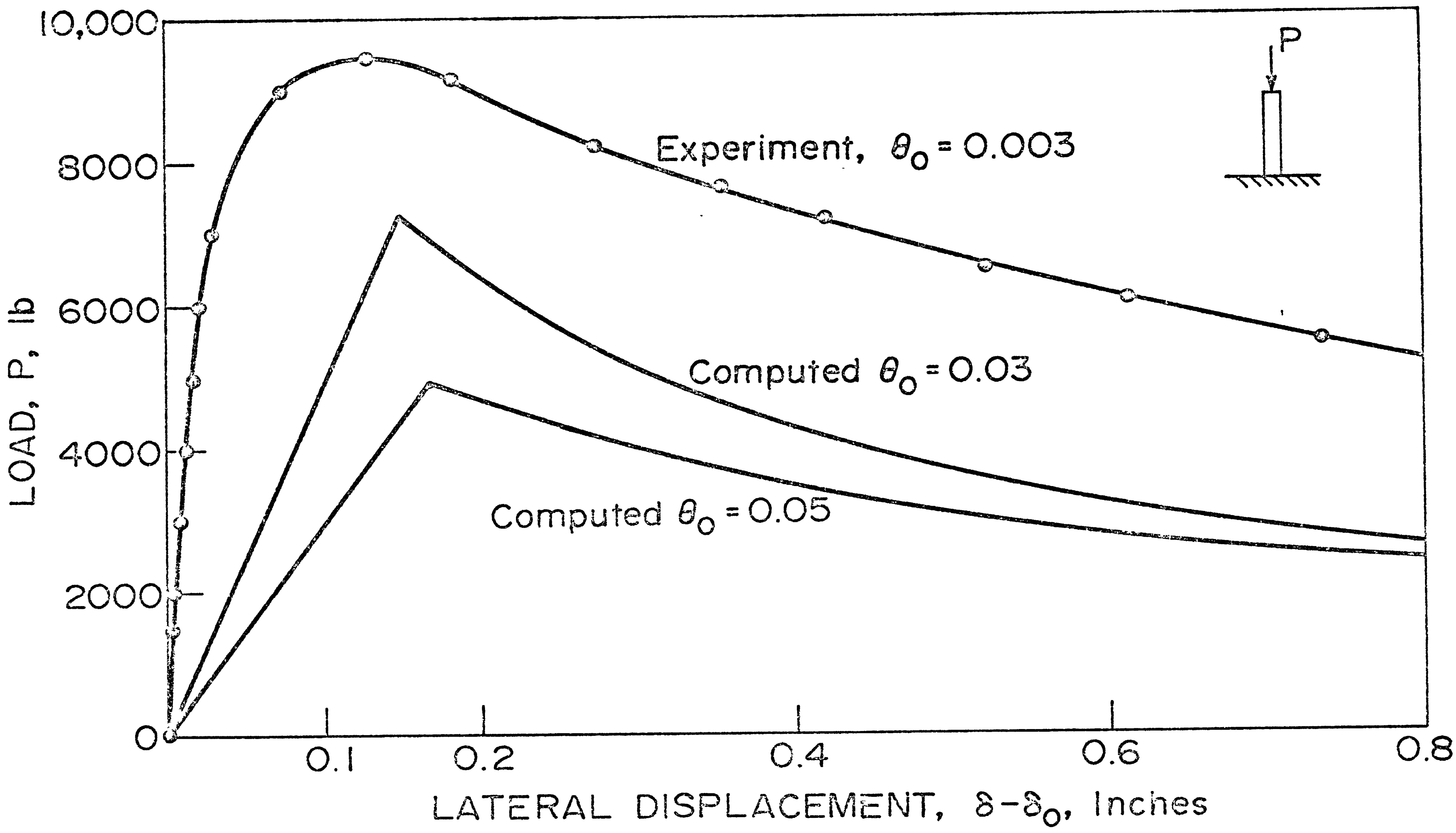

Fig. 29 Comparison of Model with Lateral Displacement

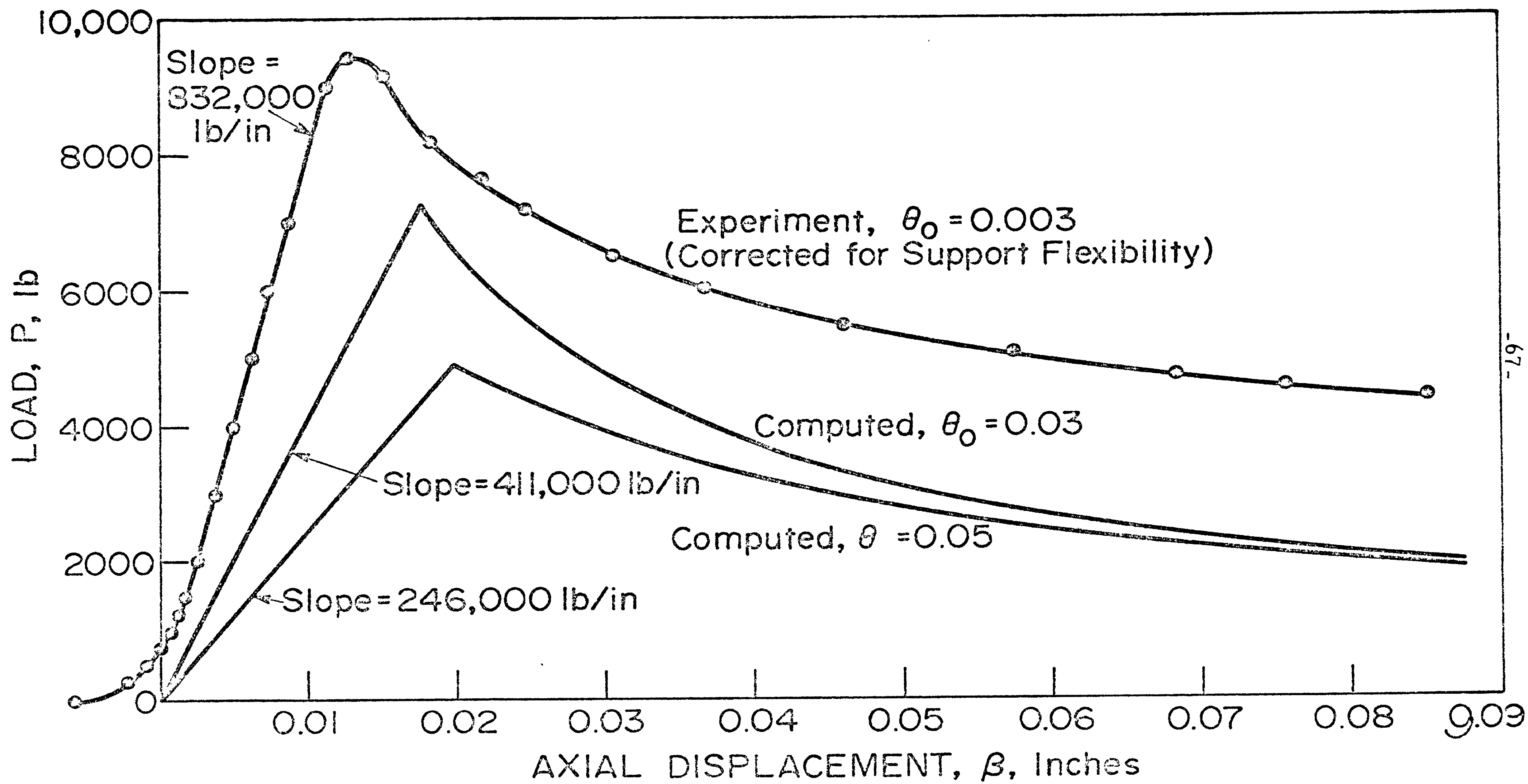

Fig. 30 Comparison of Model with Axial Displacement

3.9 SUMMARY

The experiment provides useful data for comparing with the plastic hinge model. The specimens were carefully made and tested and excellent consistency found at one coincidental data point. Support flexibility enters into the results in a small way, but is understood and can be completely removed if desired. Future, more advanced theories can also be compared with these tests.

The current computer model for the beam-column element checks out well against the experiment. Several areas of possible improvement have been noted for future development.

CHAPTER 4

QUALIFICATION STUDY

4.1 INTRODUCTION

The specific component selected for testing the three-dimensional large deformation elastic-plastic frame model was an automobile frame developed by CALSPAN Corporation. The results of a Pole Barrier Static Crush Test using this frame have been reported by CALSPAN*. This chapter contains the following items:

1) A record of the experience and considerations which arose in modeling the test frame. (Sections 1 and 2). For this purpose, this entire frame was modeled.

2) Numerical simulation of the crush test (Section 3). Because of the nature of the crush test and for computational economy, a reduced version of the frame model was used.

3) Comparison of the simulated force-deflection curve with the experimental force-deflection curve (Section 4).

4.2 SELECTION OF MODEL FRAME LAYOUT

Details regarding the automobile frame were provided by the Contract Technical Manager in the form of blueprints, clearer copies of the photographs of the crush test than which appeared in the above-mentioned CALSPAN report, and some information about material properties of the automobile frame members.

Figure 31 shows a reduced copy of one set of blueprints of the portion of the frame forward of the rear torque box.

A second set of blueprints was provided which contained

---

* Production Feasibility-Crashworthiness Structure,
Full Size Cars (Phase I), Seventh Progress Report
Contract NO. DOT-HS-053-2-487
Project No. ZM-5177-V
CALSPAN Corporation

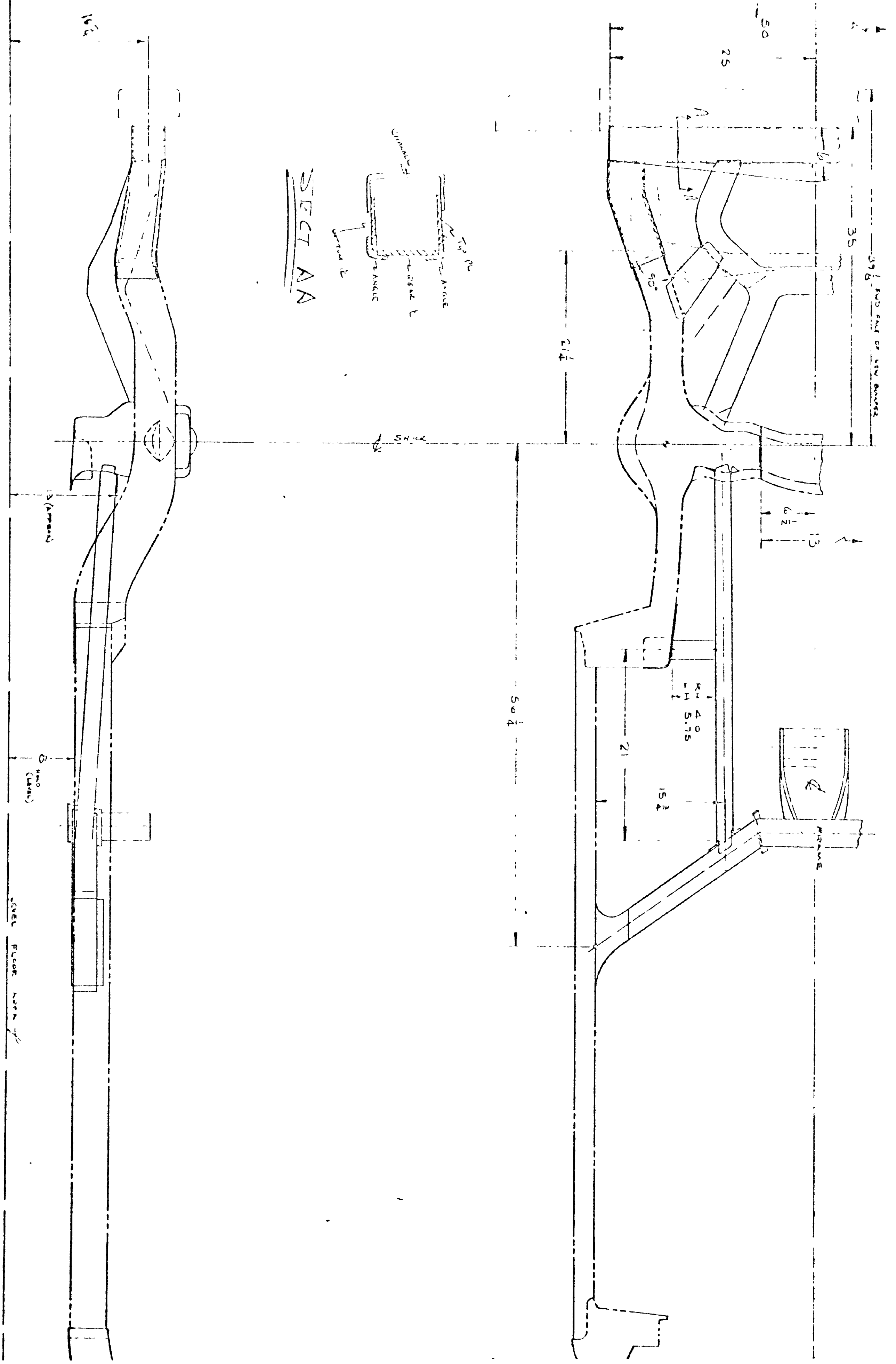

Figure 31

Reduced copy of blueprints of frame tested by CALSPAN.

more details regarding dimensions, cross-sectional properties and material properties.

Figure 1a of reference (*) shows how the frame was supported during the static crush test. A cross beam was welded to the test frame on its side rail just forward of the rear torque box. The cross beam, which is rigidly attached to the loading frame, prevented motion of the frame at its points of attachment. Consequently, the portion of the frame behind this support was never loaded and plays no part in the modeling discussed here. Constraints which could be removed during the test were also attached to the frame at the front wheel supports. Figure 32 of this discussion shows the location of these constraints on the blueprints and also the point at which load was applied to the test frame by the pole barrier.

The side view of the test frame in Figure 31 shows a channel section which is separated from the first cross member. In the test frame, this separation is provided by a piece of crushable foam. The apparent purpose of this foam-channel section assembly is to model the response of a shock absorbing bumper in low speed impacts. This assembly is ignored in the modeling of the test frame.

Selection of the nodal points was based on an understanding of the deformation mechanism of the test frame by a detailed study of its initial configuration and photographs of the crush test. Nodal points were selected for one or more of the following reasons:

1) A nodal point should be placed at the intersection of several frame members.

2) Nodal points are placed at a support or loading constraints, or point of frame symmetry.

3) Nodes were placed at points where intuition and evidence provided by photographs suggests hinges form.

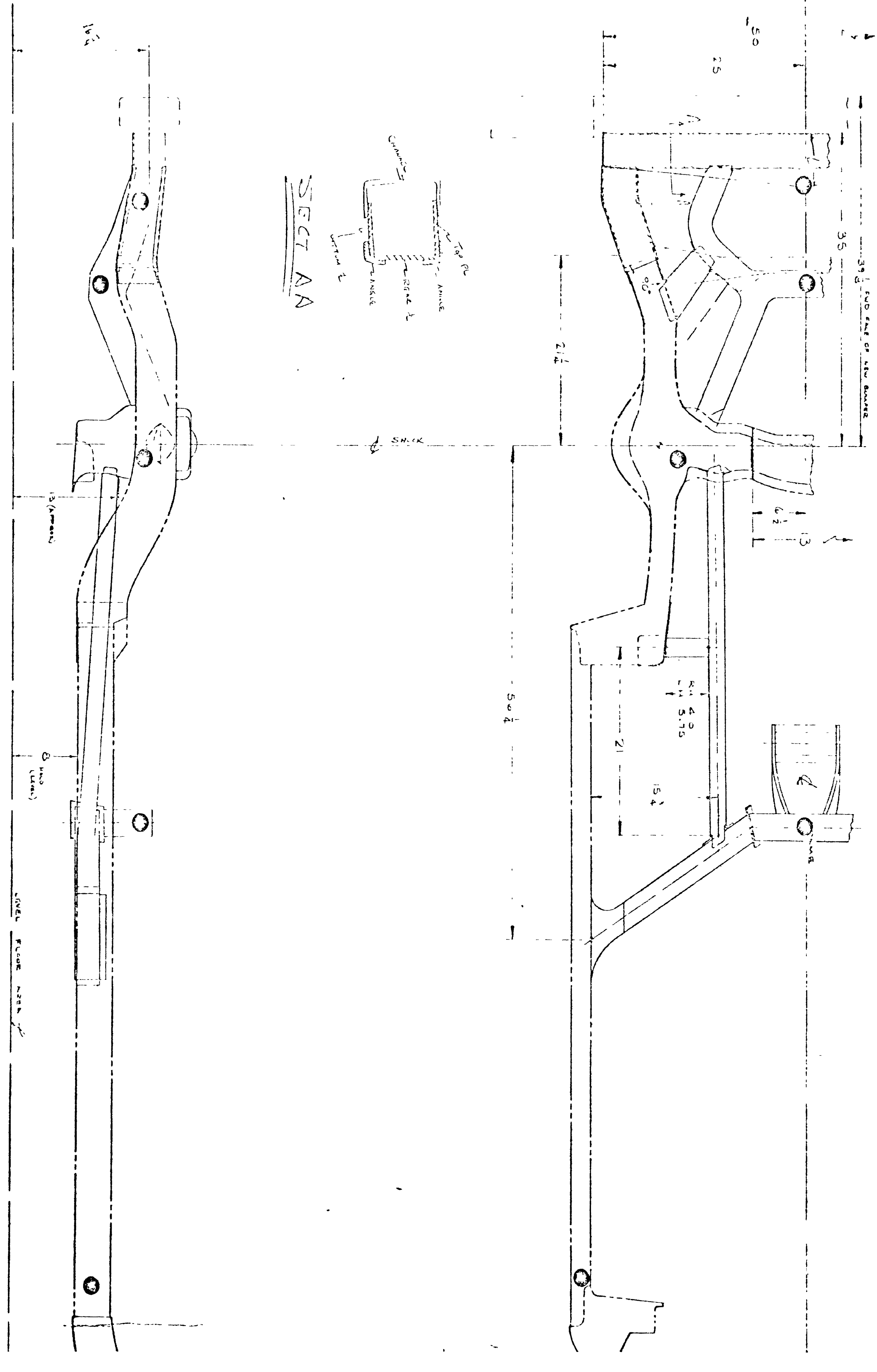

Figure 32

Location of constraints due to loading, symmetry and support.

4) Certain portions of the test frame have a complicated shape which could only be approximated by an equivalent beam structure. Nodal points were selected with the approximation in mind.

The frame model consists of 26 nodes and 34 beams. Figure 33 shows the location of the nodes and their numbers. Figure 34 contains an isometric view showing the nodes and beams of the idealized frame. Unless specified differently in the following discussion, all nodes are located on beam centerlines. The reasons for selecting each node is as follows:

Node Number	Bases For Selection
1	This is placed where the axis of symmetry intersects the first cross member.
2, 3	These are placed where the first cross member is connected to frame members. The first cross member is tapered, being 6" deep at the centerline and 4" deep at the outside rail. Nodes were placed on the inside slanted edge because it was felt that the response of the front structure of the frame would be sensitive to variations in the relative orientation of frame members.
4	Photographs indicate the formation of a plastic hinge at the bend in the frame member.
5	The member begins to curve at this point. Photographs indicate a hinge develops at this location.
6	The frame member changes direction. Photographs indicate the formation of a hinge at this location.
7	Two frame members intersect at this location.

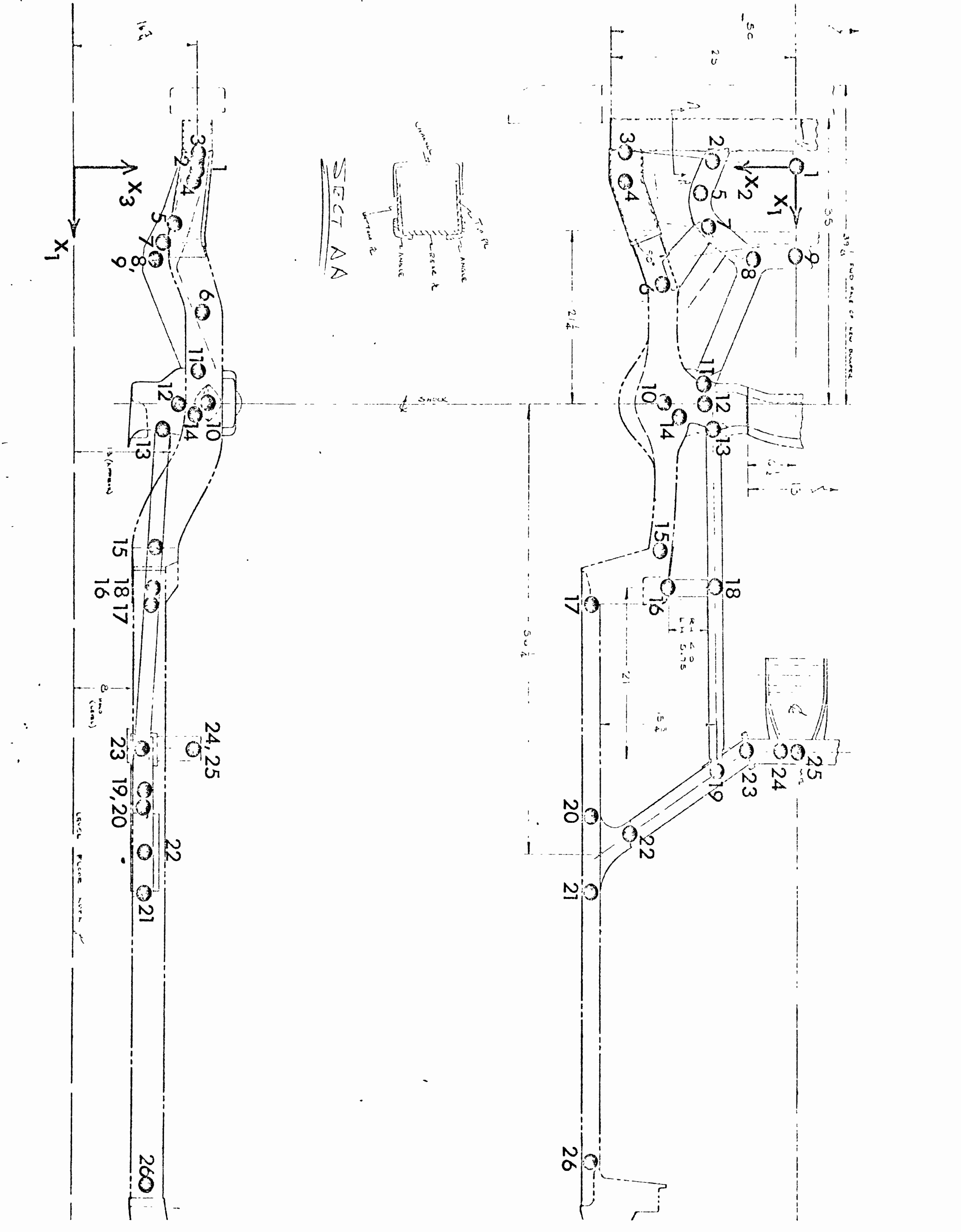

Figure 33

Location of nodes and their nodal numbers.

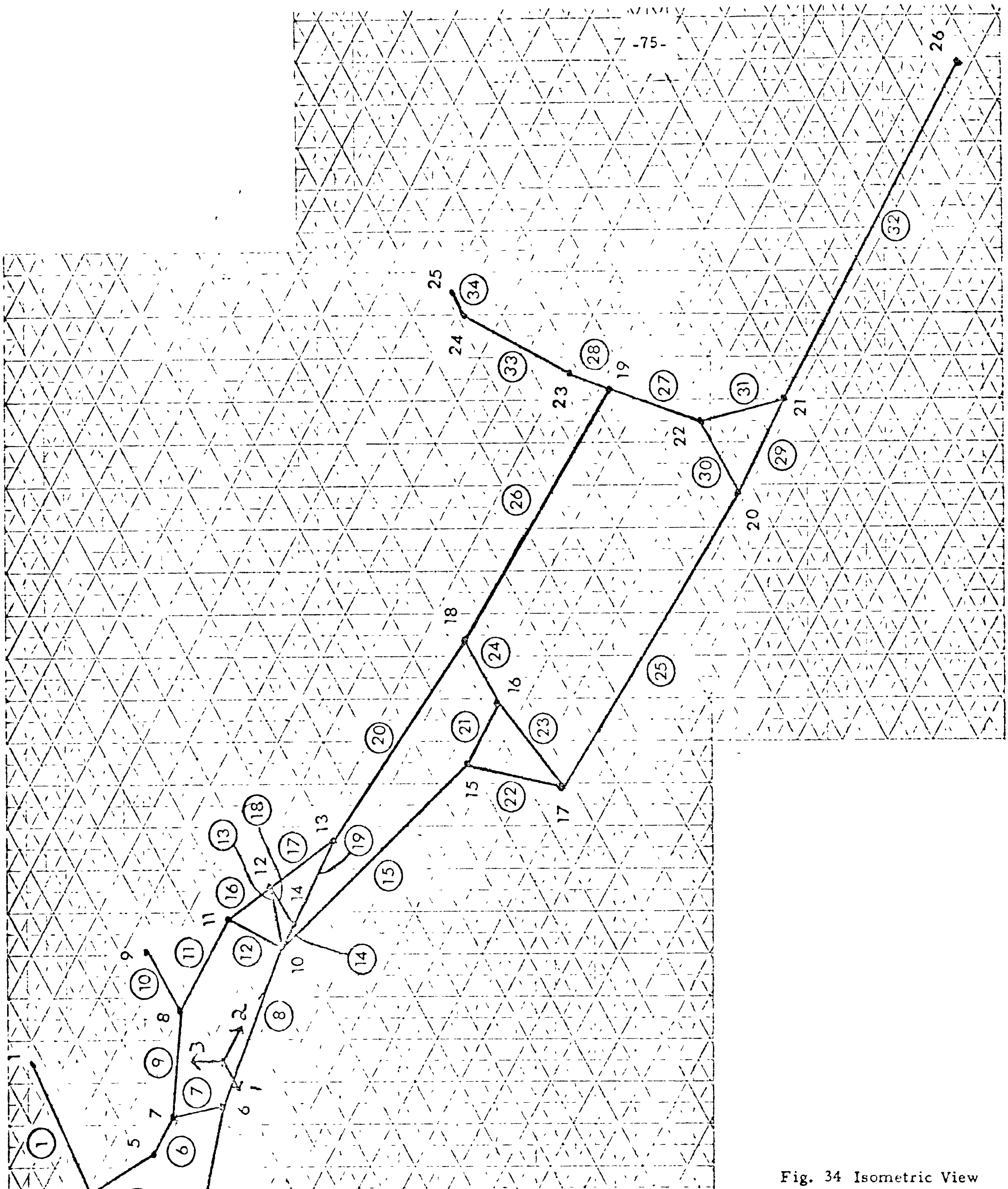

Fig. 34 Isometric View of Frame Showing Node and Beam Numbers

Node Number	Bases For Selection
8	Three frame members intersect at this location.
9	This is placed where the axis of symmetry intersects the second cross member.
10,11,12,13	This part of the frame is a large metal dome with openings in the bottom. Its purpose appears to be to support the front suspension system. It has no obvious idealization as an assembly of beam elements. Node 10 is placed at its apparent center as indicated by the blueprints. This defines a beam connecting nodes 6 and 10 on the outside part of the frame. Nodes 11 and 13 indicate where beam-like frame members are attached to the wheel support. Photographs suggest that this wheel support behaves as if it were composed of triangular segments 10-11-12 and 10-12-13 sharing a base connecting nodes 10 and 12. During the crush test, these segments rotate about the axis connecting nodes 10-12 so that nodes 10 and 13 approach each other. Node 12 is on the line connecting nodes 11 and 13.
14	This node represents the point of support of the front part of the frame during the first part of the crush test. It is placed on the line connecting nodes 10 and 13 at the same height as the center line of the first cross member.
15,16,17	Photographs indicate the large portion of the frame is almost rigid and that hinges form at location 15 and 17. Node 16 is placed where the short cross member is attached.
18,19	Frame members intersect at these locations.

Node Number	Bases for Selection
20,21,22	The photographs indicate that hinges form at the extremities of the faired region, where nodes 20 and 21 are located. This region appeared to rotate rigidly which suggested placing node 22 on the cross member at the end of the faired region.
23,24	The cross member changes directions at these points.
25	The axis of symmetry intersects the cross member at this location.
26	This node was placed at the point of support on this rear part of the frame.

4.3 PREPARATION OF INPUT DATA

a. Coordinate System

The origin is located directly below node 1 on the line designated on the blueprints as "Level Floor Area." The orientation of the coordinate system can be seen in Figure 33.

b. Nodal Coordinates

The nodal coordinates were measured directly from the blueprints using a scale of 1/4" equals 1". The coordinates are given in Table I.

c. Beam Numbering

The beam numbers are shown encircled in the isometric view of the idealized frame in Figure 34. The members of the test frame all have rectangular tubular cross sections. Only the yield function and gradient for this cross section arises in this model.

Thus for each pair of node numbers I and J, J>I, the beam identification matrix IELM(IJ) has either the value 0 if no beam connects these nodes, or 1 if a beam does connect the nodes. Table II shows the elements of this matrix.

TABLE I

NODAL COORDINATES

NODE #	x_1	x_2	x_3	NODE #	x_1	x_2	x_3
1	0	0	16.75	15	18.5	47	11
2	11	-0.75	16.75	16	17.5	51.75	10.625
3	23	-1.75	16.75	17	27.875	53.625	10.25
4	23	1.15	15.75	18	11.25	51.75	10.625
5	13.25	4.75	15.00	19	11.25	75.00	9.00
6	18.25	14.5	16.50	20	27.875	79.50	9.00
7	11.75	7.25	14.0	21	27.875	90.25	9.00
8	5.5	11.0	12.25	22	21.75	82.00	9.00
9	0	11.0	12.25	23	7.50	72.75	9.00
10	18.0	29.00	18.125	24	2.00	72.75	16.00
11	12.625	26.5	18.75	25	0	72.75	16.00
12	12	29.00	16.125	26	27.875	123.25	9.00
13	11.25	32.25	12				
14	16.5	29.75	16.75				

TABLE II

BEAM-NODE RELATION MATRIX IELM(I,J)

I = 1,...,NUMP-1; J = I+1, ..., NUMP

All entries for J = I+6 to J = NUMP are zero.

I	I+1	I+2	I+3	I+4	I+5
1	1	0	0	0	0
2	1	0	1	0	0
3	1	0	0	0	0
4	0	1	0	0	0
5	0	1	0	0	0
6	1	0	0	1	0
7	1	0	0	0	0
8	1	0	1	0	0
9	0	0	0	0	0
10	1	1	0	1	1
11	1	0	0	0	0
12	1	1	0	0	0
13	1	0	0	0	1
14	0	0	0	0	0
15	1	1	0	0	0
16	1	1	0	0	0
17	0	0	1	0	0
18	1	0	0	0	0
19	0	0	1	1	0
20	1	1	0	0	0
21	1	0	0	0	1
22	0	0	0	0	
23	1	0	0		
24	1	0			
25	0				

d. Direction Cosines of Beam Coordinate Frames

For each beam, the i and j ends coincide with the lower and higher nodal members, respectively. At t=0 the beam frames at the i and j ends are parallel. Hence, it is only necessary to specify the beam frame at the i end. The beam frame x_3 axis lies along the length of the beam directed from the lower to the higher node number. The beam frame x_1 and x_2 axes lie along the principal directions of the cross section. Since all beams have rectangular tubular cross sections, the beam frame x_1 and x_2 axes are easy to identify.

From the nodal coordinates, the beam length and the unit vector directed from the lower to the higher nodes number were computed. The components of the unit vector represent the direction cosines of the beam frame x_3 axis with respect to the global system. In order to determine the remaining direction cosines, the beams were placed into three categories:

1. the beam frame axes are parallel to the global axes. In this case, direction cosines are determined by observation.

2. The beam frame x_3 axis lies in one of the coordinate planes. In this case, the beam frame axes are obtained by a rotation about one of the global axes. All of the direction cosines are known from the components of the unit vector along the beam frame x_3 axis. For example, for beam 1 this unit vector has component (0.99773, -0.06803, 0). The local axes are oriented with respect to the global axes as shown in Figure 35a. The direction cosine matrix for beam 1 is

$$\begin{bmatrix} 0 & 0 & 1 \\ -.06803 & -.99773 & 0 \\ .99773 & -.06803 & 0 \end{bmatrix}$$

a.

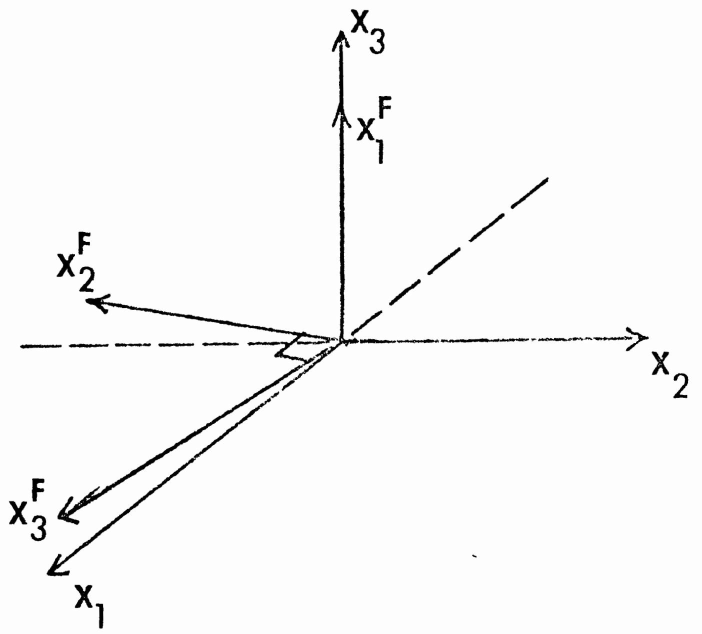

b.

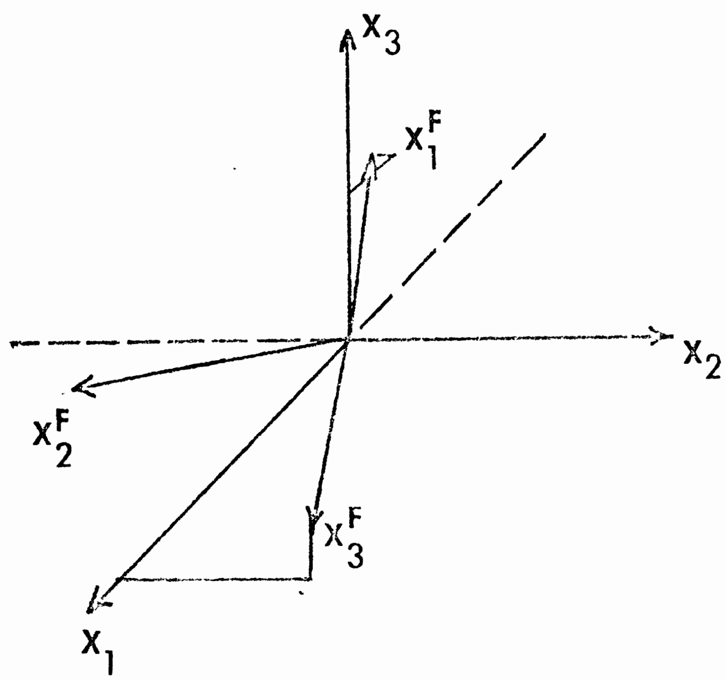

Figure 35. a. Orientation of beam frame axes (X_1^F, X_2^F, X_3^F) for beam 1 with respect to global axes

b. Orientation of beam frame axes (X_1^F, X_2^F, X_3^F) for a general beam with respect to global axes

3. The beam frame x_3 axis has a general orientation with respect to the global coordinates. Because of the test frame layout and the fact that the frame members all have rectangular tubular cross-sections, one principal direction of the cross-section always lies in the global x_1-x_2 plane. This was selected on the beam frame x_2 axis. The beam frame x_1 axis then lies in the plane formed by the global and beam frame x_3 axis. (See Figure 35b.)

The components of the unit vector in the beam frame give the desired direction cosines. Letting the components of the unit vector along the x_1, x_2, x_3 axes be, respectively (x_{11}, x_{12}, x_{13}), $(x_{21}, x_{22}, 0)$, (x_{31}, x_{32}, x_{33}), they satisfy the following system of equations where (x_{31}, x_{32}, x_{33}) are considered given:

$$x_{21}\, x_{31} + x_{22}\, x_{32} = 0$$

$$x_{21}\, x_{11} + x_{22}\, x_{12} = 0$$

$$x_{11}\, x_{31} + x_{12}\, x_{32} + x_{13}\, x_{33} = 0$$

$$x_{11}^{2} + x_{12}^{2} + x_{13}^{2} = 1$$

$$x_{21}^{2} + x_{22}^{2} = 1$$

The solution of this system is

$$x_{21} = \frac{x_{32}}{\{(x_{31})^2 + (x_{32})^2\}^{1/2}}, \quad x_{22} = \frac{x_{31}}{\{(x_{31})^2 + (x_{32})^2\}^{1/2}}$$

$$x_{11} = \frac{Ax_{22}}{(1+A^2)^{1/2}} \quad x_{12} = \frac{-Ax_{21}}{\{1+A^2\}^{1/2}}, \quad x_{33} = \frac{1}{(1+A^2)^{1/2}}$$

$$A = \frac{x_{33}}{x_{21}\, x_{32} - x_{31}\, x_{22}}$$

These equations are easily programmed and the results are given in Table III.

TABLE III

DIRECTION COSINES OF BEAM FRAMES WITH RESPECT TO THE GLOBAL FRAME

DCIK

BEAM #	$\underline{e}_1^F \cdot \underline{e}_1$	$\underline{e}_1^F \cdot \underline{e}_2$	$\underline{e}_1^F \cdot \underline{e}_3$	$\underline{e}_2^F \cdot \underline{e}_1$	$\underline{e}_2^F \cdot \underline{e}_2$	$\underline{e}_2^F \cdot \underline{e}_3$	$\underline{e}_3^F \cdot \underline{e}_1$	$\underline{e}_3^F \cdot \underline{e}_2$	$\underline{e}_3^F \cdot \underline{e}_3$
1	0	0	1	-.06803	-.99773	0	.99773	-.06803	0
2	0	0	1	-.08306	-.99668	0	+.99668	-.08306	0
3	.10697	.26147	.95927	.92555	-.37864	0	+.36320	.88781	-.28249
4	-1	0	0	0	.32605	.94555	0	.94555	-.32605
5	.01772	-.04980	.99860	.94214	.33522	0	-.33477	.94087	.05286
6	-.16680	.27814	.94595	.85761	.51429	0	-.4867	.81116	-.32446
7	-.16488	-.18391	.96902	-.74457	.66754	0	-.64657	-.72118	-.24864
8	.00192	-.11133	.99378	.99985	.01724	0	-.01713	.99363	.11135
9	-.20019	.12012	.97236	.51450	.85749	0	-.83378	.50027	-.23346
10	0	0	1	0	1	0	-1	0	0
11	-.14871	-.32352	.93446	.90866	-.41766	0	.39030	.84908	.35607
12	.09507	.04422	.99449	.42173	.90672	0	.90169	-.41939	.10485
13	-.316	0	.949	0	1	0	-.949	0	-.316
14	-.56709	.28355	.77331	.44721	.89443	0	-.69156	.34578	-.63393
15	.01022	.36778	.92986	.99961	.02777	0	.02582	.92951	-.36793
16	-.17300	.69201	.70085	.97014	.24254	0	-.16943	.67972	-.71370
17	-.17486	.75769	.62876	.97439	.22487	0	-.14138	.61263	-.77757
18	-.134	-.022	.991	.166	-.996	0	.977	.163	.136
19	-.57118	.27199	.77445	-.42994	-.90286	0	.69925	-.33298	.63266
20	-1	0	0	0	.07034	.99754	0	.99754	-.07034

TABLE III, continued

1	-.01587	.07537	.99703	.97855	.20601	0	-.20538	.97556	-.07702
2	.05382	.03824	.99782	.57914	-.81523	0	.81059	.57589	-.06519
3	.03498	.00632	.99937	.17784	-.98406	0	.98351	.17774	-.03555
4	0	0	1	0	1	0	-1	0	0
5	-1	0	0	0	.04825	.99884	0	.99884	-.04825
6	-1	0	0	0	.06972	.99755	0	.99755	-.06972
7	0	0	1	.55472	-.83208	0	.83208	.55472	0
8	0	0	1	-.51452	.85753	0	-.85753	-.51452	0
9	-1	0	0	0	0	1	0	1	0
0	0	0	1	.37787	.92579	0	-.92579	.37787	0
1	0	0	1	-.80292	.59611	0	-.59611	-.80292	0
2	-1	0	0	0	0	1	0	1	0
3	-.78634	0	-.61784	0	-1	0	-.61784	0	.78634
4	0	0	1	0	1	0	-1	0	0

e. Beam Sectional Properties

The sectional properties which must be provided are the base, height, wall thickness, area, second moments of inertia, and polar moment of inertia of each rectangular tubular cross-section. The base, height and wall thickness could be read directly off the second set of blueprints. Sectional properties were computed using the following expressions for this walled cross-section:

$$I_{11} = (6b + 2h)h^2t/12$$

$$I_{22} = (6h + 2b)b^2t/12$$

$$A = (2b + 2h)t$$

$$J = \frac{2b^2h^2t}{b + h}$$

The relation between the principal axes of the cross-section and b and h is shown in Figure 36. In preparing this input data, it was necessary to orient the principal axes before labeling one of the cross-section dimensions as the base. Table IV shows the complete set of sectional properties.

Many of the test frame members have well defined cross-sections which do not vary along their length. In accordance with the beam numbering in Figure 34 these are beams 3, 4, 6, 9, 10, 11, 20, 24, 25, 26, 27, 28, 32, 33, 34. Beams 1 and 2 form the first cross member. Since this member is tapered in the test frame, the reported depth of the cross section is the mean between the end values. The same is true for beams 5 and 7. One end of beam 8 starts from the dome shaped wheel support, while the other half has a length of uniform cross-section section. Sectional properties were chosen for this uniform portion.

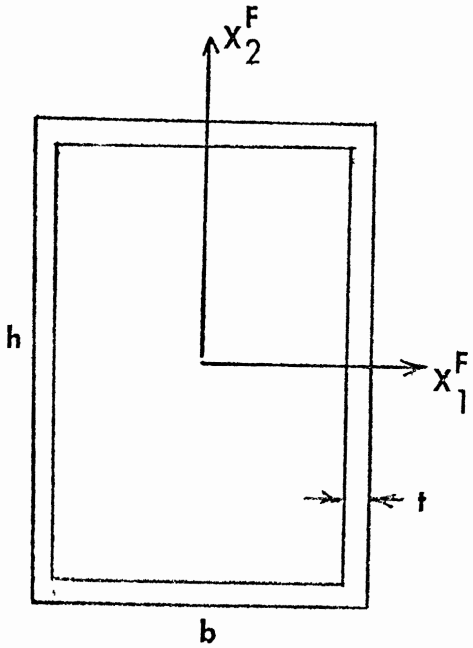

I_{11} = second area moment about X_1^F axis

I_{22} = second area moment about X_2^F axis

Figure 36. Definition of area second moments with respect to beam frame axes X_1^F and X_2^F.

TABLE IV

MATERIAL AND SECTIONAL PROPERTIES

BEAM #	E	G	AJ	AI1	AI2	A	AL	B	H	T	Y1	Y2	CF	YF
1	3.D7	12.D6	10.519	9.294	5.567	1.925	11.025	4.0	5.625	.1	1.0	1.0	1.0	5.D4
2	3.D7	12.D6	7.936	5.927	4.767	1.725	12.04	4.0	4.625	.1	1.0	1.0	1.0	5.D4
3	3.D7	12.D6	4.937	2.700	4.160	1.680	6.195	4.0	3.0	.120	1.0	1.0	1.0	3.5D4
4	3.D7	12.D6	6.400	4.267	4.267	1.600	3.067	4.0	4.0	.1	1.0	1.0	1.0	3.5D4
5	3.D7	12.D6	7.624	4.667	5.569	1.70	14.189	4.5	4.0	0.1	1.0	1.0	1.0	3.5D4
6	3.D7	12.D6	4.937	2.700	4.160	1.680	3.082	4.0	3.0	0.12	1.0	1.0	1.0	3.5D4
7	3.D7	12.D6	4.13606	2.567	2.975	1.144	10.053	4.0	3.625	.075	1.0	1.0	1.0	3.5D4
8	3.D7	12.D6	8.889	5.067	7.083	1.800	14.593	5.0	4.0	0.1	1.0	1.0	1.0	3.5D4
9	3.D7	12.D6	4.937	2.700	4.160	1.680	7.496	4.0	3.0	.120	1.0	1.0	1.0	3.5D4
10	3.D7	12.D6	4.937	2.700	4.160	1.680	5.5	4.0	3.0	.120	1.0	1.0	1.0	3.5D4
11	3.D7	12.D6	4.937	2.700	4.160	1.680	18.255	4.0	3.0	.120	1.0	1.0	1.0	3.5D4
12	3.D7	12.D6	4.4	2.2	2.2	5.0	5.961	5.0	5.0	1.0	1.0	1.0	1.0	3.5D4
13	5.D7	2.D7	10.0	10.0	10.0	5.0	6.325	1.0	1.0	1.0	1.0	1.0	1.0	5.D4
14	5.D7	2.D7	10.0	10.0	10.0	5.0	2.169	1.0	1.0	1.0	1.0	1.0	1.0	5.D4
15	3.D7	12.D6	7.2000	3.1500	9.000	1.8000	19.365	6.0	3.0	0.1	1.0	1.0	1.0	3.6D4
16	3.D7	12.D6	4.4	2.2	2.2	5.0	3.678	5.0	5.0	1.0	1.0	1.0	1.0	3.5D4
17	3.D7	12.D6	1.0	.52	.52	3.0	5.305	4.0	4.0	1.0	1.0	1.0	1.0	3.5D4
18	5.D7	2.D7	10.0	10.0	10.0	5.0	4.605	1.0	1.0	1.0	1.0	1.0	1.0	5.D4
19	3.D7	12.D6	1.0	.52	.52	3.0	7.508	4.0	4.0	1.0	1.0	1.0	1.0	3.5D4

TABLE IV, continued

	E	G	AJ	AI1	A12	A	AL	B	H	T	Y1	Y2	CF	YF
20	3.D7	12.D6	.96	.64	.64	.96	19.548	2.0	2.0	.12	1.0	1.0	1.0	3.6D4
21	3.D7	12.D6	10.0	10.0	10.0	10.0	4.869	1.0	1.0	1.0	1.0	1.0	1.0	7.D4
22	3.D7	12.D6	10.0	10.0	10.0	10.0	11.504	1.0	1.0	1.0	1.0	1.0	1.0	7.D4
23	3.D7	12.D6	10.0	10.0	10.0	10.0	10.549	1.0	1.0	1.0	1.0	1.0	1.0	7.D4
24	3.D7	12.D6	.96	.64	.64	.96	6.25	2.0	2.0	.12	1.0	1.0	1.0	3.6D4
25	3.D7	12.D6	3.692	3.680	1.813	1.560	25.905	2.5	4.0	.12	1.0	1.0	1.0	3.6D4
26	3.D7	12.D6	.96	.64	.64	.96	23.307	2.0	2.0	.12	1.0	1.0	1.0	3.6D4
27	3.D7	12.D6	3.240	2.160	2.160	1.44	12.619	3.0	3.0	.12	1.0	1.0	1.0	3.6D4
28	3.D7	12.D6	3.24	2.160	2.160	1.44	4.373	3.0	3.0	.12	1.0	1.0	1.0	3.6D4
29	3.D7	12.D6	10.0	10.0	10.0	10.0	10.75	1.0	1.0	1.0	1.0	1.0	1.0	7.D4
30	3.D7	12.D6	10.0	10.0	10.0	10.0	6.616	1.0	1.0	1.0	1.0	1.0	1.0	7.D4
31	3.D7	12.D6	10.0	10.0	10.0	10.0	10.275	1.0	1.0	1.0	1.0	1.0	1.0	7.D4
32	3.D7	12.D6	3.692	3.680	1.813	1.560	33.0	2.5	4.0	.12	1.0	1.0	1.0	3.6D4
33	3.D7	12.D6	1.728	1.620	0.88	1.2	8.902	2.0	3.0	.188	1.0	1.0	1.0	3.6D4
34	3.D7	12.D6	1.728	1.620	0.88	1.2	2.0	2.0	3.0	.188	1.0	1.0	1.0	3.6D4

The properties of the bars forming a structure to approximate the behavior of the wheel support were chosen in accordance with the discussion in Section 4.2. Beams 13-14-18 form a rigid backbone about which the triangles formed by nodes 10-11-12 (beams 12-16-13) and nodes 10-12-13 (beams 17-18-19) could fold. Bars 14 and 18 were made rigid so as to hold fixed node 14, where strong external constraint is applied. Beams 12 and 16 were designed to have high axial stiffness but lower bending resistance as compared to beam 11. These beams were given equal second area moments whose value is 0.8 that of beam 11. Similar comments apply to beams 17 and 19, whose second area moments were .8 that of beam 20.

Beams 21, 22, 23 and 29, 30, 31 model segments of the test frame which appeared to be quite rigid. Their sectional properties were accordingly chosen quite large.

f. Material Properties

Except for beams 13, 14 and 18 all bars were assigned the same tensile and shear moduli. Bars 13, 14 and 18 were given larger moduli in order to increase their stiffness. The first cross member was specified as Hot Rolled 4130 which has a yield stress of at least 50,000 psi. Beams 3 through 12, 15, 16, 17, 19, 20, 28-28, and 32-34 are made of SAE 1020 steel with a yield stress of at least 35,000 psi. The actual yield stress specified in the input data was higher for two reasons: (a) the yield stress was reported to vary in magnitude throughout the test frame (b) the ratio of the fully plastic moment to the maximum elastic moment is about 1.7. As indicated in Figure 37, higher yield stress results in a more reasonable

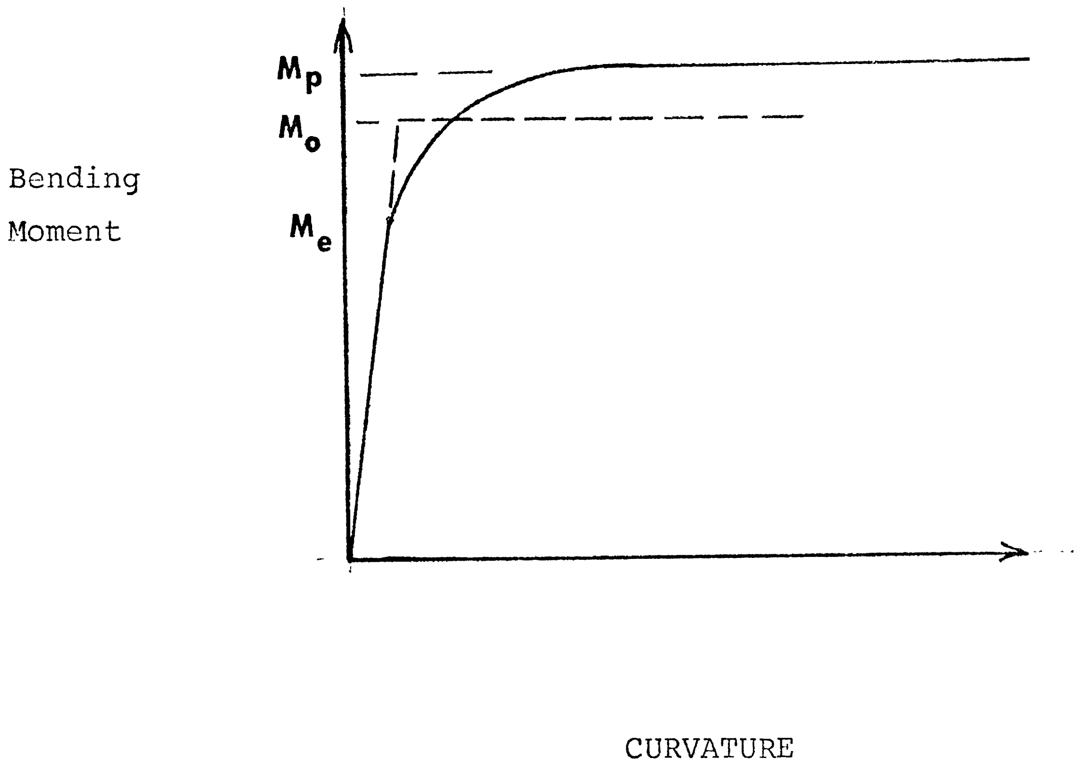

Me . . . elastic limit moment

M_p . . . fully plastic moment

Mo . . . moment in elastic-perfectly plastic idealization

Figure 37. Moment curvature relation for a rectangular cross-section, showing elastic-perfectly plastic idealization.

elastic-plastic moment-curvature relation. Beams 13, 14, 18, 21, 22, 23 and 29, 30, 31 were given higher yield stresses in accordance with their special functions. The material properties are listed in Table IV.

4.4 FORCE AND DISPLACEMENT CONDITIONS

In order to carry out the numerical simulation of the crush test, a number of reasons led to the decision to use a reduced frame. In the first part of the crush test, the frame was constrained at node 14 as well as node 26. Engineering intuition suggests that the rear part of the frame carries relatively little load because of the constraint at node 14. Also, because of the size of the problem and the number of matrix assembly and plastic hinge test and decision operations, it was felt that computer runs would be fairly expensive. Consequently, it was decided that only the first part of the crush test would be modeled using the portion of the frame model consisting of the first 15 nodes and 19 beams.

The following increments in nodal displacement Δu_i, nodal rotation $\Delta\theta_i$ and nodal force ΔF_i and nodal moment ΔM_i were prescribed.

<u>Node 1</u> $\Delta u_1 = \Delta u_3 = 0$, $\Delta u_2 = \Delta$, to be prescribed

$\Delta M_1 = 0,\quad \Delta\theta_2 = \Delta\theta_3 = 0$

<u>Node 9</u> $\Delta u_1 = 0 \quad \Delta F_1 = \Delta F_2 = 0$

$\Delta M_1 = 0 \quad \Delta\theta_2 = \Delta\theta_3 = 0$

<u>Node 14</u> $\Delta u_1 = \Delta u_2 = \Delta u_3 = 0$

$\Delta\theta_1 = \Delta\theta_2 = \Delta\theta_3 = 0$

For all other nodes, $\Delta F_i = \Delta M_i = 0$, $i = 1, 2, 3$.

4.5 DISCUSSION OF COMPUTED RESULTS

A simulated force deflection curve was computed using the following displacement increments:

$$
\begin{array}{ll}
\text{for } K = 1,2,3, & \Delta u_2 = 0.002 \\
K = 4,5,6,7 & \Delta u_2 = 0.004 \\
K = 8,9,10,11 & \Delta u_2 = 0.006 \\
K = 12,13,14,15 & \Delta u_2 = 0.008 \\
K \geq 16 & \Delta u_2 = 0.01
\end{array}
$$

For these computations KMAX = 66. The above increments were non-dimensionalized by reference length ALR = 10.0.

During the computation, all beams were assumed to undergo continuous loading.

Figure 38 shows the force deflection curve for a crush of 4.64 inches. The curve consists of an initial loading range up to 2.634 inches, where a maximum load of 32,453 pounds was reached, followed by a general softening range.

Within the loading range, all the plastic hinges except one formed within the first 1.334 inches of crush. In this region of formation of plastic hinges, the force-deflection curve oscillates about a general loading trend. For deflections greater than 1.334 inches, when hinges have stopped forming, the curve shows a much smoother monotonic increase. The oscillatory behavior may be due to numerical inaccuracy due to the large step size, or it may be due to temporary softening caused by the formation of various plastic hinges. That softening does occur in certain structures undergoing large deformation elastic-plastic behavior was discussed in the 11th monthly report. In the absence of a detailed numerical error analysis, it is not clear how much of the oscillation of the curve can be attributed to numerical and how much to physical explanation. However, since the force-deflection curve is much smoother when no hinges form, it is reasonable to assume that some of the oscillation is due to softening caused by hinge

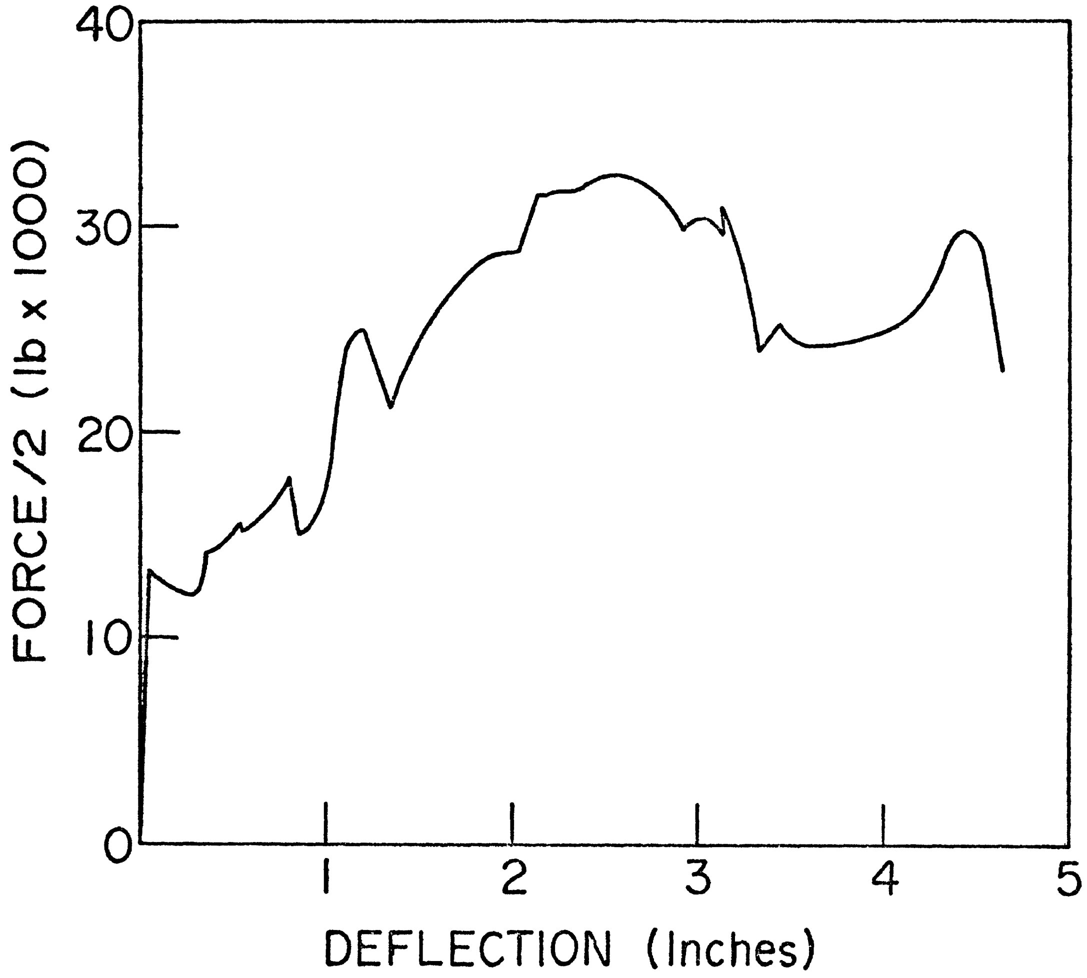

Fig. 38 Force Vs. Deflection of Node 1
Along X_2 Direction

formation. This explanation is further supported by the experimental results quoted in the 11th monthly report, which showed a hardening and softening oscillation which arose because plastic hinges did not occur simultaneously.

In support of this latter conclusion, note that during the first oscillation, from a deflection of 0.0322 inches to 0.264 inches, beam 6 has formed hinges at both ends, that is, at nodes 5 and 7. The location of this beam in the forestructure, as seen in Figure 39, suggests that its weakening could lead to some softening. The second oscillation, from .804 inches to .844 inches, corresponds to formation of hinges in beams 4 and 5 at node 4, and beam 1 at node 1. Again as seen in Figure 39, this suggests local weakening. The last dip, from 1.202 inches to 1.334 inches, corresponds to hinges forming in beam 3 at node 5 and beams 2 and 3 at node 2.

In the softening range, following the peak value at 2.634 inches, the only hinge to form occurs at 3.139 inches when the force is 30,995 lbs. The force drops to 23,940 lbs. and then stays reasonably constant until it rises quickly and drops to 23,704 lbs. This last peak is probably due more to accumulated numerical error associated with large increment size than any stiffening of the structure.

Figure 39 shows the distribution of plastic hinges after 4.64 inches of crush. Only the forward part of the structure, which was involved in the computation, is shown.

Figure 40 shows the computed force-deflection curve plotted on the same scale as the pole barrier static crush test data presented in the CALSPAN report. Photos of their test show the front bumper covered with foam and a channel section, which was not included in the model. Because of uncertainty as to how much force was required to crush the foam and channel, it was not clear how to choose the origin for plotting data. Projecting back on the steep part of the curve suggested choosing 2.5 inches as the origin.

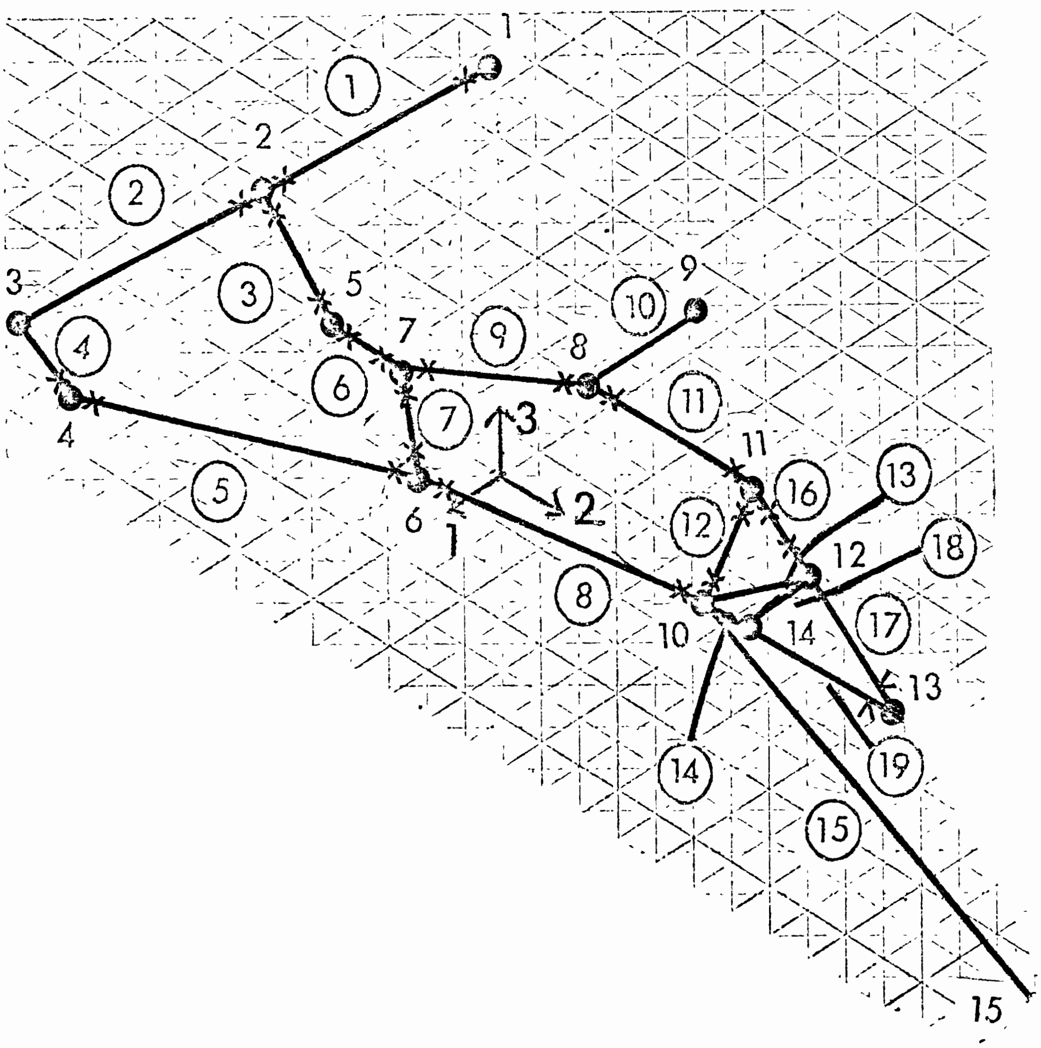

Figure 39. Final Plastic Hinge Distribution

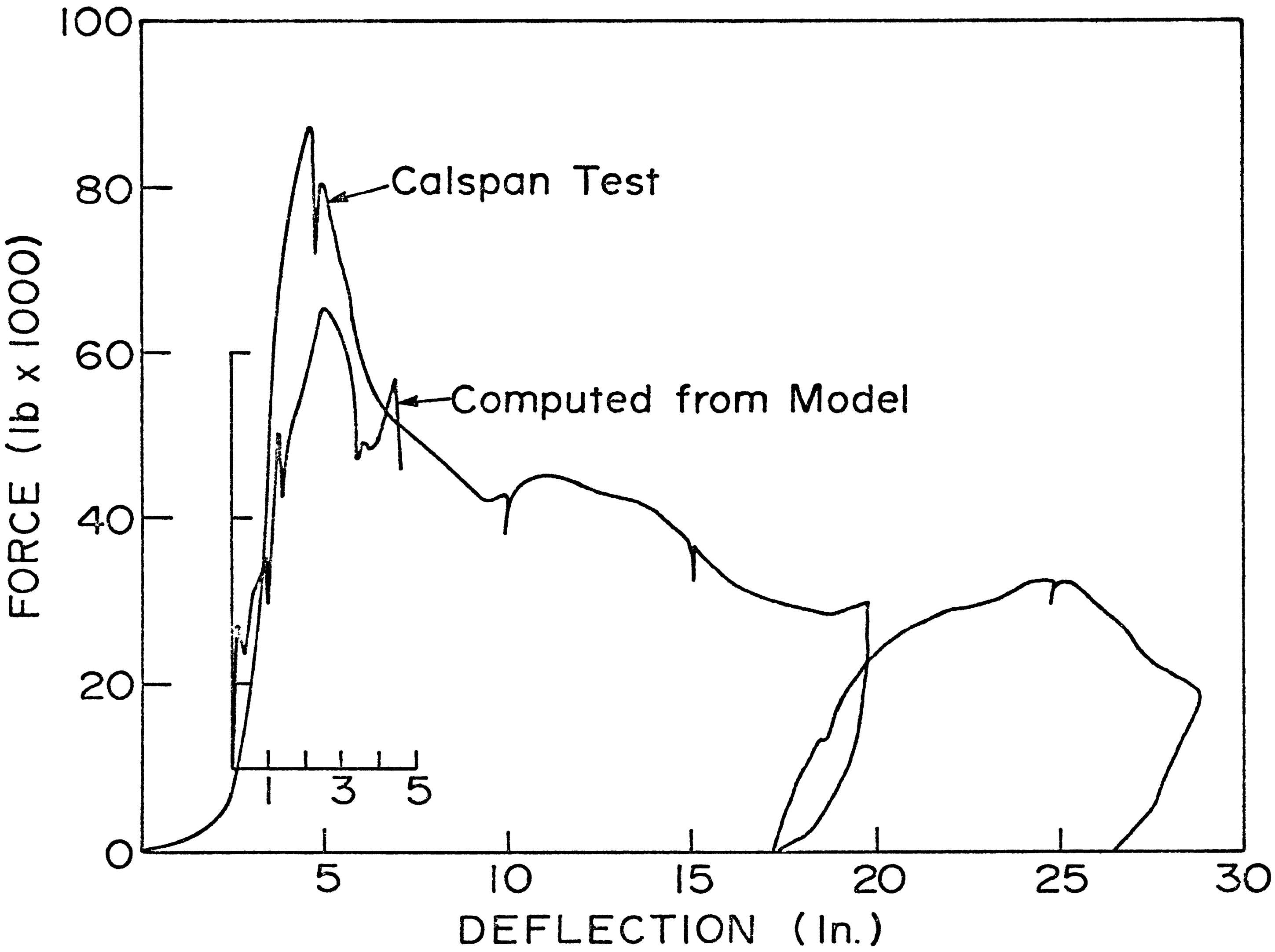

Fig. 40 Force Deflection Curve for Pole Barrier Static Crush Test

The computed results agree reasonably well with the experimental results. There is a rapid rise in force, a peak value of force and subsequent softening. The slope of the initial rise is comparable with that of the test data. The peak values have comparable magnitude (87,000 lbs. vs 64,906), and occur at about the same deflection. The softening range in the computed results has about the same slope as in the test results, except for the oscillation, whose cause, as discussed above, is uncertain.

APPENDIX A

USERS GUIDE

A.1 INPUT INFORMATION

The following discussion on the preparation of input data is divided into several subsections:

A. Discussion of Preparation of Input Data

B. List of Program Input Variables

C. Layout and Format of Input Data

D. An Example of Input Data

E. Layout and Sample of Output

The discussion in section A defines many of the input variables which are listed in section B. The order of data discussed follows that in the table of input card contents in section C.

A. Preparation of Input Data

Node Numbering (See Figure 43.).

After selecting node #1, the nearest node is assigned #2. The number of a node increases with its distance from node #1, as shown in Figure 43. The total number of nodes (mass points) is denoted by NUMP.

Beam Numbering

Consider nodes I and J, where J = I+1, ..., NUMP. If a beam connects I and J, it is assigned the next beam number in sequence. If no beam connects nodes I and J, no beam number is assigned. In Figure 43 , the beam numbers are circled. The total number of beams is denoted by NUB.

Basic Input Parameters

The first data card lists the number of nodes or mass points NUMP, the number of beams NUB, the number of time steps KMAX, print out switch control IPS and dissipation switch control IDS. These switch controls are defined in section B.

Specifying the Type of Beam Cross-Section

The type of beam cross-section is specified by assigning to each pair of nodes I and J an integer, denoted by IELM(I,J), as follows:

IELM(I,J)	= 0	If no beam connects nodes I and J
	= 1	If the beam connecting nodes I and J has cross-section type 1
	= 2	If the beam connecting nodes I and J has cross-section type 2

etc.

The program, as currently written, allows for up to four different kinds of cross-sections. For each type of cross-section there are subroutines for calculating the corresponding yield function and the gradient of the yield function. At present, subroutines have been written only for rectangular tubular (type 1) and open channel (type 2) cross-sections.

Reference Values

The next card specifies the reference beam length ALR, reference beam depth DR, reference elastic modulus ER, reference second area moment AIR and allowable error for logic test EPS.

Beam Sectional and Material Properties

For each beam, the following material properties are to be specified: elastic tensile modulus E, elastic shear modulus G, yield stress YF.

In addition to the beam length AL, the required cross-sectional properties are: base B, height H, wall thickness T, area A, principal second area moments AI1 and AI2, area polar moment AJ, distance from base of cross-section to centroid Y1, distance from centroid to top of cross-section Y2, and stress concentration factor at base of fillet in closed tubular section CF.

The input data assumes that the beam has either a rectangular or open channel section. The definition of the B, H, AI1 and AI2 with respect to the principal axes of these cross-sections is shown in Figure 41. In part C, this data is designated set A.

Direction Cosines

The direction cosines with respect to a global reference system of a coordinate frame attached to a beam in its original orientation must be specified. The X_3 axis of the attached frame is directed along the beam from the end with the lowest number node to the end with the highest number node. The X_1 and X_2 axes of the attached frame coincide with the principal axes of the beam cross-section (shown in

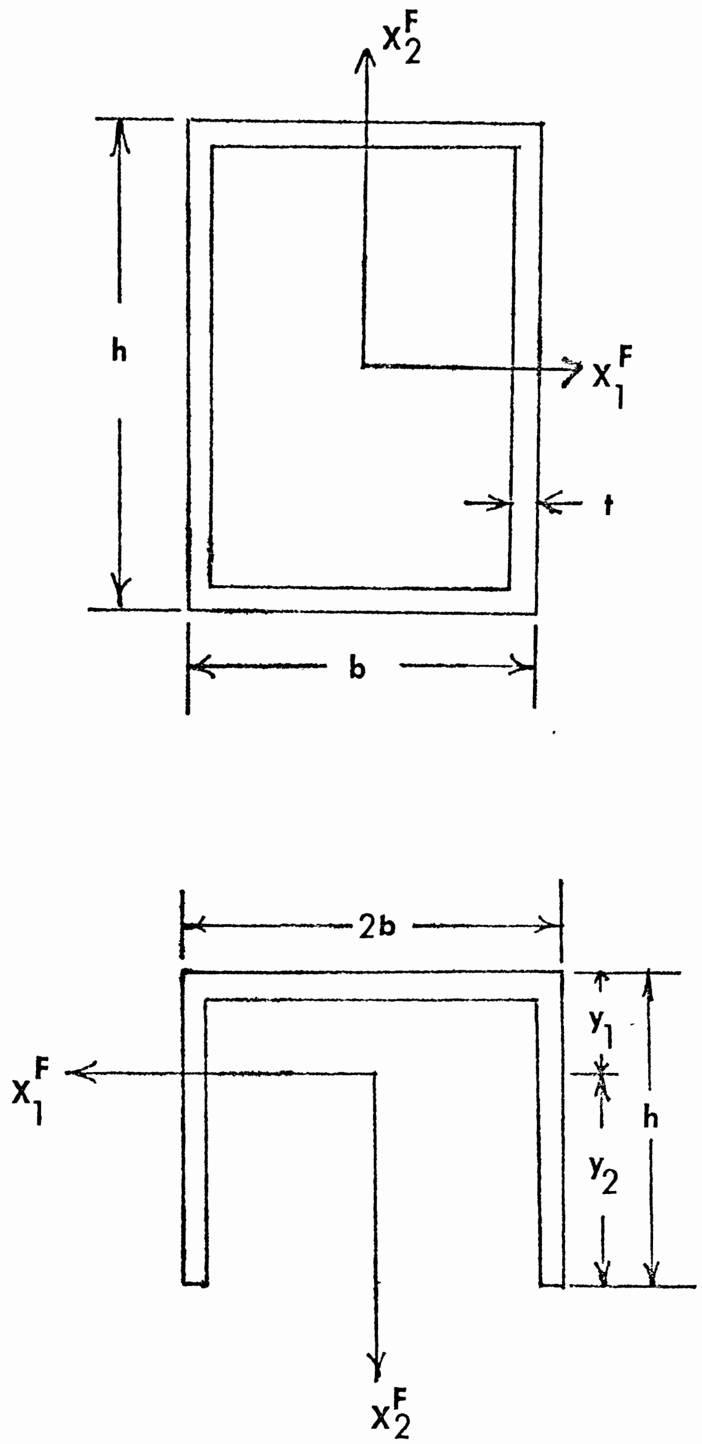

I_{11} second area moment about X_1^F axis

I_{22} second area moment about X_2^F axis

Figure 41. Relation of beam frame axes to cross-sectional dimensions for rectangular tubular and open channel cross-sections

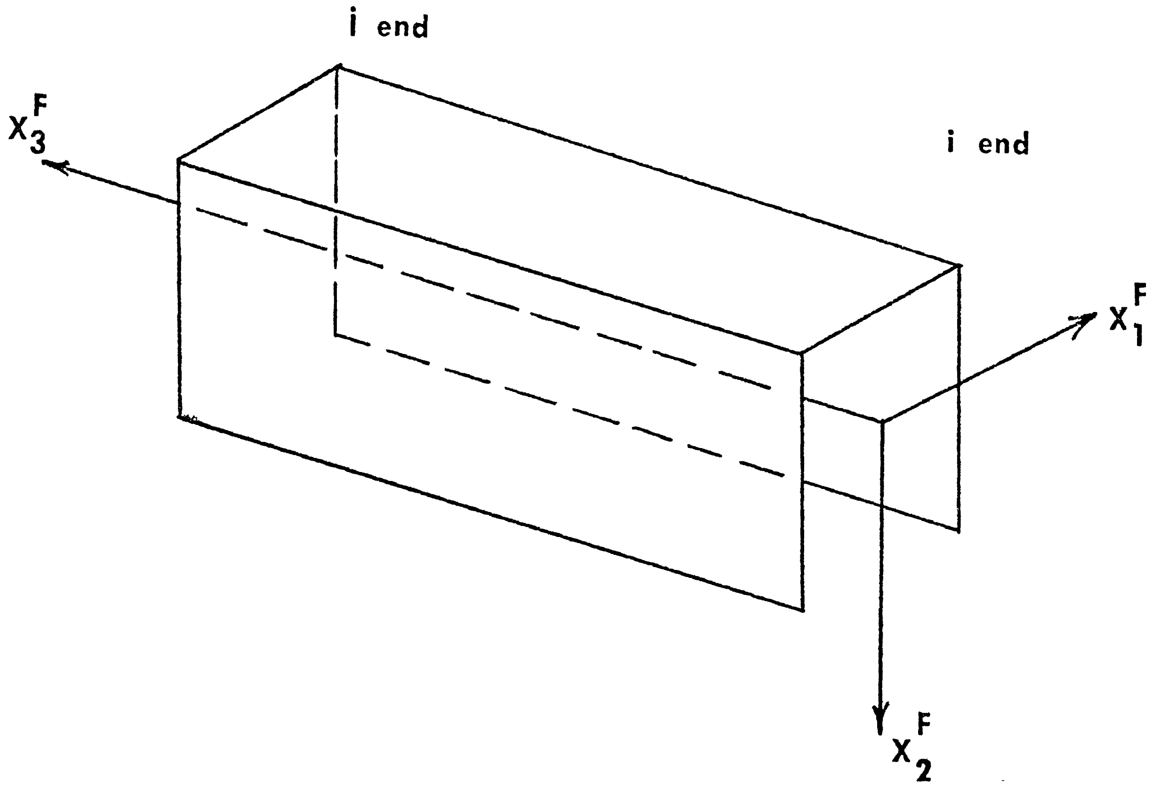

Figure 42. Beam frame axes related to cross-section principal directions

Figure 42 so as to form a right handed coordinate system.

The direction cosines are denoted by DC1K(LB,I,J) which gives the angle between the I axis of the local attached coordinate frame and the J axis of the global frame for beam number LB.

In part C, this set of data is designated set B.

Initial Coordinates of Nodes

The initial coordinates and angles of the mass frames, which are attached to the nodes, with respect to the global reference system must be specified. These are denoted by DISK(LMP,I), where LMP is the mass point number.

$$\begin{aligned} \text{DISK(LMP,I)} &= X_I \ , \ I = 1,2,3 \\ &= \theta_I \ , \ I = 4,5,6 \end{aligned}$$

where θ_I is the initial angle of the local frame axes with respect to the global frame axes.

In part C, this set of data is designated set C.

Nodal Displacement and Force Increments

The increments in the generalized displacements of the nodes form the components of the vector denoted by DU(I), I = 1,..., 6*NUMP. The LMPth group of six components correspond to mass point LMP. In each group of six, the first three components represent the components of the displacement increment vector of mass point LMP. The second three components represent the components of the rotation increment vector of mass point LMP.

The increments in the generalized forces of the nodes form the components of the vector denoted by DR(I),I = 1,..., 6*NUMP. The LMPth group of six components correspond to mass point LMP. In each group of six, the first three components represent the components of the force increment vector of mass point LMP. The second three components represent the components of the moment increment vector of mass point LMP.

At each mass point, either a displacement increment component or the corresponding force increment component is known. Also, either a rotation increment component or a moment increment component is known. However, input data requires a value for each displacement and rotation increment. If a displacement or rotation increment is unknown, its value is specified as 100. If a force or moment increment is unknown, its value can be specified arbitrarily.

Rotation increments are specified in radians, displacement increments are non-dimensionalized by the reference length ALR, forces are non-dimensionalized by the expression $(ER)(AIR)/(ALR)^2$ and moments are non-dimensionalized by the expression (ER)(AIR)/ALR.

Nodal force and displacement increments are not specified by preparing input data cards as is the above data. Because of the large number of increments and nodal conditions, it is usually easier and more efficient to specify these by means of an increment program. A different program is necessary for each problem and set of increment conditions. A sample increment program is presented in Section D.

B. LIST OF PROGRAM INPUT VARIABLES

A. . . . . beam area

AIR . . . . reference moment of inertia

ALR . . . . reference beam length

AJ . . . . beam polar moment of inertia

AI1 . . . . beam moment of inertia about 1st principal axis

AI2 . . . . beam moment of inertia about 2nd principal axis

AL . . . . beam length

B . . . . beam cross-section width dimension

CF . . . . beam cross-section torsional stress concentration factor

DC1K(LB,I,J) . . . direction cosine matrix for the initial configuration of beam member LB

(LB = 1,...,NUB; I = 1,2,3; J = 1,2,3)

DISK(LMP,I) .... Initial coordinates of mass point LMP

$DISK(LMP,I) = X_I$, $I = 1,2,3$

$DISK(LMP,I) = \theta_I$, $I = 4,5,6$

θ_I ..initial angle of mass frame axes with global frame axes

(LMP = 1,...,NUMP;I = 1,..,6)

DR .... reference beam depth

DR(I) .... nodal generalized force increment vector (I = 1,..., 6*NUMP) The LMPth group of six components correspond to mass point LMP. In each group of six, the first three components are those of the force increment vector of mass point LMP. The second three components are those of the moment increment vector of mass point LMP.

DU(I) ....Nodal generalized displacement increment vector (I = 1,...,6*NUMP). The LMPth group of six components correspond to mass point LMP. In each group of six, the first three components are those of the displacement increment vector of mass point LMP. The second three components are those of the rotation increment vector of mass point LMP.

E .... beam material elastic modulus

EPS .... allowable error for logic test

ER .... reference elastic modulus

G .... beam material shear modulus

H .... beam cross-section height dimension

IDS .... dissipation switch control

IDS = 0 no unloading at a negative dissipation increment

IDS = 1 if the dissipation increment is negative, the program allows unloading

IELM(I,J)....... type of beam relation between node I and node J

(I = 1,...,NUMP-1; J = I+1,...,NUMP)

IELM(I,J) = 0 if no beam connects I & J

= L if beam connecting I & J has cross-section type L

IPS..............print out switch control

IPS = 0 standard print out

1 print out yield function at each beam end

2 full optional output

KMAX ....maximum number of time steps

NUB .... number of beams

NUMP .... number of mass points

T .... beam wall thickness

Y1 .... distance from bottom of beam cross-section to centroid

Y2 .... distance from top of beam cross-section to centroid

YF .... yield stress for beam material

C. LAYOUT AND FORMAT OF INPUT CARD CONTENTS

CARD #	Col. 1-4	Col. 5-8	Col. 9-12	Col.13-16	Col.17-20	
1	NUMP	NUB	KMAX	IPS	IDS	

CARD #	Col. 1-2	Col. 3-4	Col. 5-6			Col.79-80
2	IELM(1,2)	IELM(1,3)				IELM(1,NUMP)
3	IELM(2,3)				IELM(2, NUMP-1)	
	⋮					
NUMP	IELM(NUMP-1, NUMP)					

THE ABOVE INPUT DATA ARE IN I FORMAT

THE FOLLOWING INPUT DATA ARE IN D FORMAT

	Col. 1-8	Col. 9-16	Col. 17-24	Col. 25-32	Col. 33-40	Col. 41-48	Col. 49-56	Col. 57-64
NUMP+1	ALR	DR	ER	AIR	EPS			
NUMP+2	E	G	AJ	AI1	AI2	A	AL	B
NUMP+3	H	T	Y1	Y2	CF	YF		
⋮								
NUMP+ 2xNUB	E	G	AJ	AI1	AI2	A	AL	B
NUMP+1 +2xNUB	H	T	Y1	Y2	CF	YF		

SET A TOTAL 2xNUB CARDS

CARD #	Col. 1-10	Col. 11-20	Col. 21-30	Col. 31-40	Col. 41-50	Col. 51-60	
NUMP+2 +2XNUB	DC1K(1,1,1)	DC1K(1,1,2)	DC1K(1,1,3)				
	DC1K(1,2,1)	DC1K(1,2,2)	DC1K(1,2,3)				
	DC1K(1,3,1)	DC1K(1,3,2)	DC1K(1,3,3)				SET B
	DC1K(2,1,1)						TOTAL
	DC1K(2,2,1)						3XNUB
	DC1K(2,3,1)						CARDS
	⋮ DC1K(NUB,1,1)						
	DC1K(NUB,2,1)						
NUMP+1 +5XNUB	DC1K(NUB,3,1)						
NUMP+2 +5XNUB	DISK(1,1)	DISK(1,2)	DISK(1,3)	DISK(1,4)	DISK(1,5)	DISK(1,6)	SET C
	⋮						TOTAL NUMP
2XNUMP+1 +5XNUB	DISK(NUMP,1)	DISK(NUMP,2)	DISK(NUMP,3)	DISK(NUMP,4)	DISK(NUMP,5)	DISK(NUMP,6)	CARDS

D. EXAMPLE OF INPUT DATA

A simple example has been selected to illustrate the preparation of input data.

The initial configuration of a structure is defined as shown in Figure 43.

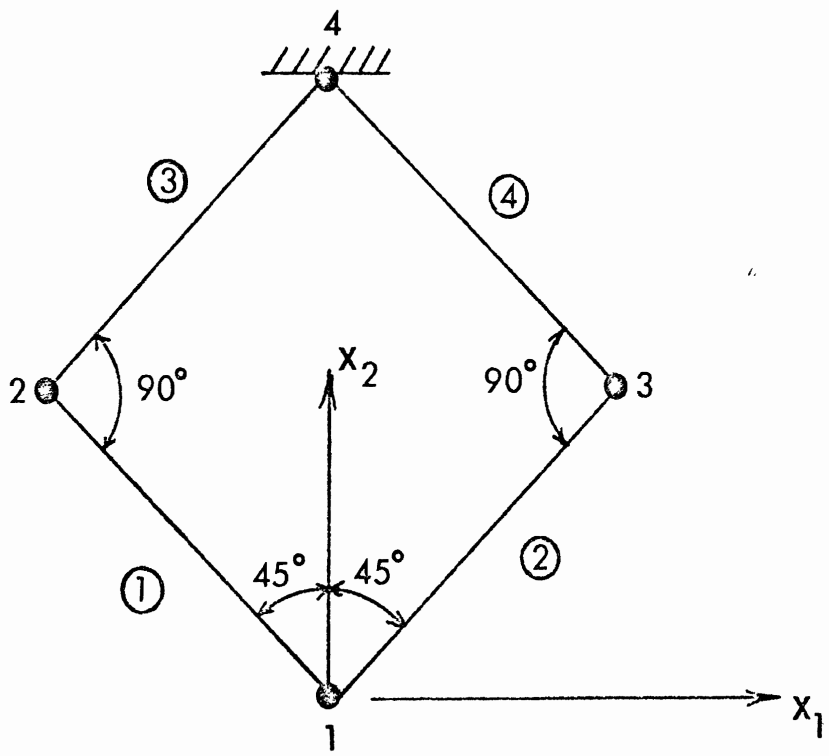

Figure 43. Four bar example frame

The structure is planar and consists of four node points, numbered as shown, connected by four beams, whose numbers are encircled. Node point 4 is fixed for all time. The prescribed conditions at node point 1 are:

a. displacement increments in the X_2 direction are known

b. there is no external force in the X_1 and X_3 directions

c. there is no external moment

At nodes 2 and 3 there are no external forces or moments. At node 4, the mass point is fixed.

All four beams have the same dimensions. These are: 2" square cross-section tube with wall thickness of 0.25 inches, lengths are 12 inches. Beams 1 and 2 have the same material, with properties

$$E = 30X10^6 psi$$

$$G = 12X10^6 psi$$

$$Y_F = 60,000psi$$

Beams 3 and 4 have the same material, with properties

$$E = 20X10^6 psi$$

$$G = 12X10^6 psi$$

$$Y_F = 45,000psi$$

The input data is given in the order shown in section C.

The displacement increments have been non-dimensionalized using reference length ALR = 12 inches. The increment program for this example is given at the end of the input data.

NUMP=4 NUB=4 KMAX=20

IELM(1,2)=1 IELM(1,3)=1 IELM(1,4)=0

IELM(2,3)=0 IELM(2,4)=1

IELM(3,4)=1

ALR=12 DR=1 $ER=30X10^{6}$ AIR=1 EPS=.005

$E=30X10^{6}$	$G=12X10^{6}$	AJ=1	AI1=1	AI2=1	A=1	AL=12	B=2	BEAM
H=2	T=0.25	Y1=1	Y2=1	CF=1	YF=60,000			1
$E=30X10^{6}$	$G=12X10^{6}$	AJ=1	AI1=1	AI2=1	A=1	AL=12	B=2	BEAM
H=2	T=0.25	Y1=1	Y2=1	CF=1	YF=60,000			2
$E=20X10^{6}$	$G=12X10^{6}$	AJ=1	AI1=1	AI2=1	A=1	AL=12	B=2	BEAM
H=2	T=0.25	Y1=1	Y2=1	CF=1	YF=45,000			3
$E=20X10^{6}$	$G=12X10^{6}$	AJ=1	AI1=1	AI2=1	A=1	AL=12	B=2	BEAM
H=2	T=0.25	Y1=1	Y2=1	CF=1	YF=45,000			4

$$DC1K(1,I,J)=\begin{bmatrix} 0 & 0 & 1 \\ .707107 & .707107 & 0 \\ -.707107 & .707107 & 0 \end{bmatrix} \qquad DC1K(2,I,J)=\begin{bmatrix} 0 & 0 & 1 \\ .707107 & -.707107 & 0 \\ .707107 & .707107 & 0 \end{bmatrix}$$

$$DC1K(3,I,J)=\begin{bmatrix} 0 & 0 & 1 \\ .707107 & -.707107 & 0 \\ .707107 & .707107 & 0 \end{bmatrix} \qquad DC1K(4,I,J)=\begin{bmatrix} 0 & 0 & 1 \\ .707107 & .707107 & 0 \\ -.707107 & .707107 & 0 \end{bmatrix}$$

DISK(1,I)=[0,0,0,0,0,0]

DISK(2,I)=[-4.242642, 4.242642, 0,0,0,0]

DISK(3,I)=[4.242642, 4.242642, 0,0,0,0]

DISK(4,I)=[0,8.485284,0,0,0,0]

DU(1)=0	DU(2)=.002	DU(3)=0	DU(4)=100	DU(5)=.01	DU(6)=100
DR(1)=0	DR(2)=0	DR(3)=0	DR(4)=0	DR(5)=0	DR(6)=0
DU(7)=100	DU(8)=100	DU(9)=100	DU(10)=100	DU(11)=100	DU(12)=100
DR(7)=0	DR(8)=0	DR(9)=0	DR(10)=0	DR(11)=0	DR(12)=0
DU(13)=100	DU(14)=100	DU(15)=100	DU(16)=100	DU(17)=100	DU(18)=100
DR(13)=0	DR(14)=0	DR(15)=0	DR(16)=0	DR(17)=0	DR(18)=0
DU(19)=0	DU(20)=0	DU(21)=0	DU(22)=0	DU(23)=0	DU(24)=0
DR(19)=0	DR(20)=0	DR(21)=0	DR(22)=0	DR(23)=0	DR(24)=0

DU(I), DU(J) ARE THE SAME FOR EACH TIME STEP.

```
MICHIGAN TERMINAL SYSTEM FORTRAN G(41336 TEST)          INCRE            08-30-73            14:12.25          PAGE P001

   0001                SUBROUTINE INCRE(M,DU,DR,K)                                                          5.000
   0002                REAL*8 DU,DR                                                                         6.000
   0003                DIMENSION DU(1),DR(1)                                                                7.000
   0004                M6=M*6                                                                               8.000
   0005                DO 10 I=1,M6                                                                         9.000
   0006                DR(I)=0.D0                                                                          10.000
   0007             10 DU(I)=100.D0                                                                        11.000
   0008                DO 16 I=1,6                                                                         12.000
   0009             16 DU(I)=0.D0                                                                          13.000
   0010                DU(2)=0.0005D0                                                                      14.000
   0011                DU(5)=0.0025D0                                                                      15.000
   0012                DO 15 I=19,M6                                                                       16.000
   0013             15 DU(I)=0.D0                                                                          17.000
   0014                RETURN                                                                              18.000
   0015                END                                                                                 19.000
    *OPTIONS IN EFFECT*  ID,EBCDIC,SOURCE,LIST,NODECK,LOAD,NOMAP
    *OPTIONS IN EFFECT*  NAME = INCRE    , LINECNT =       57
    *STATISTICS*    SOURCE STATEMENTS =       15,PROGRAM SIZE =       586
    *STATISTICS*  NO DIAGNOSTICS GENERATED
NO ERRORS IN INCRE

NO STATEMENTS FLAGGED IN THE ABOVE COMPILATIONS.
```

E. LAYOUT AND SAMPLE OF OUTPUT

The program output consists of a standard output and two optional outputs. The standard output lists forces, moments and displacements for beams and masses with respect to the global reference system. The first optional output lists the yield function values at the beam ends. The second optional output also lists the forces and moments at the beam ends relative to the local beam reference frames.

The choice of output is selected at input by the print out switch control:

IPS =	0	standard print out
	1	standard print out plus yield function values at beam ends
	2	standard print out, yield function values and local forces and moments

Samples of these outputs are shown at the end of the following discussion.

Standard Output

The first line gives the step number K and the minimum value SCFA of all loading scale factors in this step.

The output consists of two subsets, the first providing information about the masses and the second providing information about the beams. In the first line of the first output subset, labelled FORCE, columns 1-3 contain global force components F_1, F_2, F_3 and columns 4-6 contain global moment components M_1, M_2, M_3. In the second line, labelled COORD, columns 1-3 give the new coordinates and columns 4-6 give the accumulated rotation.

In the second set of output, columns 1-3 give the global force components F_1, F_2, F_3 and columns 4-6 give the global moment components M_1, M_2, M_3 of the beam at the mass number stated on that line. Each line also contains the switch setting SW, the loading scale factor SCFP and the accumulated dissipation.

First Optional Output (IPS = 1)

Lines are labelled YF I J. The first number gives the yield function value at the mass I end of the beam connecting masses I and J and the second number gives the yield function value at the mass J end.

Second Optional Output (IPS = 2)

The explanation for lines labelled YF I J was given above. In lines labelled LF @ IJ, the first six columns correspond to the local beam frame at end I and the second six columns correspond to the local beam frame at end J. The first three columns of each set of six give the local force and the second three columns give the local moment.

K= 5 SCFA= 0.65000

	1	2	3	4	5	6	SW	SCFP	DISSP
MASS 1									
FORCE	0.19723D 02	0.86968D 04	-0.49311D 01	-0.16675D 03	0.37517D 05	-0.11692D 03			
COORD	0.0	0.27900D-01	0.0	0.0	0.11625D-01	0.0			
MASS 2									
FORCE	0.16957D-10	-0.23983D-10	-0.22569D-11	0.55185D-11	0.25449D-10	-0.36524D-11			
COORD	-0.84967D 01	0.84998D 01	0.55607D-01	-0.34035D-02	0.68146D-02	0.45033D-03			
MASS 3									
FORCE	-0.14986D-10	-0.22548D-10	0.14371D-11	-0.39659D-11	0.16984D-10	0.39506D-11			
COORD	0.84968D 01	0.84997D 01	-0.55570D-01	0.34026D-02	0.68232D-02	-0.41014D-03			
MASS 4									
FORCE	-0.19723D 02	-0.86968D 04	0.49311D 01	0.83439D 02	-0.37504D 05	-0.21907D 03			
COORD	0.0	0.16971D 02	0.0	0.0	0.0	0.0			

FORCE & MOMENT ON EACH BEAM ENDS

	1	2	3	4	5	6	SW	SCFP	DISSP
BM 1@ 1	-0.21084D 03	-0.43409D 04	-0.17032D 04	-0.15951D 05	-0.18742D 05	0.20396D 05	0	1.00000	0.0
BM 1@ 2	-0.21084D 03	-0.43409D 04	-0.17032D 04	-0.18392D 04	-0.42742D 04	-0.18224D 05	0	1.00000	0.0
BM 2@ 1	0.19112D 03	-0.43560D 04	0.17082D 04	0.16118D 05	-0.18775D 05	-0.20279D 05	0	1.00000	0.0
BM 2@ 3	0.19112D 03	-0.43560D 04	0.17082D 04	0.19653D 04	-0.42660D 04	0.18302D 05	0	1.00000	0.0
BM 3@ 2	-0.21084D 03	-0.43409D 04	-0.17032D 04	-0.18392D 04	-0.42742D 04	-0.18224D 05	0	1.00000	0.0
BM 3@ 4	-0.21084D 03	-0.43409D 04	-0.17032D 04	0.12918D 05	-0.18736D 05	0.16805D 05	0	0.67700	0.0
BM 4@ 3	0.19112D 03	-0.43560D 04	0.17082D 04	0.19653D 04	-0.42660D 04	0.18302D 05	0	1.00000	0.0
BM 4@ 4	0.19112D 03	-0.43560D 04	0.17082D 04	-0.12834D 05	-0.18768D 05	-0.17024D 05	1	0.65000	0.0

```
K=  5  YIELD FUNCTION & LOCAL FORCES AT EACH BEAM END

YF @ MB  1     0.64671D 00     0.18910D 00
LF@BM  1 -0.171D 04-0.320D 04-0.293D 04 0.202D 05-0.247D 05-0.181D 04 -0.172D 04-0.321D 04-0.292D 04-0.183D 05-0.419D 04-0.176D 04
YF @ MB  2     0.64681D 00     0.19065D 00
LF@BM  2  0.171D 04 0.320D 04-0.296D 04-0.201D 05 0.248D 05-0.171D 04  0.172D 04 0.320D 04-0.295D 04 0.183D 05 0.427D 04-0.167D 04
YF @ MB  3     0.37043D 00     0.98832D 00
LF@BM  3 -0.172D 04 0.292D 04-0.321D 04-0.183D 05 0.176D 04-0.419D 04 -0.170D 04 0.292D 04-0.322D 04 0.168D 05 0.224D 05-0.411D 04
YF @ MB  4     0.37413D 00     0.99992D 00
LF@BM  4  0.172D 04-0.295D 04-0.320D 04 0.183D 05-0.167D 04-0.427D 04  0.171D 04-0.294D 04-0.322D 04-0.170D 05-0.223D 05-0.420D 04
```

A.2 PROGRAM INFORMATION

The discussion concerning the program is divided into several subsections

A. List of Major Program Variables

B. List of Subroutines and Switches

C. Flow Diagrams
   (i) Main Flow Diagram
   (ii) Assembling Global Stiffness Matrix
   (iii) Solving for Unknown Nodal Force and Displacement Components

A. List of Major Program Variables

All equation numbers refer to Chapter 2, Analysis

Program Listing Notation	Analysis Notation	Description
AJF(I,J)	$\bar{J}$	matrix in equation (42) I = 1,2,3; J = 1,2,3
DC1K(LB,I,J)	$L_k^{F_i}$	direction cosine matrix at end 1(i) of beam LB at end of step K. LB = 1,...,NUB; I = 1,2,3; J = 1,2,3
DC1KP1(LB,I,J)	$L_{k+1}^{F_i}$	direction cosine matrix at end 1 of beam LB at end of step K+1. LB = 1,...,NUB; I = 1,2,3; J = 1,2,3
DC2K(LB,I,J)	$L_k^{F_j}$	direction cosine matrix at end 2(j) of beam LB at end of step K. LB = 1,...,NUB; I = 1,2,3; J = 1,2,3
DC2KP1(LB,I,J)	$L_{k+1}^{F_j}$	direction cosine matrix at end 2 of beam LB at end of step K+1. LB = 1,...,NUB; I = 1,2,3, J = 1,2,3
DDK(LB,I)	$\Delta\dot{d}_k$	accumulated plastic energy dissipation at beam LB, end I at end of step K. LB = 1,...,NUB; I = 1,2
DISK(I)	$\begin{bmatrix} X_i \\ \theta_i \end{bmatrix}_k$	location and orientation of mass point LMP in global system at end of step K. I = 1, ...,6 *NUMP
DISKP1(I)	$\begin{bmatrix} X_i \\ \theta_i \end{bmatrix}_{k+1}$	location and orientation of mass point LMP in global system at end of step K+1. I = 1,...,6*NUMP
DISSK(LB,I)	$\dot{d}_{k+1}$	increment of plastic energy dissipation at beam LB, end I at end of step K+1. LB = 1,...,NUB; I = 1,2.

Program Listing Notation	Analysis Notation	Description
DR(I)		nodal generalized force increment vector in global system. (I = 1,..., 6*NUMP). The LMPth group of six components correspond to mass point LMP In each group of six, the first three components are those of the force increment vector at LMP. The second three components are those of the moment increment vector at mass point LMP.
DRN(LB,I)		matrix in which the elements of row LB are the components of the generalized force increment DRS acting on beam LB, LB = 1,...,NUB; I = 1,...,12
DRS(I)	$\dot{\underline{R}}$	generalized force vector increment acting on a beam, I = 1,...,12. (Eq(8))
DU(I)		nodal generalized displacement incremen vector in global system. (I = 1,..., 6*NUMP) The LMPth group of six components correspond to mass point LMP In each group of six, the first three components are those of the displacement increment vector of mass point LMP. The second three components are those of the rotation increment vector of mass point LMP.
DUP(I)	$\dot{K}^i$	plastic deformation rate vector I = 1,...,4 (Eq (51))
DUS(I)	$\dot{D}$	generalized displacement increment acting on a beam, I = 1,...,12. (Eq(8))
EBI(I,J)	$\hat{E}_i$	matrices defined in Eq(67),I = 1,2,3; J = 1,...,6.
EBJ(I,J)	$\hat{E}_j$	
EBHI(I,J)	$\hat{\bar{E}}_i$	matrices defined in Eq(67), I,J = 1,2,3.
EBHJ(I,J)	$\hat{\bar{E}}_j$	

Program Listing Notation	Analysis Notation	Description
FK(LB,I)		matrix in which the elements of row LB are the values of the yield function at the ends of beam LB at step K. LB = 1,...,NUB; I = 1,2.
FKP1(I)		yield function at the two ends of a beam, I = 1,2
FRK(I)	$\begin{bmatrix} F_{i_{R_i}} \\ F_{i_{R_j}} \end{bmatrix}_k$	generalized force vector on beam ends in local frames at end of step K. I = 1,...,12
FRKL(I)		temporary storage for force vectors at beam ends in local frames, I = 1,...,12.
FRKP(I)	$\begin{bmatrix} F_{i_{R_i}} \\ F_{j_{R_j}} \end{bmatrix}_{k+1}$	generalized force vector on beam ends in local frames at end of step K+1, I = 1,...,12.
G1(I,J) G2(I,J)	G^i G^j	matrices for i & j ends of a beam, appearing in Eq(55)-(58). I = 1,...,4; J = 1,...,6.
G1RJ(I,J)	$\bar{J}\cdot G^i_R$	product of matrix AJF and the lower three rows of G1, (see Eq(69)) I = 1,2,3; J = 1,...,6
G1S(LB,I,J) G2S(LB,I,J)		matrices G^1 and G^2 of Eq(55)-(58) corresponding to beam LB, LB = 1,..., NUB; I = 1,...,4; J - 1,...,6.
GBI(I,J) GBJ(I,J)	$\bar{G}^i$ $\bar{G}^j$	matrices for i & j ends of a beam appearing in Eq(55)-(58), I = 1,...,4; J = 1,2,3.
GBIT(LB,I,J) GBJT(LB,I,J)		matrices $\bar{G}^i$ and $\bar{G}^j$ of Eq(55)-(58) corresponding to beam LB, LB = 1,..., NUB; I = 1,...,4; J = 1,...,3.

Program Listing Notation	Analysis Notation	Description
GRF(I)	∇f	gradient of yield function (Eq(49)), I = 1,...,4.
HBIP(I,J)	$\bar{H}^{ip}$	matrices for i and j ends of a beam appearing in Eqs(60) and (61). I,J = 1,2,3
HBJP(I,J)	$\bar{H}^{jp}$	
HBIPT(LB,I,J)		matrices $\bar{H}^{ip}$, $\bar{H}^{jp}$ of Eqs(60) and (61) corresponding to beam LB, LB = 1,...,NUB; I,J = 1,2,3.
HBJPT(LB,I,J)		
HP1(I,J)	H^{ip}	matrices for i and j ends of a beam appearing in Eqs(60) and (61) I = 1,2,3; J = 1,...,6.
HP2(I,J)	H^{jp}	
HP1S(LB,I,J)		matrices H^{ip},H^{jp} of Eqs(60) and (61) corresponding to beam LB, LB = 1,...,NUB; I,J = 1,2,3
HP2S(LB,I,J)		
HR(I,J)	H_R	matrix defined by Eq(26) I,J = 1,2,3
IELM(I,J)		type of beam relation between node I and node J I = 1,...,NUMP-1; J = I+1,...,NUMP.
KRT(I,J)	KRT	matrices appearing in Eq(68) I,J = 1,...,6; M = 1,...,6; N = 1,2,3
KRTB(M,N)	$\overline{KRT}$	
P(I,J)	$(T^{F_i})^T A(T^{F_i})$	matrix appearing in Eq(44), using A defined by Eq(32),I,J = 1,...,6
RK(I)		vector of force and moment components with respect to the global system at end of step K, I = 1,...,NUMP*6. The LMPth group of six components correspond to mass LMP. In each group of six, the first three components are those of the force vector on mass point LMP. The second three components are those of the moment vector on mass point LMP.

Program Listing Notation	Analysis Notation	Description
RKP1(I)		vector of force and moment components with respect to the global system at end of step K+1, I = 1,...,6*NUMP. See definition of RK(I) for component definition.
RNK(LB,I)	$\begin{bmatrix} R_i \\ R_j \end{bmatrix}_k$	matrix in which the elements of row LB are the global components of the generalized force vector on beam LB at step K, LB = 1,...,NUB; I = 1,...,K.
RNKP(I)		global components of the generalized force vector on a beam at step K+1, I = 1,...,12
RNKP1(LB,I)		matrix in which the elements of row LB are the global components of the generalized force vector acting on beam LB at step K+1, LB = 1,...,NUB; I = 1,...,12
SCFA		minimum value of set of scaling factors SCFP.
SCFD(LB,I)		scaling factor at end I of beam LB due to unloading, LB = 1,...,NUB; I = 1,2.
SCFP(LB,I)		scaling factor at end I of beam LB due to loading from the elastic to the plastic state. LB = 1,...,NUB; I = 1,2
SK(LB,I,J)		matrix $H^{-1}B$ defined by Eq(72) for beam LB; LB = 1,...,NUB; I,J = 1,...,12
STIF1(I,J)	$\begin{bmatrix} K_U \\ \hline K_L \end{bmatrix}$	matrix defined by Eq(65),I,J = 1,...,6

Program Listing Notation	Analysis Notation	Description
STK(I,J)	$K = H^{-1}B$	matrix defined by Eq(72) I,J = 1,...,12.
SW(LB,I)	S^{i}	switch setting for end I of beam LB, defined by Eq(73),LB = 1,...,NUB, I = 1,2.
TK(I,J)		global stiffness matrix; I,J = 1,...,6*NUMP.

B. List of Subroutines and Switches

List of Subroutines

1. DISSP(G,GB,DR,DU,N,AL,DUP,DC)

    Purpose: to compute the dissipation

    Input quantities:

    G,GB = G1,GBI or G2,GBJ

    DR: nodal force increment vector

    DU: nodal displacement increment vector

    N: N = 1 is beam end i
    2 is beam end j

    AL: beam length

    DC: direction cosine

    Output quantity

    DUP: plastic displacement vector

2. DMAX(A,B,NUB)

    Purpose: to determine the maximum component of a vector

    Input quantities:

    A: input array

    NUB: number of beams

    Output quantity

    B : maximum element of A

3. DMIN(A,B,NUB)

    Purpose: to determine the minimum component of a vector

    Input quantities:

    A: input array

    NUB: number of beams

    Output quantity

    B: minimum element of A

4. FRKS(RKP1,DC1KP1,DC2KP1,FRKP1)

Purpose: to compute force and moment components with respect to local coordinates.

Input quantities:

RKP1: global components of generalized force vector on a beam

DC1KP1: direction cosine matrix at i end (end 1)

DC2KP1: direction cosine matrix at j end (end 2)

Output quantity

FRKP1: generalized force vector on a beam in local frame

5. GHP(DC,AL,G,HP,FRK,GRF,N,HB,EBH,GB)

Purpose: to find the G,HP,HB,EBH,GB matrices at each node point

Input quantities:

AL: beam length

DC: direction cosine

FRK: local generalized force vector

GRF: gradient of yield function

N: N = 1 if beam end is i
   2 if beam end is j

Output quantities

If N = 1: G1	If N = 2: G2
HP1	HP2
HBIP	HBJP
EBHI	EBHJ
GBI	GBJ

6. GMPRD(A,B,R,N,M,L)

Purpose: matrix multiplication

Input quantities:

A: NXM matrix

B: MXL matrix

Output quantity

R: NXL matrix

7. GRYF1(LB,FRK,GRF,N)

Purpose: to find gradient of the yield function for the rectangular tube section

Input quantities:

LB: beam number

FRK: generalized force vector on beam ends in local frame

N: N = 1 if end I
= 2 if end j

Output quantity

GRF: gradient vector at end N

8, HINVB(ST1F1,P,HR,HIP,HJP,AJF,DC1,ST1F, EBI,EBJ,GRB1,HBIP,HBJP,EBHI,EBHJ)

Purpose: to find the matrix $K = H^{-1}B$ for a beam

Input quantities:

P, AJF, HR	matrices defined in List of Program Variables.
HIP, HJP	matrices HP1,HP2 in List of Program Variables
EBI, EBJ, HBIP, HBJP, EBHI, EBHJ, ST1F1	matrices defined in List of Program Variables
GRBI	lower three rows of GBI matrix
DC1	direction cosine matrix

Output quantity

STIF: matrix $H^{-1}B$, local stiffness matrix

9. INCRE(M,DU,DR,K)

Purpose: to read in the increment of displacement and force

Input quantities:

M: mass point number

K: step number

Output quantities

DU: displacement increment vector

DR: force increment vector

10. INPUT(M,NEN,IELM)

Purpose: to read in the initial position, forces and switch setting and material properties of each beam

Input quantities:

M: mass point number

NEN: beam number

IELM: relation between mass points I and J

11. INV(M,N,A,IM,L,B)

(Library Subroutine, University of Michigan Computing Center)

Purpose: matrix inversion

Input quantities:

A: matrix to be inverted

M: size of matrix A

N: maximum size of matrix A

IM: 2M dimension vector

Output quantity

B: matrix A^{-1}

12. SUBROUTINE KR1(DC,HIP,HB1P,FL,LB,AL,KRT,KRTB)

Purpose: to comput the matrices KRT and $\overline{KRTB}$ in the H and B matrices

Input quantities:

DC: direction cosine

HIP: H^{ip}

HBIP: $\overline{H}^{ip}$

FC: force at local frame (12 elements)

LB: beam number

AL: beam length

Output quantity

KRT: KRT

KRTB: $\overline{KRT}$

13. KUKL(DCI,ST1F1,P,HR,G1RJ,LB,AL)

Purpose: to find the elastic stiffness matrix and associated matrices P and HR

Input quantities:

DCI: direction cosine

G1RJ: matrix from list of variables

LB: beam number

AL: beam length

Output quantities

$\left.\begin{array}{r}\text{ST1F1}\\ \text{P}\\ \text{HR}\end{array}\right\}$ matrices defined in List of Program Variables

14. NEWDC (HIP,HJP,DR,DD,DCI,DCJ,D1,D2,HBIP,HBJP)

Purpose: to compute new direction cosines

<u>Input quantities:</u>

HIP,HJP: matrices HP1,HP2 in List of Program Variables

HBIP,HBJP: matrices in List of Program Variables

DCI,DCJ: direction cosine matrices at I and J ends

DR: increment in generalized force vector

DD: increment in generalized displacement

<u>Output quantities</u>

D1:
D2: new direction cosines at $\frac{i}{j}$ ends

15. OUTP(K,IELM,RK,D1SK,RNKP1,SW,SCF,SCF1,
SCFA,IPS,NUMP,NUB,FK1,FRK1)

Purpose: to print out the final force components and coordinates

<u>Input quantities:</u>

RK: total force at each mass

RNKP1: total force at each beam end

K: step number

IELM: type of beam relation between mass points I and J

D1SK: location and orientation of mass points

SW: switch setting

NUMP: number of mass point

NUB: beam number

SCF: loading scale factor

SCF1: unloading scale factor

SCFA: minimum loading scale factor

SCFB: minimum unloading scale factor

IPS: print out switch control

FK1: yield function values at beam ends

FRK1: beam end force vector in local frame

16. SCFS1(FRKP1,FR,D,N,I,LB)

Purpose: to scale displacement increment so that resulting force stays on the yield surface

Input quantities:

FRKP1: local force vector at step K+1

FR: local force vector at step K

N: beam end i or j

LB: beam number

Output quantity

D: scaling factor

J: number of iterations

17. YFCT1(LB,FR,FK)

Purpose: to compute the yield function for the rectangular tube section

Input quantities:

LB: beam number

FR: local force vector

Output quantity

FK: value of yield function

List of Control Switches

1. IDS dissipation switch control

   Purpose: to allow choice of loading or unloading at a negative dissipation increment

IDS = 0	at a negative dissipation increment, switch SW stays = 1
1	at a negative dissipation increment, switch SW is set = 0 causing unloading

2. IPS print out switch control

   Purpose: to select amount of print out

IPS = 0	standard print out
1	standard print out plus yield function values at beam ends
2	standard print out, yield function values and local forces and moments

C. Flow Diagrams

(i) Main Flow Diagram

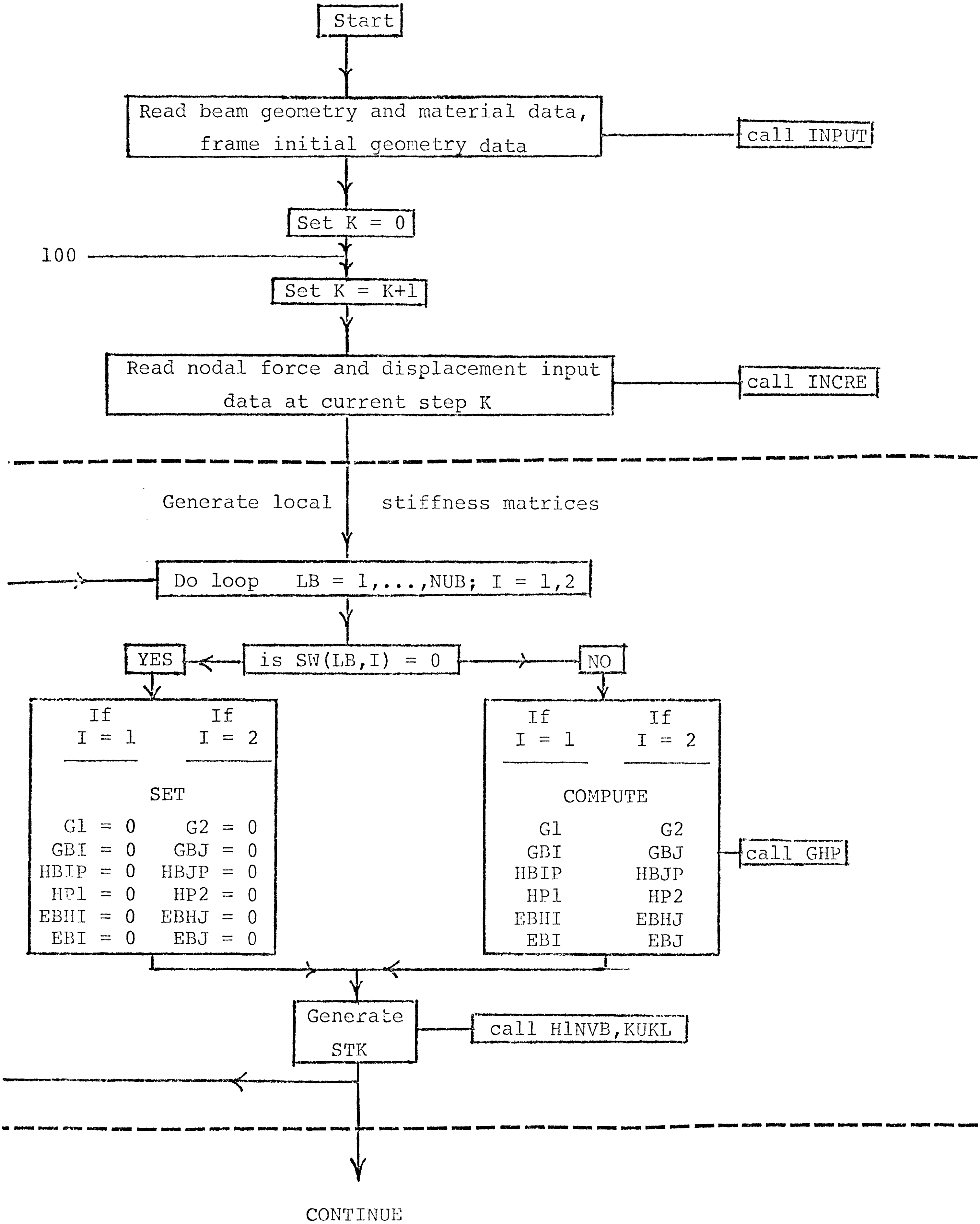

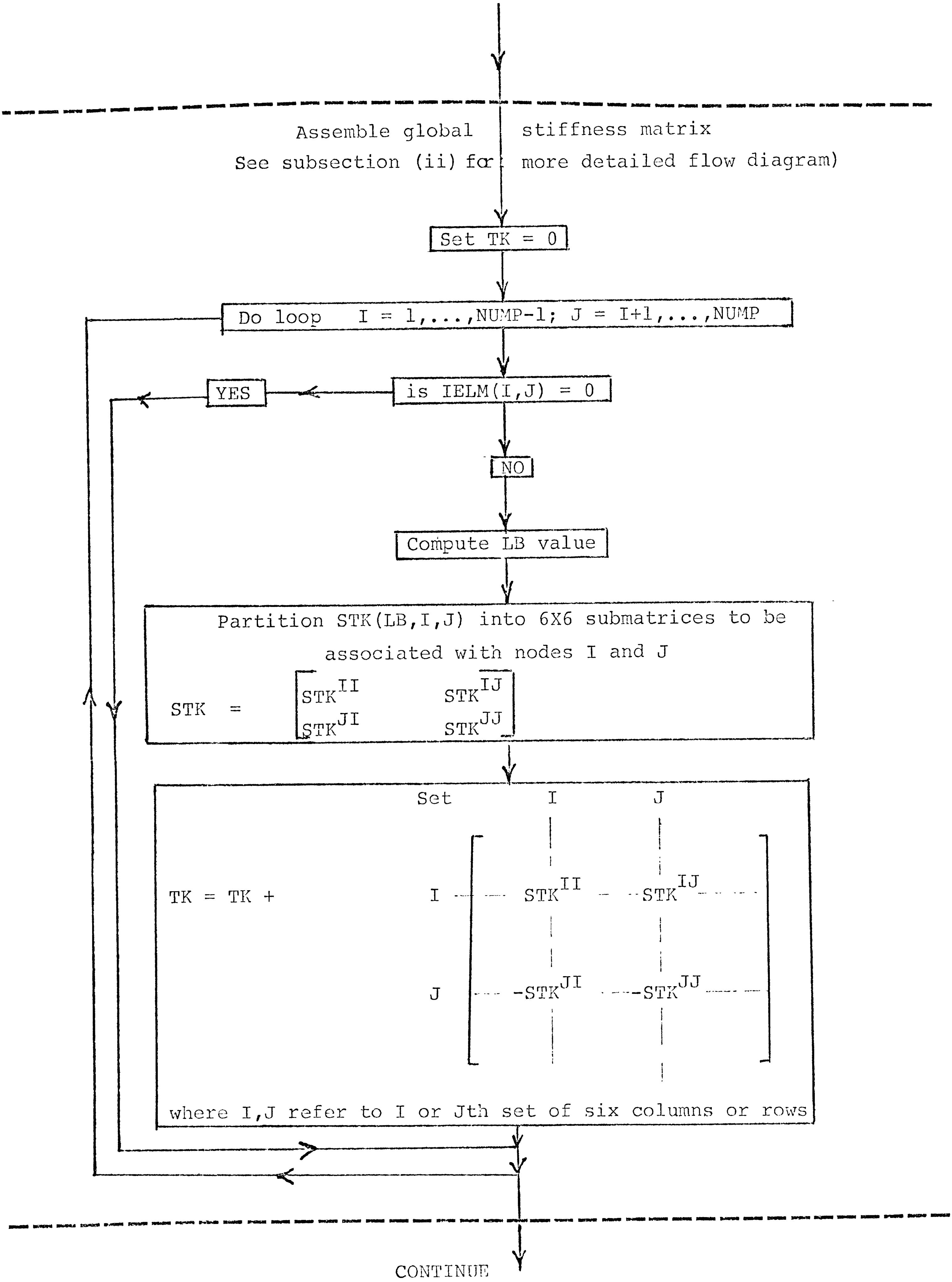
Assemble global stiffness matrix
See subsection (ii) for more detailed flow diagram)
Set TK = 0
Do loop I = 1,...,NUMP-1; J = I+1,...,NUMP
is IELM(I,J) = 0
YES
NO
Compute LB value
Partition STK(LB,I,J) into 6X6 submatrices to be associated with nodes I and J
STK = [STK^II STK^IJ; STK^JI STK^JJ]
Set
I
J
TK = TK +
I
STK^II
STK^IJ
J
-STK^JI
-STK^JJ
where I,J refer to I or Jth set of six columns or rows
CONTINUE

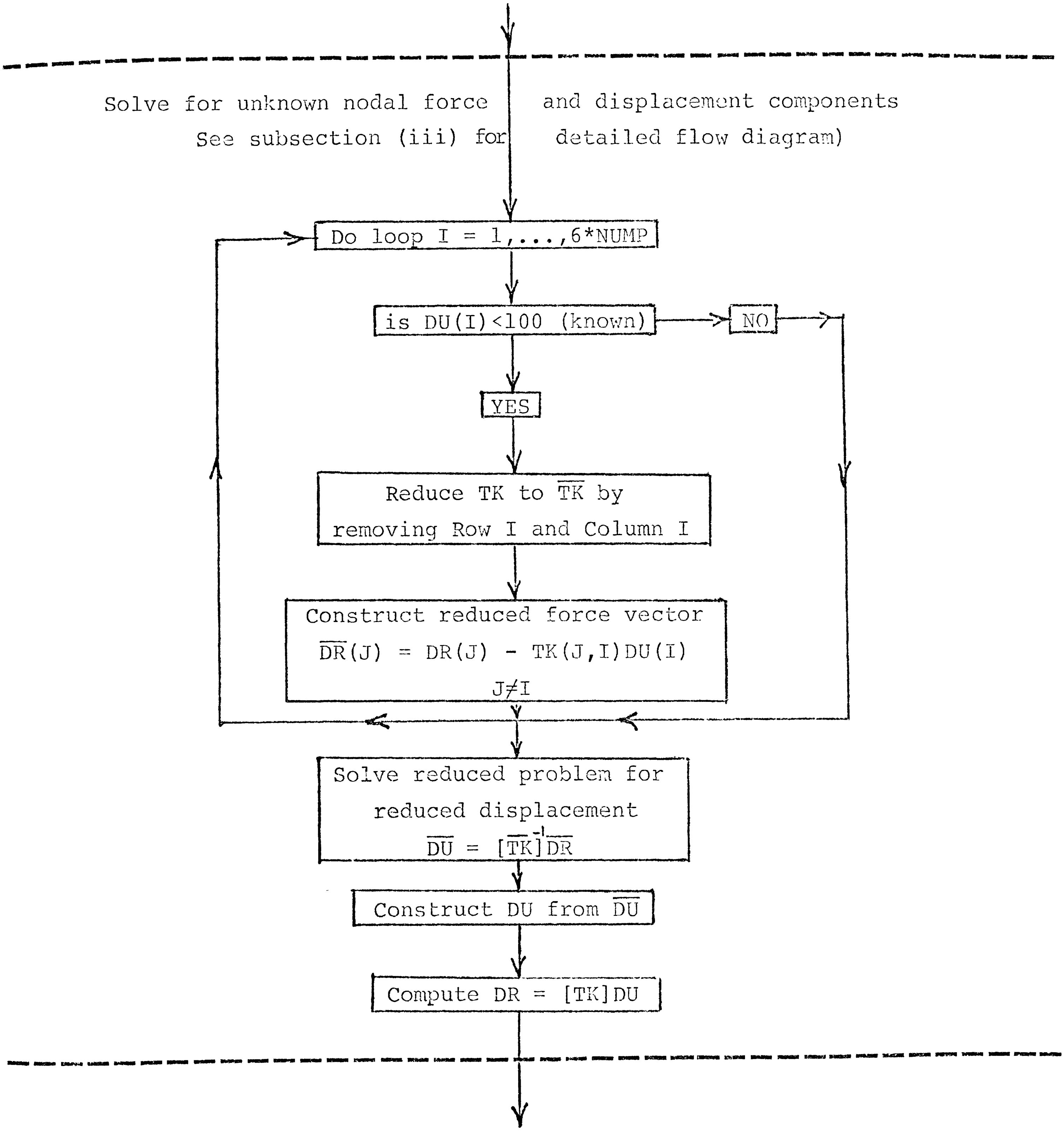
Solve for unknown nodal force and displacement components
See subsection (iii) for detailed flow diagram)
Do loop I = 1,...,6*NUMP
is DU(I)<100 (known)
NO
YES
Reduce TK to $\overline{TK}$ by removing Row I and Column I
Construct reduced force vector
$\overline{DR}(J) = DR(J) - TK(J,I)DU(I)$
$J \neq I$
Solve reduced problem for reduced displacement
$\overline{DU} = [\overline{TK}]^{-1}\overline{DR}$
Construct DU from $\overline{DU}$
Compute DR = [TK]DU

CONTINUE

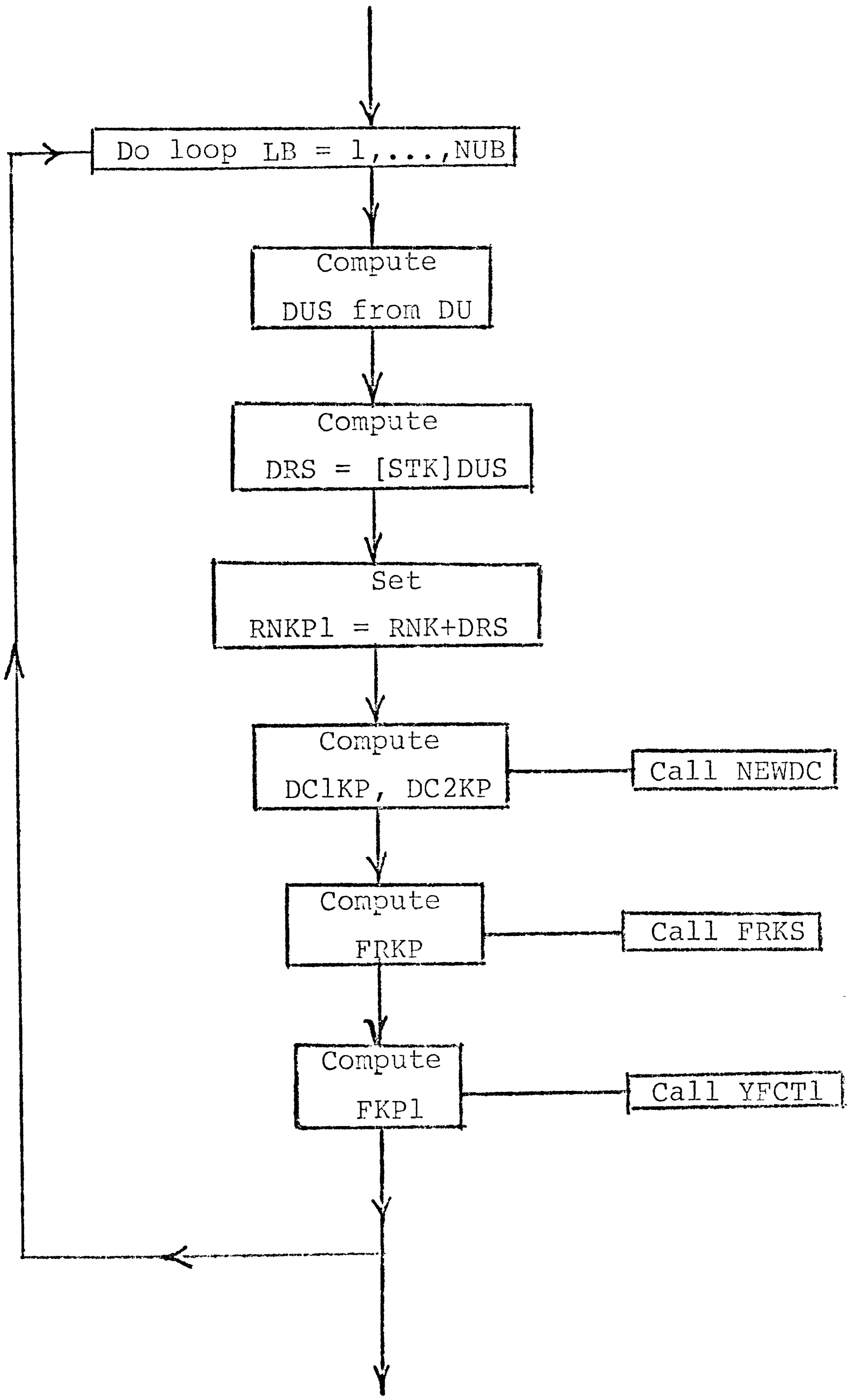
Do loop LB = 1,...,NUB
Compute
DUS from DU
Compute
DRS = [STK]DUS
Set
RNKP1 = RNK+DRS
Compute
DC1KP, DC2KP
Call NEWDC
Compute
FRKP
Call FRKS
Compute
FKP1
Call YFCT1

CONTINUE

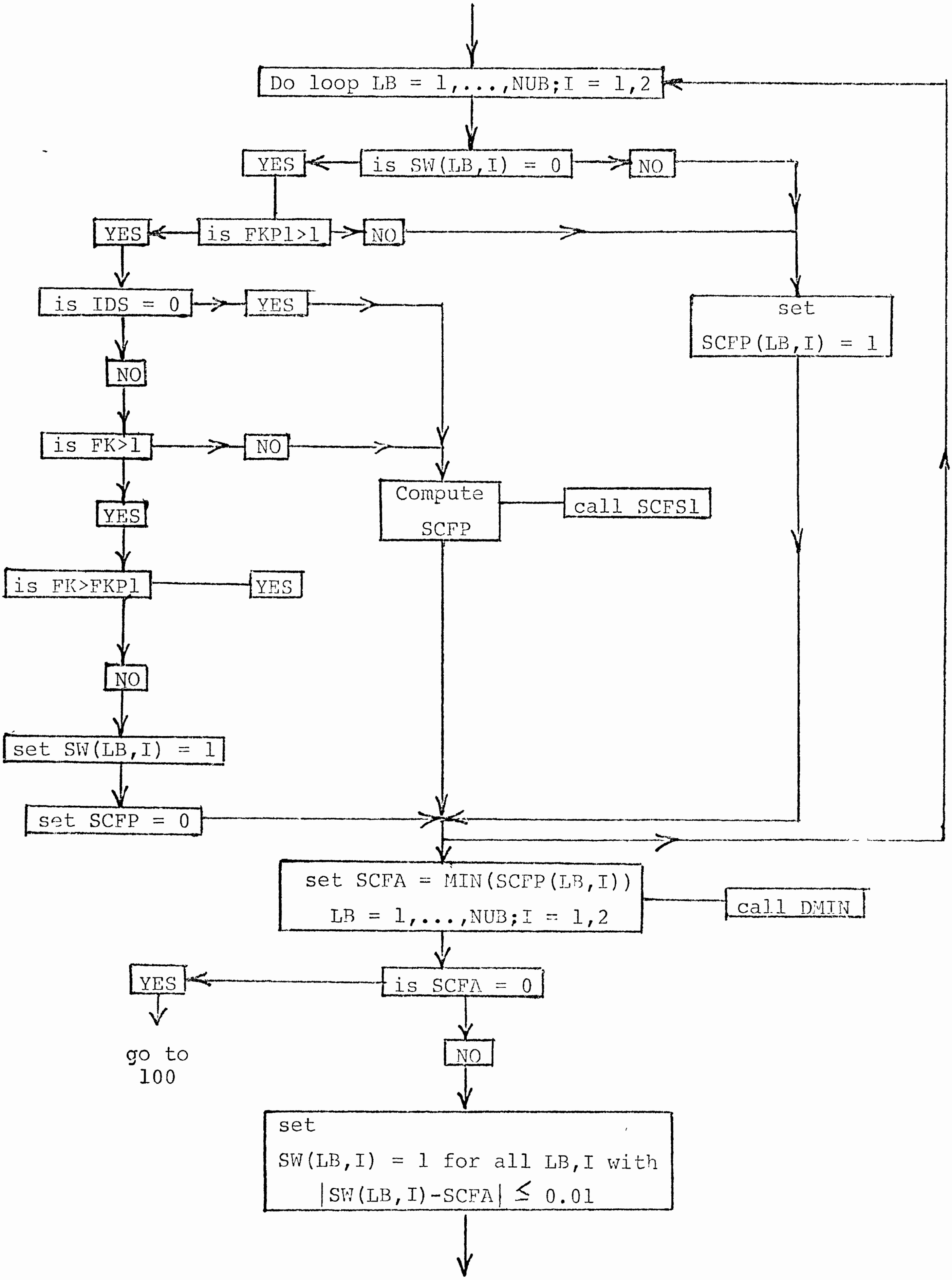
Do loop LB = 1,...,NUB;I = 1,2
is SW(LB,I) = 0
YES
NO
is FKP1>1
YES
NO
is IDS = 0
YES
NO
set
SCFP(LB,I) = 1
is FK>1
NO
Compute
SCFP
call SCFS1
YES
is FK>FKP1
YES
NO
set SW(LB,I) = 1
set SCFP = 0
set SCFA = MIN(SCFP(LB,I))
LB = 1,...,NUB;I = 1,2
call DMIN
YES
is SCFA = 0
go to
100
NO
set
SW(LB,I) = 1 for all LB,I with
|SW(LB,I)-SCFA| ≤ 0.01
CONTINUE

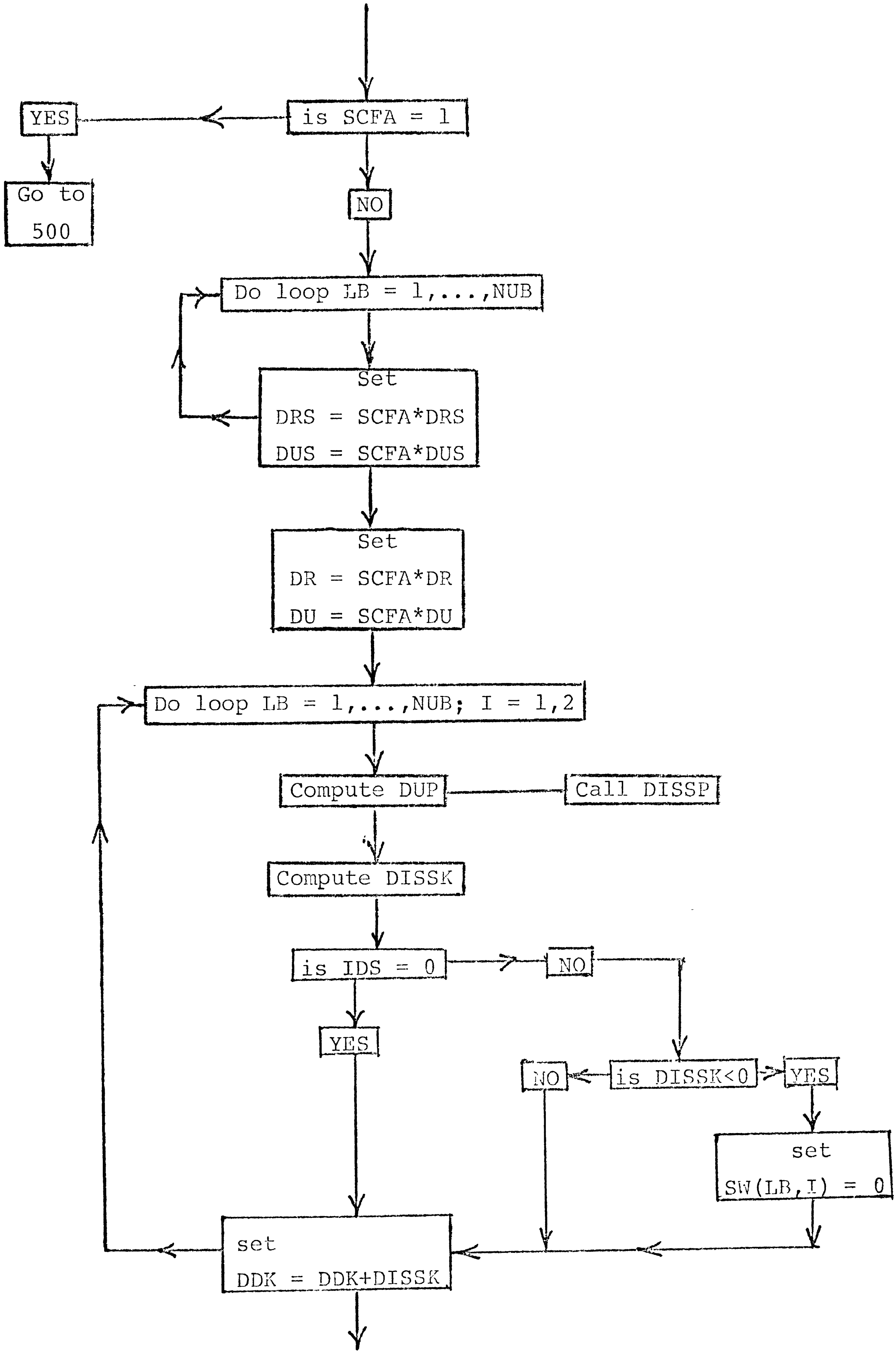
is SCFA = 1
YES
Go to 500
NO
Do loop LB = 1,...,NUB
Set
DRS = SCFA*DRS
DUS = SCFA*DUS
Set
DR = SCFA*DR
DU = SCFA*DU
Do loop LB = 1,...,NUB; I = 1,2
Compute DUP
Call DISSP
Compute DISSK
is IDS = 0
NO
YES
is DISSK<0
NO
YES
set
SW(LB,I) = 0
set
DDK = DDK+DISSK

CONTINUE

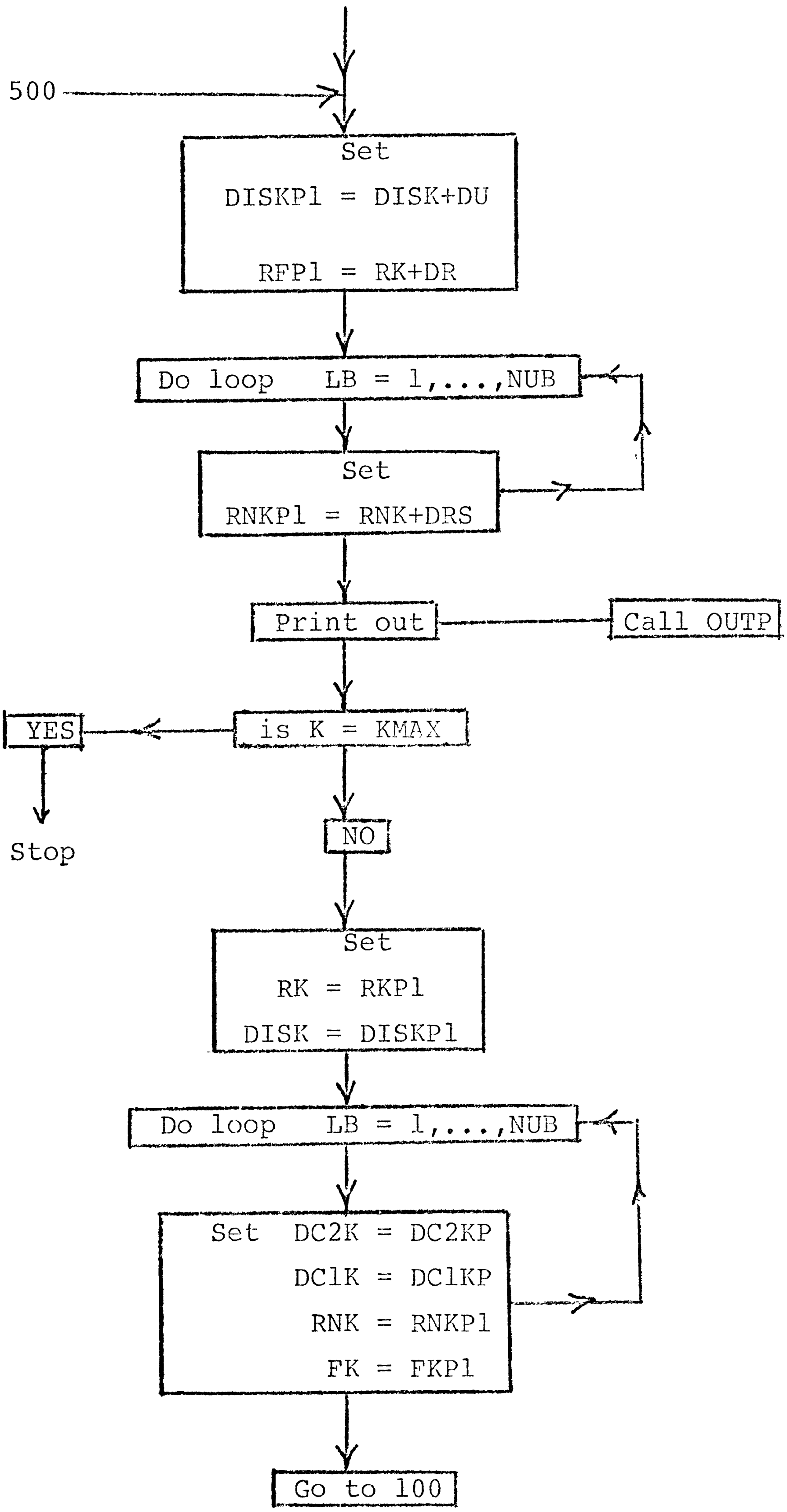

500
Set
DISKP1 = DISK+DU
RFP1 = RK+DR
Do loop LB = 1,...,NUB
Set
RNKP1 = RNK+DRS
Print out
Call OUTP
is K = KMAX
YES
Stop
NO
Set
RK = RKP1
DISK = DISKP1
Do loop LB = 1,...,NUB
Set DC2K = DC2KP
DC1K = DC1KP
RNK = RNKP1
FK = FKP1
Go to 100

(ii) Assembling Global Stiffness Matrix

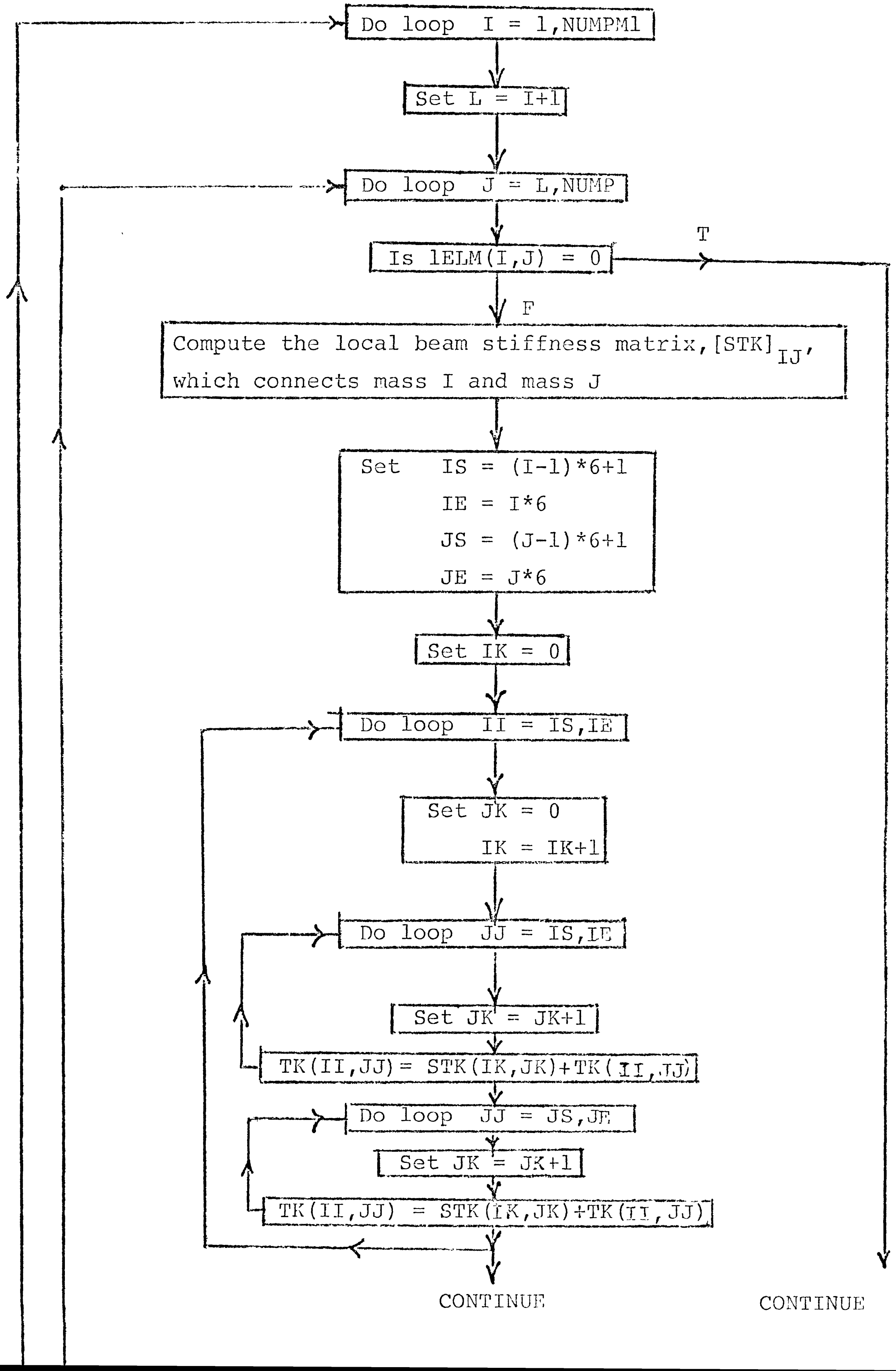

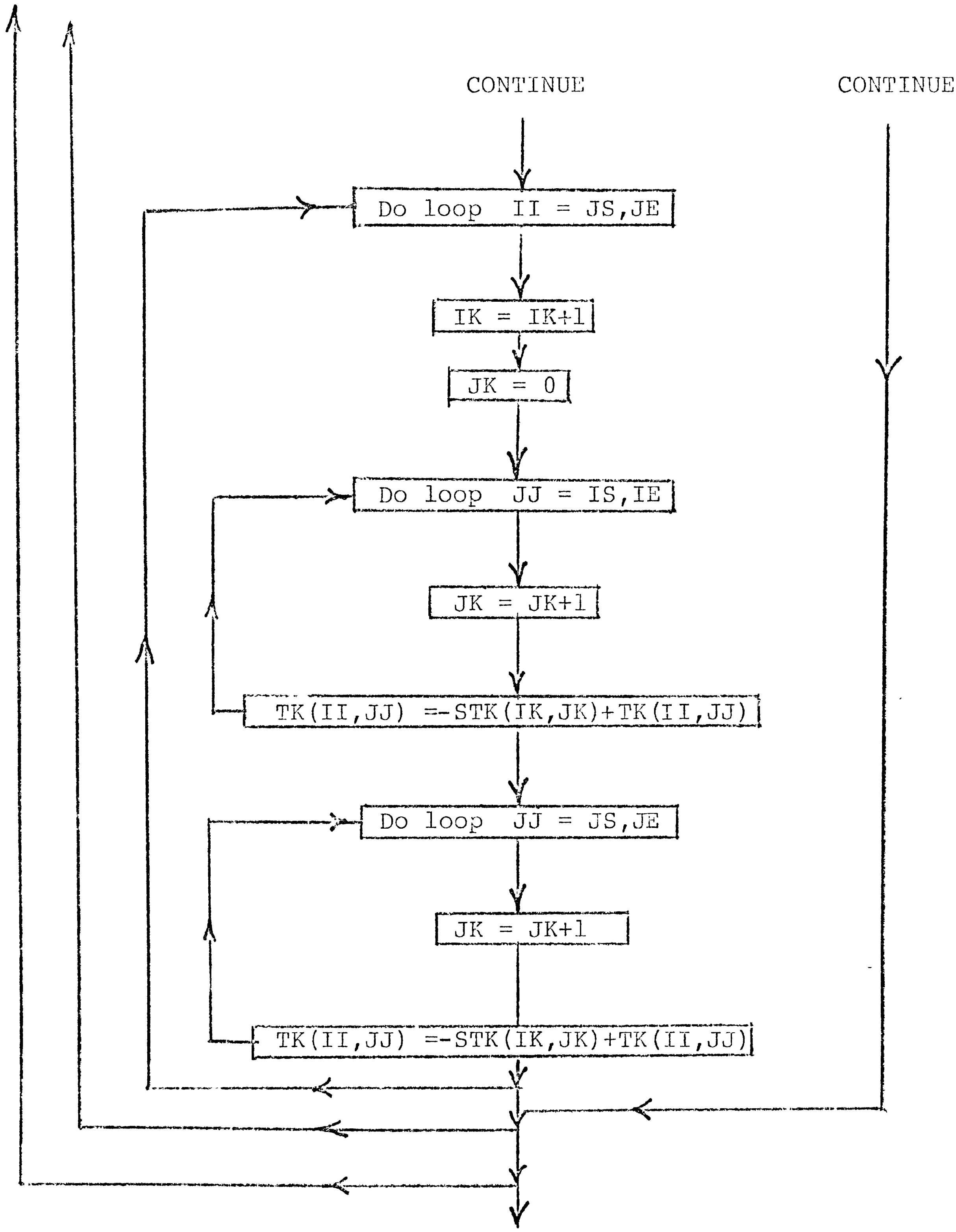
CONTINUE
CONTINUE
Do loop II = JS,JE
IK = IK+1
JK = 0
Do loop JJ = IS,IE
JK = JK+1
TK(II,JJ) =-STK(IK,JK)+TK(II,JJ)
Do loop JJ = JS,JE
JK = JK+1
TK(II,JJ) =-STK(IK,JK)+TK(II,JJ)

CONTINUE

(iii) Solving for Unknown Nodal Force and Displacement Components

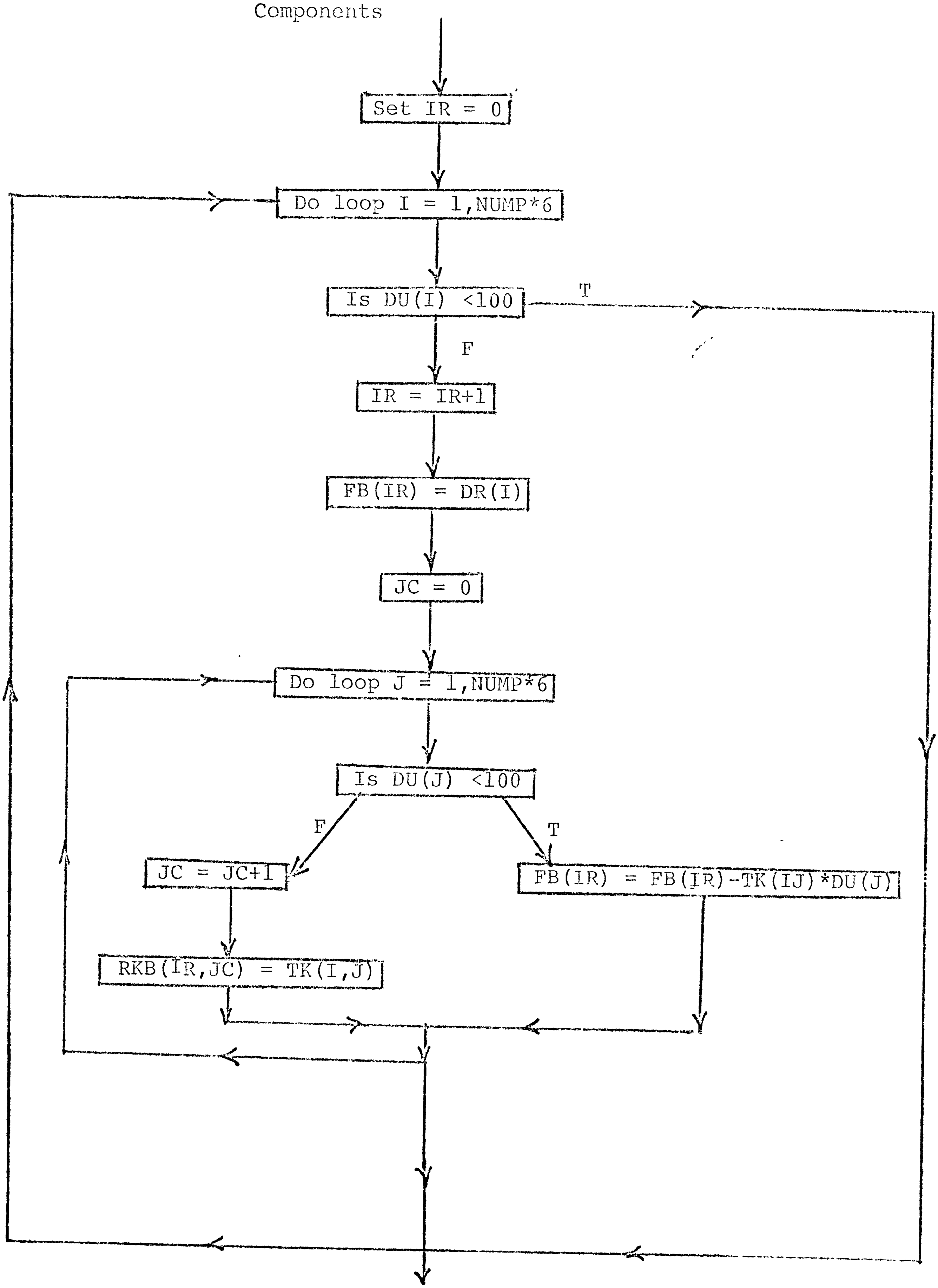

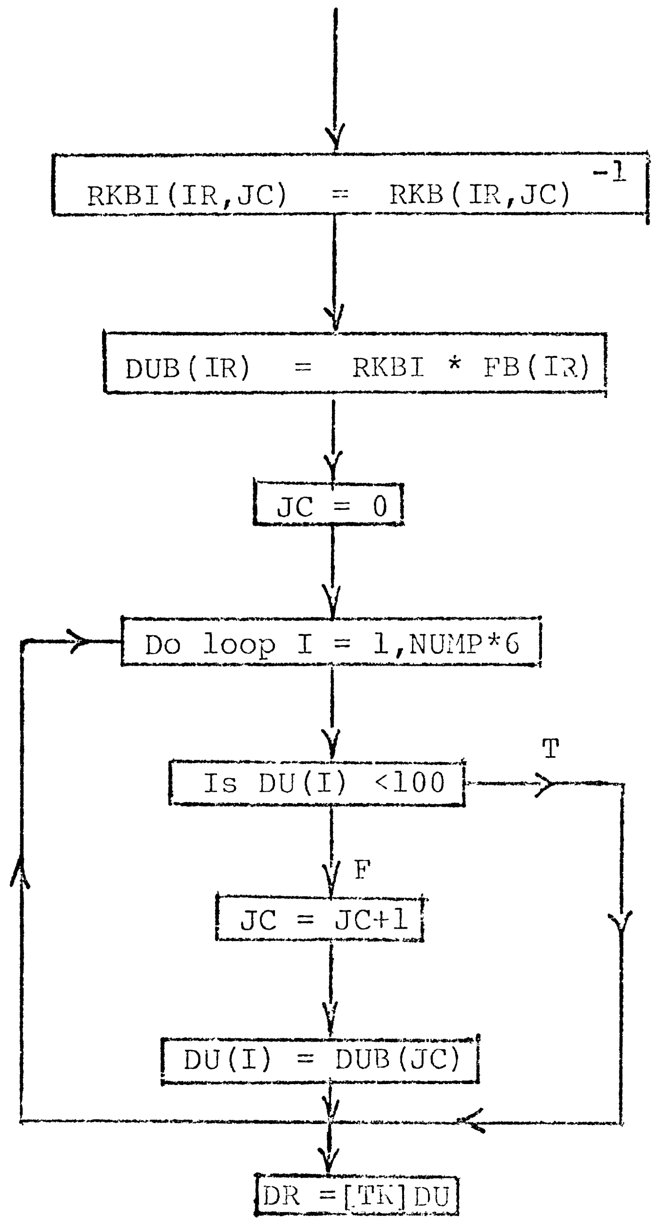
RKBI(IR,JC) = RKB(IR,JC) -1
DUB(IR) = RKBI * FB(IR)
JC = 0
Do loop I = 1,NUMP*6
Is DU(I) <100
T
F
JC = JC+1
DU(I) = DUB(JC)
DR =[TK] DU

APPENDIX B

B.1 PROGRAM LISTING

```
0001             IMPLICIT REAL *8(A-H,P-Z)
           C     MAIN PROGRAM
           C     THIS PROGRAM CAN BE USED FOR MAXIMUM 15 MASSES &20 BEAMS
0002             INTEGER SW,SWT
0003             REAL *8 M10,M20,M30
0004             DIMENSION AKRT(6,6),BKRT(6,3)
0005             DIMENSION IELM(14,15),RK(90),RKP1(90),DISK(90),DISKP1(90),
               1  FRK(20,12),FRKP(20,12),SW(20,2),SCFP(20,2),SCFD(20,2),DC1(3,3),
               2  DC2(3,3),DC1P1(3,3),DC2P1(3,3),DC1K(20,3,3),DC2K(20,3,3),
               3  DC1KP1(20,3,3),DC2KP1(20,3,3),AL(20),DDK(20,2),DISSK(20,2),
               4  TK(90,90),FRKL(12),GRF(4),G1(4,6),G2(4,6),HP1(3,6),HP2(3,6),
               5  G1S(20,4,6),G2S(20,4,6),HP1S(20,3,6),HP2S(20,3,6),G1R(3,6),
               6  AJF(3,3),G1RJ(3,6),STIF1(6,6),P(6,6),HR(3,3),STK(12,12),
               7  SK(20,12,12),DR(90),DU(90),DUS(12),DRS(12),DRN(20,12),
               8  RNKP(12),RNK(20,12),FRKP1(12),FKP1(2),FK(20,2),RNKP1(20,12),
               9  DUP(4),FB(90),DUB(90),RKB(90,90),RKBI(90,90),IMPERM(180)
0006             DIMENSION OI(6),OJ(6),FBI(3,6),FBJ(3,6)
0007             DIMENSION IT(90),NT(90),GBJT(20,4,3),GBIT(20,4,3),HBIT(20,3,3),
               1  HBJT(20,3,3),GBI(4,3),GBJ(4,3),GRBI(3,3),HBIP(3,3),HBJP(3,3),
               2  FBHI(3,3),FBHJ(3,3),DYF(20,2),FK1(20,2)
0008             COMMON/COMF/DC1K,DC2K,SW,FK,DDK,RK,FRK,DISK,AL
0009             COMMON/COMF/SCFD,SCFP
           C     READ IN NUMBER OF MASS POINTS & BEAMS
0010          10 FORMAT (20I4)
0011             READ (5,10) NUMP,NUB,KMAX,IPS,IDS
0012             NMPM1=NUMP-1
           C     READ IN THE RELATIONSHIP BETWEEN MASSES I & J
0013             DO 20 I=1,NMPM1
0014             L=I+1
0015          20 READ (5,11) (IELM(I,J),J=L,NUMP)
0016          11 FORMAT(40I2)
0017             K=0
0018             M6=NUMP*6
           C     READ IN THE GEOM. PAR. & INITIAL POSITION OF EACH BEAM
0019             CALL INPUT(NUMP,NUB,IELM)
0020             CALL OUTP(K,IELM,RK,DISK,FRK,SW,SCFP,DDK,1.,0,NUMP,NUB,FK,FRK)
0021             DO 40 I=1,NUB
0022             DO 40 J=1,12
0023          40 RNK(I,J)=FRK(I,J)
           C     READ IN INCREMENTS
0024          50 K=K+1
0025             CALL INCRE(NUMP,DU,DR,K)
           C     INITIALIZE THE TOTAL K MATRIX
0026             DO 55 I=1,M6
0027             DO 55 J=1,M6
0028          55 TK(I,J)=0.D0
           C     GENERATE THE K MATRIX OF EACH BEAM
0029             LB=0
0030             DO 200 I=1,NMPM1
0031             L=I+1
0032             DO 200 J=L,NUMP
0033             IF (IELM(I,J) .EQ. 0) GO TO 200
0034             LB=LB+1
0035             DO 131 II=1,3
0036             DO 131 JJ=1,3
```

```
  131 DC1(II,JJ)=DC1K(LB,II,JJ)
      DO 136 II=1,3
      DO 136 JJ=1,3
  136 DC2(II,JJ)=DC2K(LB,II,JJ)
      DO 105 M=1,12
  105 FRKL(M)=FRK(LB,M)
C     CHECK THE HINGE SWITCHES FOR EACH BEAM AND COMPUTE G,HP
      DO 140 N=1,2
      IF(SW(LB,N) .EQ. 0) GO TO 125
      IX=IFLM(I,J)
      GO TO (111,112,113,114,115),IX
  111 CALL GRYFI(LB,FRKL,GRF,N)
      GO TO 130
  112 GO TO 130
  113 GO TO 130
  114 GO TO 130
  115 GO TO 130
  125 IF (N.EQ. 2) GO TO 127
      DO 126 II=1,4
      DO 126 JJ=1,6
      G1(II,JJ)=0.D0
      IF(II .EQ. 4) GO TO 126
      HP1(II,JJ)=0.D0
      FBI(II,JJ)=0.D0
      IF (JJ .GE. 4) GO TO 126
      EBHI(II,JJ)=0.D0
      HBIP(II,JJ)=0.D0
  126 CONTINUE
      DO 116 II=1,4
      DO 116 JJ=1,3
  116 GBI(II,JJ)=0.D0
      GO TO 140
  127 DO 128 II=1,4
      DO 128 JJ=1,6
      G2(II,JJ)=0.D0
      IF(II .EQ. 4) GO TO 128
      HP2(II,JJ)=0.D0
      FBJ(II,JJ)=0.D0
      IF (JJ .GE. 4) GO TO 128
      EBHJ(II,JJ)=0.D0
      HBJP(II,JJ)=0.D0
  128 CONTINUE
      DO 129 II=1,4
      DO 129 JJ=1,3
  129 GBJ(II,JJ)=0.D0
      GO TO 140
  130 IF (N .EQ. 2) GO TO 135
      CALL GHP(DC1,AL(LB),G1,HP1,FRKL,GRF,1,HBIP,EBHI,GBI)
      GO TO 140
  135 CALL GHP(DC2,AL(LB),G2,HP2,FRKL,GRF,2,HBJP,EBHJ,GBJ)
  140 CONTINUE
C     STORE THE CALCULATED MATRICES
      DO 142 II=1,3
      DO 142 JJ=1,6
      HP1S(LB,II,JJ)=HP1(II,JJ)
```

```
0090             HP2S(LB,II,JJ)=HP2(II,JJ)
0091             G1S(LB,II,JJ)=G1(II,JJ)
0092             G2S(LB,II,JJ)=G2(II,JJ)
0093             IF (JJ .GE. 4) GO TO 142
0094             HBIT(LB,II,JJ)=HBIP(II,JJ)
0095             HBJT(LB,II,JJ)=HBJP(II,JJ)
0096         142 G1R(II,JJ)=G1(II+1,JJ)
0097             DO 143 JJ=1,6
0098             G1S(LB,4,JJ)=G1(4,JJ)
0099         143 G2S(LB,4,JJ)=G2(4,JJ)
0100             DO 144 II=1,3
0101             DO 144 JJ=1,3
0102         144 AJF(II,JJ)=0.D0
0103             AJF(1,1)=-FRKL(3)*AL(LB)
0104             AJF(2,2)=AJF(1,1)
0105             AJF(3,1)=FRKL(1)*AL(LB)
0106             AJF(3,2)=FRKL(2)*AL(LB)
0107             CALL GMPRD(AJF,G1R,G1RJ,3,3,6)
0108             DO 145 II=1,4
0109             DO 145 JJ=1,3
0110             GBIT(LB,II,JJ)=GBI(II,JJ)
0111             GBJT(LB,II,JJ)=GBJ(II,JJ)
0112         145 CONTINUE
           C     FIND THE ELASTIC STIFFNESS MATRIX
0113             CALL KUKL(DC1,STIF1,P,HR,G1RJ,LB,AL(LB))
0114             CALL KR1(DC1,HP1,HBIP,FRKL,LB,AL(LB),AKRT,BKRT)
           C     COMPUTE THE FINAL K MATRIX OF EACH BEAM
0115             IF (SW(LB,1) .EQ. 0 .AND. SW(LB,2) .EQ. 0) GO TO 180
0116             DO 150 II=1,3
0117             QI(II)=0.D0
0118             QI(II+3)=0.D0
0119             QJ(II)=0.D0
0120             QJ(II+3)=0.D0
0121             DO 150 JJ=1,3
0122             QI(II)=G1(1,JJ)*DC1(JJ,II)+QI(II)
0123             QI(II+3)=G1(1,JJ+3)*DC1(JJ,II)+QI(II+3)
0124             QJ(II)=G2(1,JJ)*DC2(JJ,II)+QJ(II)
0125         150 QJ(II+3)=G2(1,JJ+3)*DC2(JJ,II)+QJ(II+3)
0126         180 CONTINUE
0127             DO 152 II=1,3
0128             DO 152 JJ=1,6
0129             EBI(II,JJ)=DC1(3,II)*QI(JJ)
0130         152 EBJ(II,JJ)=DC2(3,II)*QJ(JJ)
0131             DO 182 II=1,3
0132             DO 182 JJ=1,3
0133         182 GRBI(II,JJ)=GBI(II+1,JJ)
0134             CALL HINVB(STIF1,P,HR,HP1,HP2,AJF,DC1,STK,EBI,EBJ,GRBI,HBIP,HBJP,
               1  EBHI,EBHJ,AKRT,BKRT)
0135             DO 146 II=1,12
0136             DO 146 JJ=1,12
0137         146 SK(LB,II,JJ)=STK(II,JJ)
0138             DO 148 II=7,12
0139             DO 148 JJ=1,12
0140         148 STK(II,JJ)=-STK(II,JJ)
0141             IS=(I-1)*6+1
```

```
      IE=I*6
      JS=(J-1)*6+1
      JE=J*6
      IK=0
      DO 162 II=IS,IE
      JK=0
      IK=IK+1
      DO 161 JJ=IS,IE
      JK=JK+1
  161 TK(II,JJ)=STK(IK,JK)+TK(II,JJ)
      DO 162 JJ=JS,JE
      JK=JK+1
  162 TK(II,JJ)=STK(IK,JK)+TK(II,JJ)
      DO 164 II=JS,JE
      IK=IK+1
      JK=0
      DO 163 JJ=IS,IE
      JK=JK+1
  163 TK(II,JJ)=STK(IK,JK)+TK(II,JJ)
      DO 164 JJ=JS,JE
      JK=JK+1
  164 TK(II,JJ)=STK(IK,JK)+TK(II,JJ)
  200 CONTINUE
      IR=0
      DO 410 I=1,M6
      IF (DU(I) .LT. 1.D2) GO TO 410
      IR=IR+1
      JC=0
      FB(IR)=DR(I)
      DO 409 J=1,M6
      IF (DU(J) .LT. 1.D2) GO TO 408
      JC=JC+1
      RKB(IR,JC)=TK(I,J)
      GO TO 409
  408 FB(IR)=FB(IR)-TK(I,J)*DU(J)
  409 CONTINUE
  410 CONTINUE
      CALL  INV(IR,90,RKB,IMPERM,90,RKBI)
      CALL GMPRDI(RKBI,FB,DUB,IR,IR,1)
      JC=0
      DO 420 I=1,M6
      IF (DU(I) .LT. 1.D2)GO TO 420
      JC=JC+1
      DU(I)=DUB(JC)
  420 CONTINUE
      CALL GMPRDI(TK,DU,DR,M6,M6,1)
C     COMPUTE THE FORCE VECTOR AT EACH NODE POINT
  202 SCFA=1.D0
  201 LB=0
      DO 300 I=1,NMPM1
      IS=(I-1)*6
      L=I+1
      DO 300 J=L,NUMP
      IF (IELM(I,J) .EQ. 0) GO TO 300
      JS=(J-1)*6
```

```
0196             LB=LB+1
0197             DO 210 II=1,6
0198             DUS(II)=DU(IS+II)
0199         210 DUS(II+6)=DU(JS+II)
0200             IF (SCFA .LT. 0.99999D0) GO TO 215
0201             DO 212 II=1,12
0202             DO 212 JJ=1,12
0203         212 STK(II,JJ)=SK(LB,II,JJ)
0204             CALL GMPRD(STK,DUS,DRS,12,12,1)
0205             DO 214 M=1,12
0206         214 DRN(LB,M)=DRS(M)
0207             IF (SCFA .GT. 0.99999D0) GO TO 217
0208         215 DO 216 M=1,12
0209         216 DRS(M)=DRN(LB,M)*SCFA
0210         217 DO 218 M=1,12
0211         218 RNKP(M)=RNK(LB,M)+DRS(M)
0212             DO 220 II=1,3
0213             DO 220 JJ=1,6
0214             HP1(II,JJ)=HP1S(LB,II,JJ)
0215         220 HP2(II,JJ)=HP2S(LB,II,JJ)
0216             DO 222 II=1,3
0217             DO 222 JJ=1,3
0218             HBIP(II,JJ)=HBIT(LB,II,JJ)
0219             HBJP(II,JJ)=HBJT(LB,II,JJ)
0220             DC1(II,JJ)=DC1K(LB,II,JJ)
0221         222 DC2(II,JJ)=DC2K(LB,II,JJ)
           C     COMPUTE THE NEW DIRECTION COSINES AND FORCES AT LOCAL FRAME OF
           C     EACH NODE POINT
0222             CALL NEWDC(HP1,HP2,DRS,DUS,DC1,DC2,DC1P1,DC2P1,HBIP,HBJP)
0223             DO 230 II=1,3
0224             DO 230 JJ=1,3
0225             DC1KP1(LB,II,JJ)=DC1P1(II,JJ)
0226         230 DC2KP1(LB,II,JJ)=DC2P1(II,JJ)
0227             CALL FRKS(RNKP,DC1P1,DC2P1,FRKP1)
0228             DO 232 M=1,12
0229             RNKP1(LB,M)=RNKP(M)
0230         232 FRKP(LB,M)=FRKP1(M)
           C     EVALUATE THE YIELD FORCE AT I & J TH ENDS
0231             IX=IELM(I,J)
0232             GO TO (241,242,243,244,245),IX
0233         241 CALL YFCT1(LB,FRKP1,FKP1)
0234             GO TO 260
0235         242 GO TO 260
0236         243 GO TO 260
0237         244 GO TO 260
0238         245 GO TO 260
0239         260 CONTINUE
0240             DO 262 N=1,2
0241         262 FK1(LB,N)=FKP1(N)
0242             IF (SCFA .LT. 0.99999D0) GO TO 300
           C     CHECK THE HINGE SWITCHES AND DETERMINE THE SCALING FACTOR
0243             DO 290 N=1,2
0244             IF (SW(LB,N) .EQ. 1) GO TO 289
0245             IF (FKP1(N) .GT. 1.D0) GO TO 265
0246             SCFP(LB,N)=1.D0
```

```
0247          GO TO 290
0248      265 IF (FK(LB,N) .LE. 1.DO) GO TO 270
0249          IF (FK(LB,N) .GT. FKP1(N)) GO TO 289
0250          SW(LB,N)=1
0251          SCFP(LB,N)=0.DO
0252          GO TO 290
0253      270 IX=IELM(I,J)
0254          GO TO (271,272,273,274,275),IX
0255      271 CALL SCFS1(FRKP1,FRK,ALAMDA,N,NI,LB)
0256          IF (NI .GT. 100 .OR. ALAMDA .EQ. 0.DO .OR. ALAMDA .GE. 1.DO) GO TO
         1 1001
0257          GO TO 288
0258      272 GO TO 288
0259      273 GO TO 288
0260      274 GO TO 288
0261      275 GO TO 288
0262      288 SCFP(LB,N)=ALAMDA
0263          GO TO 290
0264      289 SCFP(LB,N)=1.DO
0265      290 CONTINUE
0266      300 CONTINUE
0267          IF (SCFA .LT. 0.99999DO) GO TO 320
        C     DETERMINE THE MIN. SCALING FACTOR
0268          CALL DMIN(SCFP,SCFA,NUB)
0269          IF (SCFA .LE. 0.00001DO) GO TO 50
0270          IF (SCFA .GT. 0.99999DO) GO TO 320
0271          DO 310 I=1,M6
0272          DR(I)=DR(I)*SCFA
0273      310 DU(I)=DU(I)*SCFA
0274          GO TO 201
0275      320 CONTINUE
0276      321 DO 322 M=1,M6
0277          RKP1(M)=RK(M)-DR(M)
0278      322 DISKP1(M)=DISK(M)+DU(M)
0279          IF (SCFA .GT. 0.99999DO) GO TO 325
0280          DO 305 I=1,NUB
0281          DO 305 N=1,2
0282          IF (SCFP(I,N) .GT. SCFA+0.01DO) GO TO 305
0283          IF (SCFP(I,N) .EQ. 1.DO) GO TO 305
0284          SW(I,N)=1
0285      305 CONTINUE
0286      325 CALL DMAXI(SW,SWT,NUB)
0287          SCFB=1.DO
0288          IF (SWT .EQ. 0) GO TO 500
        C     CHECK THE DISSIPATION
0289          I=0
0290          DO 370 MI=1,NMPM1
0291          IS=(MI-1)*6
0292          L=MI+1
0293          DO 370 MJ=L,NUMP
0294          IF (IELM(MI,MJ) .EQ. 0) GO TO 370
0295          I=I+1
0296          JS=(MJ-1)*6
0297          DO 330 II=1,6
0298          DUS(II)=DU(IS+II)
```

MICHIGAN TERMINAL SYSTEM FORTRAN G(41336 TEST)   MAIN   08-29-73   17:44.30   PAGE P007

```
0299        330 DUS(II+6)=DU(JS+II)
0300            DO 334 M=1,12
0301        334 DRS(M)=DPN(I,M)
0302            DO 360 N=1,2
0303            DISSK(I,N)=0.D0
0304            IF (SW(I,N) .NE. 1) GO TO 359
0305            IF (N .EQ. 2) GO TO 340
0306            DO 335 II=1,4
0307            DO 335 JJ=1,3
0308        335 GBI(II,JJ)=GBIT(I,II,JJ)
0309            DO 336 II=1,4
0310            DO 336 JJ=1,6
0311        336 G1(II,JJ)=G1S(I,II,JJ)
0312            DO 337 II=1,3
0313            DO 337 JJ=1,3
0314        337 DC1(II,JJ)=DC1K(I,II,JJ)
0315            CALL DISSP(G1,GBI,DRS,DUS,1,AL(I),DUP,DC1)
0316            GO TO 350
0317        340 DO 341 II=1,4
0318            DO 341 JJ=1,3
0319        341 GBJ(II,JJ)=GBJT(I,II,JJ)
0320            DO 342 II=1,4
0321            DO 342 JJ=1,6
0322        342 G2(II,JJ)=G2S(I,II,JJ)
0323            DO 343 II=1,3
0324            DO 343 JJ=1,3
0325        343 DC2(II,JJ)=DC2K(I,II,JJ)
0326            CALL DISSP(G2,GBJ,DRS,DUS,2,AL(I),DUP,DC2)
0327        350 M=(N-1)*6+2
0328            DO 351 J=1,4
0329            F1=FRK(I,J+M)
0330        351 DISSK(I,N)=DISSK(I,N)+F1*DUP(J)
0331            IF (IDS .EQ. 0) GO TO 360
0332            IF (DISSK(I,N) .GE. 0.D0) GO TO 360
0333            SW(I,N)=0
0334        359 CONTINUE
0335        360 DDK(I,N)=DISSK(I,N)+DDK(I,N)
0336        370 CONTINUE
0337        500 CALL OUTP(K,IELM,RKP1,DISKP1,RNKP1,SW,SCFP,DDK,SCFA,IPS,NUMP,NJB,
               1 FK1,FRKP)
0338            IF (K .GE. KMAX) GO TO 1000
0339            DO 505 I=1,M6
0340            RK(I)=RKP1(I)
0341        505 DISK(I)=DISKP1(I)
0342            DO 520 I=1,NUB
0343            DO 508 N=1,2
0344        508 FK(I,N)=FK1(I,N)
0345            DO 510 J=1,12
0346            FRK(I,J)=FRKP(I,J)
0347        510 RNK(I,J)=RNKP1(I,J)
0348            DO 515 II=1,3
0349            DO 515 JJ=1,3
0350            DC1K(I,II,JJ)=DC1KP1(I,II,JJ)
0351        515 DC2K(I,II,JJ)=DC2KP1(I,II,JJ)
0352        520 CONTINUE
```

```
            GO TO 50
      1001 WRITE (6,1002) NI,ALAMDA
      1002 FORMAT  ('TRY',I4,'  TIMES LAMDA=',D15.5)
      1000 CONTINUE
      1101 FORMAT (1H1,'K=    ',I3)
      1108 FORMAT ('L F @',2I3,12D10.3)
      1109 FORMAT ('YF    ',2I3,2D15.5)
      1110 FORMAT (//'K=',I3,'ISCF=',I3/)
           END
  *OPTIONS IN EFFECT*  ID,EBCDIC,SOURCE,LIST,NODECK,LOAD,NOMAP
  *OPTIONS IN EFFECT*  NAME = MAIN     , LINECNT =        57
  *STATISTICS*     SOURCE STATEMENTS =       361,PROGRAM SIZE =    272822
  *STATISTICS*  NO DIAGNOSTICS GENERATED
NO ERRORS IN MAIN

NO STATEMENTS FLAGGED IN THE ABOVE COMPILATIONS.
```

APPENDIX B

B.2 SUBROUTINE LISTING

```
0001              SUBROUTINE INPUT(M,NEN,IELM)
           C      INPUT DATA & INITIAL POSITION
0002              IMPLICIT REAL *8(A-H,P-Z)
0003              REAL *8 M10,M20,M30
0004              INTEGER SW
0005              DIMENSION AL(20),Y1(20),Y2(20),CF(20),M10(20),M20(20),M30(20),
                1  P0(20),Z11(20),Z12(20),Z21(20),Z22(20),Z31(20),Z32(20),ZA(20),
                2  ZG(20),DC1K(20,3,3),DC2K(20,3,3),SW(20,2),FK(20,2),DDK(20,2),
                3  RK(90),FRK(20,12),DISK(90),IELM(14,15),INB(20),SCFD(20,2),
                4  SCFP(20,2)
0006              COMMON/COMA/ZA,ZG,Z11,Z12,Z21,Z22,Z31,Z32
0007              COMMON/COMB/M10,M20,M30,P0,Y1,Y2,CF
0008              COMMON/COMC/AMR,FR,ALR/COMD/EPS
0009              COMMON/COME/DC1K,DC2K,SW,FK,DDK,RK,FRK,DISK,AL
0010              COMMON/COMF/SCFD,SCFP
           C      READ IN REFERENCE UNITS
0011              READ(5,12) ALR,DR,ER,AIR,EPS
0012              RR=ALR/DR
0013              AMR=ER*AIR/ALR
0014              FR=AMR/ALR
0015              AR=AIR/DR/DR
0016              LB=0
0017              M1=M-1
0018              DO 20 I=1,M1
0019              L=I+1
0020              DO 20 J=L,M
0021              IF (IELM(I,J) .EQ. 0) GO TO 20
0022              LB=LB+1
0023              INB(LB)=IELM(I,J)
0024           20 CONTINUE
           C       READ IN MATERIAL PROPERTIES, DIMENSIONS OF EA. MEM. AND CAL.
           C      NONDIMENSIONAL QUANTITIES
0025              DO 1 I=1,NEN
0026              READ(5,10) E,G,AJ,AI1,AI2,A,AL(I),B,H,T,Y1(I),Y2(I),CF(I),YF
0027              E=E/ER
0028              G=G/ER
0029              AJ=AJ/AIR
0030              AI1=AI1/AIR
0031              AI2=AI2/AIR
0032              A=A/AR
0033              AL(I)=AL(I)/ALR
0034              B=B/DR
0035              H=H/DR
0036              T=T/DR
0037              Y1(I)=Y1(I)/DR
0038              Y2(I)=Y2(I)/DR
0039              YF=YF/ER
0040              IF (INB(I) .EQ. 1) GO TO 21
0041              M10(I)=2.D0*AI1*YF*RR/H
0042              M20(I)=2.D0*AI2*YF*RR/B
0043              M30(I)=2.D0*A*T*YF*RR/1.732D0
0044              GO TO 22
0045           21 M10(I)=2.D0*AI1*YF*RR/H
0046              M20(I)=2.D0*AI2*YF*RR/B
0047              M30(I)=2.D0*A*T*YF*RR/1.732D0
```

```
MICHIGAN TERMINAL SYSTEM FORTRAN G(41336 TEST)          INPUT          08-29-73          19:03.44          PAGE P002
 0048          22 PO(I)=A*YF*RR*RR                                                61.000
 0049             Z11(I)=AL(I)/(E*AI1)                                            62.000
 0050             Z12(I)=AL(I)/(E*AI2)                                            63.000
 0051             Z21(I)=AL(I)*AL(I)/(2.DO*E*AI1)                                 64.000
 0052             Z22(I)=AL(I)*AL(I)/(2.DO*E*AI2)                                 65.000
 0053             Z31(I)=AL(I)*AL(I)*AL(I)/(3.DO*E*AI1)                           66.000
 0054             Z32(I)=AL(I)*AL(I)*AL(I)/(3.DO*E*AI2)                           67.000
 0055             ZA(I)=AL(I)/(A*E)/RR/RR                                         68.000
 0056           1 ZG(I)=AL(I)/(G*AJ)                                              69.000
             C    READ IN INITIAL POSITION AND FORCES FOR ELEMENT ENDS, SET I.C.  70.000
 0057             DO 2 I=1,NEN                                                    71.000
 0058             DO 2 J=1,3                                                      72.000
 0059             READ(5,12) (DC1K(I,J,K),K=1,3)                                  73.000
 0060             DO 2 K=1,3                                                      74.000
 0061           2 DC2K(I,J,K)=DC1K(I,J,K)                                         75.000
 0062             M6=M*6                                                          76.000
 0063             DC 3 I=1,M                                                      77.000
 0064             J=(I-1)*6+1                                                     78.000
 0065             L=I*6                                                           79.000
 0066           3 READ (5,12) (DISK(N),N=J,L)                                     80.000
 0067             DO 6 I=1,NEN                                                    81.000
 0068             DO 4 J=1,2                                                      82.000
 0069             SW(I,J)=0                                                       83.000
 0070             FK(I,J)=0.DO                                                    84.000
 0071             SCFP(I,J)=1.DO                                                  85.000
 0072             SCFD(I,J)=1.DO                                                  86.000
 0073           4 DDK(I,J)=0.DO                                                   87.000
 0074             DO 5 J=1,12                                                     88.000
 0075           5 FRK(I,J)=0.DO                                                   89.000
 0076           6 CONTINUE                                                        90.000
 0077             DO 7 J=1,M6                                                     91.000
 0078           7 RK(J)=0.DO                                                      92.000
 0079          10 FORMAT(8D10.0)                                                  93.000
 0080          12 FORMAT(6D10.0)                                                  94.000
 0081          14 FORMAT(5D10.0,I3)                                               95.000
 0082             RETURN                                                          96.000
 0083             END                                                             97.000
  *OPTIONS IN EFFECT*  ID,EBCDIC,SOURCE,LIST,NODECK,LOAD,NOMAP
  *OPTIONS IN EFFECT*  NAME = INPUT     , LINECNT =       57
  *STATISTICS*    SOURCE STATEMENTS =          83,PROGRAM SIZE =      2532
  *STATISTICS*  NO DIAGNOSTICS GENERATED
NO ERRORS IN INPUT
```

```
0001             SUBROUTINE GRYF1(LB,FRK,GRF,N)
           C     COMPUTE THE GRAD. OF YIELD FUNCTION
0002             IMPLICIT REAL*8(A-H,P-Z)
0003             REAL *8 M10,M20,M30,M1,M2,M3
0004             DIMENSION FRK(1),GRF(1),A(4),B(4),M10(20),M20(20),M30(20),
               1  PC(20),Y1(20),Y2(20),CF(20)
0005             COMMON/COMB/M10,M20,M30,PO,Y1,Y2,CF
0006             M1=M10(LB)
0007             M2=M20(LB)
0008             M3=M30(LB)
0009             P=PC(LB)
0010             M = (N-1)*6 + 2
0011             DO 10 I=1,4
0012          10 A (I) = 2.DO * DABS ( FRK(M+I) )
0013             DO 15 I=1,4
0014             IF ( FRK(M+I)) 12,13,14
0015          12 B(I) = -1.DO
0016             GO TO 15
0017          13 B(I) = 0.
0018             GO TO 15
0019          14 B(I) = 1.DO
0020          15 CONTINUE
0021             GRF(1) = B(1)*( A(1)/P /P   + A(2)/M1 /P   + A(3)/M2 /P   )
0022             GRF(2) = B(2)*( A(2)/M1 /M1   + A(3)/M1 /M2   + A(1)/M1 /P   )
0023             GRF(3) = B(3)*( A(3)/M2 /M2   + A(2)/M1 /M2   + A(1)/M2 /P   )
0024             GRF(4) = B(4)*A(4)/M3 /M3
0025             RETURN
0026             END
  *OPTIONS IN EFFECT*  ID,EBCDIC,SOURCE,LIST,NODECK,LOAD,NOMAP
  *OPTIONS IN EFFECT*  NAME = GRYF1    , LINECNT =       57
  *STATISTICS*    SOURCE STATEMENTS =        26,PROGRAM SIZE =       944
  *STATISTICS*  NO DIAGNOSTICS GENERATED
NO ERRORS IN GRYF1
```

```
 0001               SUBROUTINE YFCT1(LB,FR,FK)
          C         TEST YIELD CONDITION
 0002               IMPLICIT REAL*8(A-H,P-Z)
 0003               REAL *8 M10,M20,M30,M1,M2,M3
 0004               DIMENSION FR(12),FK(2),M10(20),M20(20),M30(20),PO(20),
                   1  Y1(20),Y2(20),CF(20)
 0005               COMMON/COMB/M10,M20,M30,PO,Y1,Y2,CF
 0006               M1=M10(LB)
 0007               M2=M20(LB)
 0008               M3=M30(LB)
 0009               P=PO(LB)
 0010               A1=DABS(FR(3)/P  )
 0011               A2=DABS(FR(4)/M1  )
 0012               A3=DABS(FR(5)/M2  )
 0013               A4=DABS(FR(6)/M3  )
 0014               A5=DABS(FR(9)/P  )
 0015               A6=DABS(FR(10)/M1  )
 0016               A7=DABS(FR(11)/M2  )
 0017               A8=DABS(FR(12)/M3  )
 0018               FK(1)=A1*A1+A2*A2+A3*A3+A4*A4+2.D0*A2*A3+2.D0*A1*A2+2.D0*A1*A3
 0019               FK(2)=A5*A5+A6*A6+A7*A7+A8*A8+2.D0*A6*A7+2.D0*A5*A6+2.D0*A5*A7
 0020               RETURN
 0021               END
  *OPTIONS IN EFFECT*  ID,EBCDIC,SOURCE,LIST,NODECK,LOAD,NOMAP
  *OPTIONS IN EFFECT*  NAME = YFCT1    , LINECNT =       57
  *STATISTICS*    SOURCE STATEMENTS =        21,PROGRAM SIZE =       796
  *STATISTICS*  NO DIAGNOSTICS GENERATED
NO ERRORS IN YFCT1
```

```
MICHIGAN TERMINAL SYSTEM FORTRAN G(41336 TEST)          DMIN            08-29-73           19:04.10          PAGE P001

  0001                SUBROUTINE DMIN(SCF,S,NUB)                                               149.000
              C       FIND OUT THE MIN. VALUE OF AN ARRAY SCF(20,2)                            150.000
  0002                REAL *8 SCF,S,X,Y                                                        151.000
  0003                DIMENSION SCF(20,2)                                                      152.000
  0004                X=DMIN1(SCF(1,1),SCF(1,2))                                               153.000
  0005                DO 10 I=2,NUB                                                            154.000
  0006                Y=DMIN1(SCF(I,1),SCF(I,2))                                               155.000
  0007             10 X=DMIN1(X,Y)                                                             156.000
  0008                S=X                                                                      157.000
  0009                RETURN                                                                   158.000
  0010                END                                                                      159.000
   *OPTIONS IN EFFECT*  ID,EBCDIC,SOURCE,LIST,NODECK,LOAD,NOMAP
   *OPTIONS IN EFFECT*  NAME = DMIN    , LINECNT =        57
   *STATISTICS*    SOURCE STATEMENTS =        10,PROGRAM SIZE =       524
   *STATISTICS*  NO DIAGNOSTICS GENERATED
 NO ERRORS IN DMIN
```

```
MICHIGAN TERMINAL SYSTEM FORTRAN G(41336 TEST)        GMPRD          08-29-73          19:04.11          PAGE P001

  0001              SUBROUTINE GMPRD(A,B,R,N,M,L)                                        160.000
  0002              REAL*8 A,B,R                                                         161.000
  0003              DIMENSION A(1),B(1),R(1)                                             162.000
  0004              IR=0                                                                 163.000
  0005              IK=-M                                                                164.000
  0006              DO 10 K=1,L                                                          165.000
  0007              IK=IK+M                                                              166.000
  0008              DO 10 J=1,N                                                          167.000
  0009              IR=IR+1                                                              168.000
  0010              JI=J-N                                                               169.000
  0011              IB=IK                                                                170.000
  0012              R(IR)=0.D0                                                           171.000
  0013              DO 10 I=1,M                                                          172.000
  0014              JI=JI+N                                                              173.000
  0015              IB=IB+1                                                              174.000
  0016           10 R(IR)=R(IR)+A(JI)*B(IB)                                              175.000
  0017              RETURN                                                               176.000
  0018              END                                                                  177.000
   *OPTIONS IN EFFECT*  ID,EBCDIC,SOURCE,LIST,NODECK,LOAD,NOMAP
   *OPTIONS IN EFFECT*  NAME = GMPRD   , LINECNT =       57
   *STATISTICS*    SOURCE STATEMENTS =        18,PROGRAM SIZE =       674
   *STATISTICS*  NO DIAGNOSTICS GENERATED
NO ERRORS IN GMPRD
```

```
MICHIGAN TERMINAL SYSTEM FORTRAN G(41336 TEST)        FRKS           08-29-73          19:04.13         PAGE P001

 0001                SUBROUTINE FRKS(RKP1,DC1KP1,DC2KP1,FRKP1)
             C       COMPUTE THE RESULTANT FORCE AT LOCAL COOR.
 0002                IMPLICIT REAL*8(A-H,P-Z)
 0003                DIMENSION RKP1(12),DC1KP1(3,3),DC2KP1(3,3),FRKP1(12),SRKP1(12),
                    1 F(3),FM(3),FL(3),FML(3)
 0004                DO 50 M=1,12,6
 0005                DO 40 I=1,3
 0006                N=M+I-1
 0007                F(I)=RKP1(N)
 0008             40 FM(I)=RKP1(N+3)
 0009                IF (M .GE. 7) GO TO 45
 0010                CALL GMPRD(DC1KP1,F,FL,3,3,1)
 0011                CALL GMPRD(DC1KP1,FM,FML,3,3,1)
 0012                GO TO 46
 0013             45 CALL GMPRD(DC2KP1,F,FL,3,3,1)
 0014                CALL GMPRD(DC2KP1,FM,FML,3,3,1)
 0015             46 DO 47 I=1,3
 0016                N=M+I-1
 0017                FRKP1(N)=FL(I)
 0018             47 FRKP1(N+3)=FML(I)
 0019             50 CONTINUE
 0020                CONTINUE
 0021                RETURN
 0022                END
  *OPTIONS IN EFFECT*  ID,EBCDIC,SOURCE,LIST,NODECK,LOAD,NOMAP
  *OPTIONS IN EFFECT*  NAME = FRKS     , LINECNT =       57
  *STATISTICS*    SOURCE STATEMENTS =        22,PROGRAM SIZE =       974
  *STATISTICS*  NO DIAGNOSTICS GENERATED
NO ERRORS IN FRKS
```

```
0001            SUBROUTINE GHP(DC,AL,G,HP,FRK,GRF,N,HB,EBH,GB)                          202.000
          C     COMPUTE THE G AND HP MATRICES                                           203.000
0002            IMPLICIT REAL*8(A-H,P-Z)                                                204.000
0003            DIMENSION DC(3,3),G(4,6),HP(3,6),R(6),GRF(4),A(4),T(6,6),GR(3,6),       205.000
               1AUX(3,6),FRK(12),B(3,3)                                                 206.000
0004            DIMENSION BI(4,3),GT(1,3),GB(4,3),HB(3,3),GBR(3,3),EBH(3,3),            207.000
               1  HT(3,3)                                                               208.000
0005            COMMON/CUMD/EPS                                                         209.000
0006            X=0.D0                                                                  210.000
0007            DO 10 I=1,4                                                             211.000
0008         10 X=X+GRF(I)*GRF(I)                                                       212.000
0009            X=DSQRT(X)                                                              213.000
0010            DO 12 I=1,4                                                             214.000
0011         12 A(I)=GRF(I)/X                                                           215.000
0012            M=(N-1)*6                                                               216.000
0013            DO 13 I=1,3                                                             217.000
0014         13 R(I)=FRK(M+I)                                                           218.000
0015            IF(M .EQ. 0) GO TO 19                                                   219.000
0016            R(4)=FRK(10)-AL*FRK(8)                                                  220.000
0017            R(5)=FRK(11)+AL*FRK(7)                                                  221.000
0018            R(6)=FRK(12)                                                            222.000
0019            DG=GRF(1)*(A(3)*R(1)-A(2)*R(2))+GRF(2)*(-AL*A(4)*R(1)+AL*A(2)*R(3)      223.000
               1+A(4)*R(5)-A(3)*R(6))+GRF(3)*(-AL*A(4)*R(2)+AL*A(3)*R(3)-A(4)*R(4)      224.000
               2 +A(2)*R(6))+GRF(4)*(A(3)*R(4)-A(2)*R(5))                               225.000
0020            IF(DABS(DG) .LE. EPS) DG=DSIGN(EPS,DG)                                  226.000
0021            BI(1,1)=-R(2)                                                           227.000
0022            B(1,2)=R(1)                                                             228.000
0023            B(1,3)=0.D0                                                             229.000
0024            B(2,1)=R(3)*AL                                                          230.000
0025            BI(2,2)=-R(6)                                                           231.000
0026            BI(2,3)=-R(1)*AL+R(5)                                                   232.000
0027            BI(3,1)=R(6)                                                            233.000
0028            BI(3,2)=R(3)*AL                                                         234.000
0029            BI(3,3)=-R(2)*AL-R(4)                                                   235.000
0030            BI(4,1)=-R(5)                                                           236.000
0031            BI(4,2)=R(4)                                                            237.000
0032            BI(4,3)=0.D0                                                            238.000
0033            CALL GMPRD(GRF,BI,GT,1,4,3)                                             239.000
0034            CALL GMPRD(A,GT,GB,4,1,3)                                               240.000
0035            DO 15 I=1,4                                                             241.000
0036            DO 15 J=1,3                                                             242.000
0037         15 GB(I,J)=CB(I,J)/DG                                                      243.000
0038            DO 17 I=1,4                                                             244.000
0039            G(I,1)=-A(I)*GRF(3)*AL/DG                                               245.000
0040            G(I,2)=A(I)*GRF(2)*AL/DG                                                246.000
0041            G(I,3)=A(I)*GRF(1)/DG                                                   247.000
0042            G(I,4)=G(I,2)/AL                                                        248.000
0043            G(I,5)=-G(I,1)/AL                                                       249.000
0044         17 G(I,6)=A(I)*GRF(4)/DG                                                   250.000
0045            GO TO 21                                                                251.000
0046         19 R(4)=FRK(M+4)+AL*FRK(M+2)                                               252.000
0047            R(5)=FRK(M+5)-AL*FRK(M+1)                                               253.000
0048            R(6)=FRK(M+6)                                                           254.000
0049            DG=GRF(1)*(A(3)*R(1)-A(2)*R(2))+GRF(2)*(AL*A(4)*R(1)-AL*A(2)*R(3)       255.000
               1 +A(4)*R(5)-A(3)*R(6))+GRF(3)*(AL*A(4)*R(2)-AL*A(3)*R(3)-A(4)*R(4)      256.000
```

```
              2 +A(2)*R(6))+GRF(4)*(A(3)*R(4)-A(2)*R(5))
 0050           DG=-DG
 0051           IF (DABS(DG) .LE. EPS) DG=DSIGN(EPS,DG)
 0052           BI(1,1)=-R(2)
 0053           BI(1,2)=R(1)
 0054           BI(1,3)=0.D0
 0055           BI(2,1)=-R(3)*AL
 0056           BI(2,2)=-R(6)
 0057           BI(2,3)=R(1)*AL+R(5)
 0058           BI(3,1)=R(6)
 0059           BI(3,2)=-R(3)*AL
 0060           BI(3,3)=R(2)*AL-R(4)
 0061           BI(4,1)=-R(5)
 0062           BI(4,2)=R(4)
 0063           BI(4,3)=0.D0
 0064           CALL GMPRD(GRF,BI,GT,1,4,3)
 0065           CALL GMPRD(A,GT,GB,4,1,3)
 0066           DO 18 I=1,4
 0067           DO 18 J=1,3
 0068        18 GB(I,J)=GB(I,J)/DG
 0069           DO 20 I=1,4
 0070           G(I,1)=A(I)*GRF(3)*AL/DG
 0071           G(I,2)=-A(I)*GRF(2)*AL/DG
 0072           G(I,3)=A(I)*GRF(1)/DG
 0073           G(I,4)=-G(I,2)/AL
 0074           G(I,5)=G(I,1)/AL
 0075        20 G(I,6)=A(I)*GRF(4)/DG
 0076        21 DO 22 I=1,3
 0077           DO 22 J=1,3
 0078        22 T(I,J)=DC(I,J)
 0079           DO 24 I=4,6
 0080           DO 24 J=4,6
 0081        24 T(I,J)=DC(I-3,J-3)
 0082           DO 25 I=1,3
 0083           DO 25 J=4,6
 0084        25 T(I,J)=0.D0
 0085           DO 26 I=4,6
 0086           DO 26 J=1,3
 0087        26 T(I,J)=0.D0
 0088        40 DO 41 I=1,3
 0089           DO 41 J=1,6
 0090        41 GR(I,J)=G(I+1,J)
 0091           CALL GMPRD(GR,T,AUX,3,6,6)
 0092           DO 50 I=1,3
 0093           DO 50 J=1,3
 0094        50 B(I,J)=DC(J,I)
 0095           CALL GMPRD(B,AUX,HP,3,3,6)
 0096           DO 60 I=1,3
 0097           DO 60 J=1,3
 0098        60 GBR(I,J)=GB(I+1,J)
 0099           CALL GMPRD(GBR,DC,HT,3,3,3)
 0100           CALL GMPRD(B,HT,HB,3,3,3)
 0101           DO 70 J=1,3
 0102           EBH(1,J)=0.D0
 0103           EBH(2,J)=0.D0
```

```
 0104            70 EBH(3,J)=GB(1,J)                                312.000
 0105               CALL GMPRD(EBH,DC,HT,3,3,3)                     313.000
 0106               CALL GMPRD(B,HT,EBH,3,3,3)                      314.000
 0107               RETURN                                          315.000
 0108               END                                             316.000
  *OPTIONS IN EFFECT*  ID,EBCDIC,SOURCE,LIST,NODECK,LOAD,NOMAP
  *OPTIONS IN EFFECT*  NAME = GHP      , LINECNT =       57
  *STATISTICS*    SOURCE STATEMENTS =      108,PROGRAM SIZE =     4364
  *STATISTICS*  NO DIAGNOSTICS GENERATED
NO ERRORS IN GHP
```

```
 0001              SUBROUTINE GMPRDI(X,Y,Z,IRX,JCX,JCY)
              C    MATRIX PROD.
 0002              REAL*8 X,Y,Z
 0003              DIMENSION X(90,90),Y(1),Z(1)
 0004              DO 20 I=1,IRX
 0005              Z(I)=0.D0
 0006              DO 10 J=1,JCX
 0007           10 Z(I)=Z(I)+X(I,J)*Y(J)
 0008           20 CONTINUE
 0009              RETURN
 0010              END
  *OPTIONS IN EFFECT*  ID,EBCDIC,SOURCE,LIST,NODECK,LOAD,NOMAP
  *OPTIONS IN EFFECT*  NAME = GMPRDI   , LINECNT =       57
  *STATISTICS*    SOURCE STATEMENTS =       10,PROGRAM SIZE =      522
  *STATISTICS*  NO DIAGNOSTICS GENERATED
NO ERRORS IN GMPRDI
```

```
MICHIGAN TERMINAL SYSTEM FORTRAN G(41336 TEST)          KUKL              08-29-73             19:04.29            PAGE P001

0001               SUBROUTINE KUKL(DCI,STIF1,P,HR,G1RJ,LB,AL)
            C      GENERATE THE ELASTIC STIFFNESS MATRIX
0002               IMPLICIT REAL*8(A-H,P-Z)
0003               DIMENSION DCI(3,3),STIF1(6,6),P(6,6),HR(3,3),ZA(20),ZG(20),
                  1 Z11(20),Z12(20),Z21(20),Z22(20),Z31(20),Z32(20),G1RJ(3,6)
0004               COMMON/COMA/ZA,ZG,Z11,Z12,Z21,Z22,Z31,Z32
0005               Z1=ZA(LB)
0006               Z2=ZG(LB)
0007               Z3=Z11(LB)
0008               Z4=Z12(LB)
0009               Z5=Z21(LB)
0010               Z6=Z22(LB)
0011               Z7=Z31(LB)
0012               Z8=Z32(LB)
0013               DO 20 I=1,3
0014               DO 10 J=I,3
0015            10 STIF1(I,J)=DCI(1,I)*DCI(1,J)*Z8 +DCI(2,I)*DCI(2,J)*Z7 +
                  1   DCI(3,I)*DCI(3,J)*Z1
0016               DO 20 J=4,6
0017            20 STIF1(I,J)=DCI(1,I)*DCI(2,J-3)*Z6 -DCI(2,I)*DCI(1,J-3)*Z5
0018               DO 30 I=4,6
0019               DO 30 J=I,6
0020               STIF1(I,J)=DCI(1,I-3)*DCI(1,J-3)*Z3 +DCI(2,I-3)*DCI(2,J-3)*Z4+
                  1DCI(3,I-3)*DCI(3,J-3)*Z2
0021            30 CONTINUE
0022               DO 40 J=1,5
0023               M=J+1
0024               DO 40 I=M,6
0025            40 STIF1(I,J)=STIF1(J,I)
0026               DO 50 I=1,3
0027               DO 50 J=1,3
0028               IF(I .EQ.J) GO TO 45
0029               HR(I,J)=-(DCI(2,I)*DCI(1,J)-DCI(1,I)*DCI(2,J))*AL
0030               GO TO 50
0031            45 HR(I,J)=0.D0
0032            50 CONTINUE
0033               DO 60 I=1,3
0034               DO 60 J=1,6
0035               IF(I .EQ. J) GO TO 59
0036               P(I,J)=0.D0
0037               GO TO 60
0038            59 P(I,J)=1.D0
0039            60 CONTINUE
0040               DO 70 I=4,6
0041               DO 70 J=1,6
0042            70 P(I,J)=G1RJ(I-3,J)
0043               P(4,2)=-AL+P(4,2)
0044               P(4,4)=1.D0+P(4,4)
0045               P(5,1)=AL+P(5,1)
0046               P(5,5)=1.D0+P(5,5)
0047               P(6,6)=1.D0+P(6,6)
0048               RETURN
0049               END
 *OPTIONS IN EFFECT*  ID,EBCDIC,SOURCE,LIST,NODECK,LOAD,NOMAP
 *OPTIONS IN EFFECT*  NAME = KUKL     , LINECNT =       57
```

```
MICHIGAN TERMINAL SYSTEM FORTRAN G(41336 TEST)        KUKL          08-29-73        19:04.29        PAGE E002

    *STATISTICS*    SOURCE STATEMENTS =        49,PROGRAM SIZE =      1748
    *STATISTICS*  NO DIAGNOSTICS GENERATED
NO ERRORS IN KUKL
```

```
MICHIGAN TERMINAL SYSTEM FORTRAN G(41336 TEST)        DMAXI           08-29-73          19:04.34          PAGE P001

   0001              SUBROUTINE DMAXI(SW,SWT,NUB)                                              381.000
   0002              INTEGER SW,SWT                                                            382.000
   0003              DIMENSION SW(20,1)                                                        383.000
   0004              I=MAXO(SW(1,1),SW(1,2))                                                   384.000
   0005              DO 10 M=2,NUB                                                             385.000
   0006              J=MAXO(SW(M,1),SW(M,2))                                                   386.000
   0007           10 I=MAXO(I,J)                                                               387.000
   0008              SWT=I                                                                     388.000
   0009              RETURN                                                                    389.000
   0010              END                                                                       390.000
    *OPTIONS IN EFFECT*  ID,EBCDIC,SOURCE,LIST,NODECK,LOAD,NCMAP
    *OPTIONS IN EFFECT*  NAME = DMAXI    , LINECNT =       57
    *STATISTICS*    SOURCE STATEMENTS =       10,PROGRAM SIZE =       508
    *STATISTICS*  NO DIAGNOSTICS GENERATED
NO ERRORS IN DMAXI
```

```
MICHIGAN TERMINAL SYSTEM FORTRAN G(41336 TEST)        DMAXF          08-29-73          19:04.35          PAGE P001

                  SUBROUTINE DMAXF(A,B,N)
                  REAL *8 A,B,X,Y
                  DIMENSION A(20,1)
                  X=DMAX1(A(1,1),A(1,2))
                  DO 10 I=2,N
                  Y=DMAX1(A(I,1),A(I,2))
               10 X=DMAX1(X,Y)
                  B=X
                  RETURN
                  END
  *OPTIONS IN EFFECT*  ID,EBCDIC,SOURCE,LIST,NODECK,LOAD,NOMAP
  *OPTIONS IN EFFECT*  NAME = DMAXF    , LINECNT =       57
  *STATISTICS*    SOURCE STATEMENTS =        10,PROGRAM SIZE =       524
  *STATISTICS*  NO DIAGNOSTICS GENERATED
NO ERRORS IN DMAXF
```

```
0001             SUBROUTINE KR1(DC,HIP,HBIP,FL,LB,AL,KRT,KRTB)
0002             IMPLICIT REAL*8(A-H,K,P-Z)
0003             DIMENSION DC(3,3),HIP(3,6),HBIP(3,3),FL(12),ZA(20),ZG(20),Z11(20),
                1 Z12(20),Z21(20),Z22(20),Z31(20),Z32(20),R(6),KR(6,3),T(6,6),
                2 TR(6,3),TKR(6,3),HB(3,3),KRT(6,6),KRTB(6,3)
0004             COMMON/COMA/ZA,ZG,Z11,Z12,Z21,Z22,Z31,Z32
0005             K11=Z32(LB)
0006             K15=Z22(LB)
0007             K22=Z31(LB)
0008             K24=-Z21(LB)
0009             K33=ZA(LB)
0010             K44=Z11(LB)
0011             K55=Z12(LB)
0012             K66=ZG(LB)
0013             DO 10 I=1,3
0014          10 R(I)=FL(I)
0015             R(4)=FL(4)+FL(2)*AL
0016             R(5)=FL(5)-FL(1)*AL
0017             R(6)=FL(6)
0018             KR(1,1)=K15*R(6)
0019             KR(1,2)=(K33-K11)*R(3)
0020             KR(1,3)=(K11-K22)*R(2)-(K15+K24)*R(4)
0021             KR(2,1)=(K22-K33)*R(3)
0022             KR(2,2)=-K24*R(6)
0023             KR(2,3)=(K11-K22)*R(1)+(K15+K24)*R(5)
0024             KR(3,1)=(K22-K33)*R(2)+K24*R(4)
0025             KR(3,2)=(K33-K11)*R(1)-K15*R(5)
0026             KR(3,3)=0.D0
0027             KR(4,1)=K24*R(3)
0028             KR(4,2)=(K66-K44)*R(6)
0029             KR(4,3)=-(K15+K24)*R(1)+(K44-K55)*R(5)
0030             KR(5,1)=(K55-K66)*R(6)
0031             KR(5,2)=-K15*R(3)
0032             KR(5,3)=(K15+K24)*R(2)+(K44-K55)*R(4)
0033             KR(6,1)=K15*R(1)+(K55-K66)*R(5)
0034             KR(6,2)=-K24*R(2)+(K66-K44)*R(4)
0035             KR(6,3)=0.D0
0036             DO 25 I=1,3
0037             DO 20 J=1,3
0038          20 T(I,J)=DC(I,J)
0039             DO 25 J=4,6
0040          25 T(I,J)=0.D0
0041             DO 35 I=4,6
0042             DO 30 J=1,3
0043          30 T(I,J)=0.D0
0044             DO 35 J=4,6
0045          35 T(I,J)=DC(I-3,J-3)
0046             CALL GMPRD(T,KR,TR,6,6,3)
0047             CALL GMPRD(TR,DC,TKR,6,3,3)
0048             CALL GMPRD(TKR,HIP,KRT,6,3,6)
0049             DO 40 I=1,3
0050             DO 40 J=1,3
0051             IF (I .EQ. J) GO TO 39
0052             HB(I,J)=HBIP(I,J)
0053             GO TO 40
```

```
MICHIGAN TERMINAL SYSTEM FORTRAN G(41336 TEST)        KR1           08-29-73          19:04.37        PAGE P002

  0054          39 HB(I,J)=HBIP(I,J)+1.D0                                                  456.000
  0055          40 CONTINUE                                                                457.000
  0056             CALL GMPRD(TKR,HB,KRTB,6,3,3)                                           458.000
  0057             RETURN                                                                  459.000
  0058             END                                                                     460.000
   *OPTIONS IN EFFECT*  ID,EBCDIC,SOURCE,LIST,NODECK,LOAD,NOMAP
   *OPTIONS IN EFFECT*  NAME = KR1      , LINECNT =       57
   *STATISTICS*    SOURCE STATEMENTS =        58,PROGRAM SIZE =      2570
   *STATISTICS*  NO DIAGNOSTICS GENERATED
NO ERRORS IN KR1
```

MICHIGAN TERMINAL SYSTEM FORTRAN G(41336 TEST) HINVB 08-29-73 19:04.44 PAGE P001

```
      SUBROUTINE HINVB(STIF1,P,HR,HIP,HJP,AJF,DC1,STIF,EBI,EBJ,GRBI,
     1  HBIP,HBJP,EBHI,EBHJ,AKRT,BKRT)
      IMPLICIT REAL*8(A-H,P-Z)
      DIMENSION STIF1(6,6),P(6,6),HR(3,3),HIP(3,6),HJP(3,6),AJF(3,3),
     1          DC1(3,3),STIF(12,12),DC1T(3,3),P1(3,3),P2(3,3),HT(3,3),
     2          H7(3,3),H8(3,3),H(12,12),HINV(12,12),HRR(3,6),IM(24),
     3          B6(3,3),B(12,3),BT(12,3)
      DIMENSION EBHI(3,3),EBHJ(3,3),HBIP(3,3),HBJP(3,3),GRBI(3,3),
     1  B10(3,3),B14(3,3),B16(3,3)
      DIMENSION EBI(3,6),EBJ(3,6)
      DIMENSION AKRT(6,6),BKRT(6,3)
      DO 10 I=1,3
      DO 10 J=1,3
      DC1T(I,J)=DC1(J,I)
      P1(I,J)=P(I+3,J)
   10 P2(I,J)=P(I+3,J+3)
      CALL GMPRD (P1,DC1,HT,3,3,3)
      CALL GMPRD (DC1T,HT,H7,3,3,3)
      CALL GMPRD (P2,DC1,HT,3,3,3)
      CALL GMPRD (DC1T,HT,H8,3,3,3)
      DO 20 I=1,6
      DO 20 J=1,6
      IF (I .EQ. J) GO TO 19
      H(I,J)=0.D0
      GO TO 20
   19 H(I,J)=1.D0
   20 CONTINUE
      DO 25 I=7,9
      DO 25 J=1,6
   25 H(I,J)=EBJ(I-6,J)
      DO 30 I=10,12
      DO 30 J=1,6
   30 H(I,J)=HJP(I-9,J)
      DO 40 I=1,3
      DO 40 J=7,12
   40 H(I,J)=0.D0
      H(1,7)=-1.D0
      H(2,8)=-1.D0
      H(3,9)=-1.D0
      CALL GMPRD (HR,HIP,HRR,3,3,6)
      DO 50 I=4,6
      DO 45 J=7,9
   45 H(I,J)=-H7(I-3,J-6)
      DO 50 J=10,12
   50 H(I,J)=-H8(I-3,J-9)
      DO 60 I=1,3
      DO 60 J=1,6
   60 H(I+6,J+6)=STIF1(I,J)+HRR(I,J)+EBI(I,J)+AKRT(I,J)
      DO 70 I=10,12
      DO 70 J=7,12
   70 H(I,J)=STIF1(I-6,J-6)+HIP(I-9,J-6)+AKRT(I-6,J-6)
      CALL INV(12,12,H,IM,12,HINV)
      DO 72 I=1,3
      DO 72 J=1,3
      IF (I .NE. J) GO TO 71
```

```
          P1(I,J)=1.D0+GRBI(I,J)
          B14(I,J)=-(1.D0+HBIP(I,J))-BKRT(I+3,J)
          B16(I,J)=1.D0-HBJP(I,J)
          GO TO 72
       71 P1(I,J)=GRBI(I,J)
          B14(I,J)=-HBIP(I,J) -BKRT(I+3,J)
          B16(I,J)=-HBJP(I,J)
       72 CONTINUE
          CALL GMPRD(AJF,P1,P2,3,3,3)
          CALL GMPRD(P2,DC1,HT,3,3,3)
          CALL GMPRD(DC1T,HT,B6,3,3,3)
          CALL GMPRD(HR,HBIP,P1,3,3,3)
          DO 74 I=1,3
          DO 74 J=1,3
       74 B10(I,J)=-(HR(I,J)+P1(I,J)+EBHI(I,J))-BKRT(I,J)
          DO 100 I=1,12
          DO 94 J=1,3
       94 STIF(I,J)=-HINV(I,J+6)
          DO 96 J=7,9
       96 STIF(I,J)=HINV(I,J)
      100 CONTINUE
          DO 110 J=1,3
          DO 102 I=1,3
      102 B(I,J)=0.D0
          DO 104 I=4,6
      104 B(I,J)=B6(I-3,J)
          DO 106 I=7,9
      106 B(I,J)=B10(I-6,J)
          DO 109 I=10,12
      108 B(I,J)=B14(I-9,J)
      109 CONTINUE
      110 CONTINUE
          CALL GMPRD (HINV,B,BT,12,12,3)
          DO 120 I=1,12
          DO 120 J=1,3
      120 STIF(I,J+3)=BT(I,J)
          DO 130 J=1,3
          DO 122 I=1,6
      122 B(I,J)=0.D0
          DO 123 I=7,9
      123 B(I,J)=-EBHJ(I-6,J)
          DO 124 I=10,12
      124 B(I,J)=B16(I-9,J)
      130 CONTINUE
          CALL GMPRD(HINV,B,BT,12,12,3)
          DO 140 I=1,12
          DO 140 J=1,3
      140 STIF(I,J+9)=BT(I,J)
          RETURN
          END
 *OPTIONS IN EFFECT*  ID,EBCDIC,SOURCE,LIST,NODECK,LOAD,NOMAP
 *OPTIONS IN EFFECT*  NAME = HINVB   , LINECNT =       57
 *STATISTICS*    SOURCE STATEMENTS =       100,PROGRAM SIZE =     8168
 *STATISTICS*  NO DIAGNOSTICS GENERATED
NO ERRORS IN HINVB
```

```
MICHIGAN TERMINAL SYSTEM FORTRAN G(41336 TEST)        DISSP            08-29-73           19:05.01          PAGE P001

 0001               SUBROUTINE DISSP(G,GB,DR,DU,N,AL,DUP,DC)
           C        COMPUTE DISSIPITION
 0002               IMPLICIT REAL*8(A-H,P-Z)
 0003               DIMENSION DR(12),DU(12),G(4,6),GB(4,3),DUP(4),DUPI(4),FDR(6)
 0004               DIMENSION DC(3,3),RF(3),RM(3),DUSG(3),RFL(3),RML(3)
 0005               DIMENSION DUS(3)
 0006               M=12-6*N
 0007               J=(N-1)*6+3
 0008               DO 5 I=1,3
 0009               RF(I)=DR(M+I)
 0010               RM(I)=DR(M+3+I)
 0011             5 DUSG(I)=DU(J+I)
 0012               CALL GMPRD(DC,RF,RFL,3,3,1)
 0013               CALL GMPRD(DC,RM,RML,3,3,1)
 0014               CALL GMPRD(DC,DUSG,DUS,3,3,1)
 0015               DO 10 I=1,3
 0016               FDR(I)=RFL(I)
 0017            10 FDR(I+3)=RML(I)
 0018            30 CALL GMPRD(G,FDR,DUP,4,6,1)
 0019               CALL GMPRD(GB,DUS,DUPI,4,3,1)
 0020               DO 40 I=1,4
 0021            40 DUP (I)=DUP(I)+DUPI(I)
 0022               RETURN
 0023               END
  *OPTIONS IN EFFECT*  ID,EBCDIC,SOURCE,LIST,NODECK,LOAD,NOMAP
  *OPTIONS IN EFFECT*  NAME = DISSP   , LINECNT =       57
  *STATISTICS*    SOURCE STATEMENTS =        23,PROGRAM SIZE =      1180
  *STATISTICS*  NO DIAGNOSTICS GENERATED
NO ERRORS IN DISSP
```

```
MICHIGAN TERMINAL SYSTEM FORTRAN G(41336 TEST)          NEWDC          08-29-73          19:05.03          PAGE P001

 0001                 SUBROUTINE NEWDC(HIP,HJP,DR,DD,DCI,DCJ,D1,D2,HBIP,HBJP)
              C       CCMPUTE THE NEW DIRECTION COSINE
 0002                 IMPLICIT REAL*8(A-H,P-Z)
 0003                 DIMENSION HIP(3,6),HJP(3,6),DR(12),DD(12),DCI(3,3),DCJ(3,3),
                     1DWI(3),    DWIP(3),DWJP(3),D1(3,3),D2(3,3),WI(3,3),WJ(3,3),DWJ(3)
 0004                 DIMENSION HBIP(3,3),HBJP(3,3)
 0005                 DO 10 I=1,3
 0006                 DWIP (I) = 0.DO
 0007                 DWJP (I) = 0.DO
 0008                 DC 10 J=1,6
 0009                 DWIP (I) = DWIP (I) + HIP (I,J) * DR (6+J)
 0010              10 DWJP (I) = DWJP (I) + HJP (I,J) * DR (J)
 0011                 DO 20 I=1,3
 0012                 DC 20 J=1,3
 0013                 DWIP(I)=DWIP(I)+HBIP(I,J)*DD(3+J)
 0014              20 DWJP(I)=DWJP(I)+HBJP(I,J)*DD(9+J)
 0015             100 DO 110 I=1,3
 0016                 DWIP (I) = DD (3+I) + DWIP (I)
 0017             110 DWJP (I) = DD (9+I) - DWJP (I)
 0018                 CALL GMPRD(DCI,DWIP,DWI,3,3,1)
 0019                 CALL GMPRD(DCJ,DWJP,DWJ,3,3,1)
 0020                 DO 120 I=1,3
 0021                 DO 120 J=I,3
 0022                 IF ( J .NE. I ) GO TO 120
 0023                 WI (I,J) = 1.DO
 0024                 WJ(I,J)=1.DO
 0025             120 CONTINUE
 0026                 WI (1,2) = DWI (3)
 0027                 WJ (1,2) = DWJ (3)
 0028                 WI (1,3) = -DWI (2)
 0029                 WJ (1,3) = -DWJ (2)
 0030                 WI (2,3) = DWI (1)
 0031                 WJ (2,3) = DWJ (1)
 0032                 WI (2,1) = -WI (1,2)
 0033                 WJ (2,1) = -WJ (1,2)
 0034                 WI (3,1) = -WI (1,3)
 0035                 WJ (3,1) = -WJ (1,3)
 0036                 WI (3,2) = -WI (2,3)
 0037                 WJ (3,2) = -WJ (2,3)
 0038                 CALL GMPRD(WJ,DCJ,D2,3,3,3)
 0039                 CALL GMPRD(WI,DCI,D1,3,3,3)
 0040                 RETURN
 0041                 END
  *OPTIONS IN EFFECT*  ID,EBCDIC,SOURCE,LIST,NODECK,LOAD,NOMAP
  *OPTIONS IN EFFECT*  NAME = NEWDC    , LINECNT =      57
  *STATISTICS*    SOURCE STATEMENTS =       41,PROGRAM SIZE =      1612
  *STATISTICS*  NO DIAGNOSTICS GENERATED
NO ERRORS IN NEWDC
```

```
MICHIGAN TERMINAL SYSTEM FORTRAN G(41336 TEST)        SCFS1          08-29-73          19:05.08          PAGE P001

  0001               SUBROUTINE SCFS1(FRKP1,FR,D,N,J,LB)
               C     COMPUTE THE SCALING FACTOR FOR RECTANGULAR TUBE CROSS-SECTION
  0002               IMPLICIT REAL *8(A-H,P-Z)
  0003               REAL *8 M10,M20,M30
  0004               DIMENSION FRKP1(12),FRK(12),A(4), DA(4),ADA(4),B(4),C(4),R(4),
                    1 M10(20),M20(20),M30(20),P0(20),Y1(20),Y2(20),CF(20),FR(20,12)
  0005               DIMENSION AA(4)
  0006               COMMON/COMB/M10,M20,M30,PO,Y1,Y2,CF
  0007               M=(N-1)*6+2
  0008               R(1)=PO(LB)
  0009               R(2)=M10(LB)
  0010               R(3)=M20(LB)
  0011               R(4)=M30(LB)
  0012               DO 5 I=1,12
  0013             5 FRK(I)=FR(LB,I)
  0014               DO 10 I=1,4
  0015               A(I)=FRK(M+I)/R(I)
  0016               AA(I)=DABS(A(I))
  0017               DA(I)=FRKP1(M+I)/R(I)-A(I)
  0018            10 ADA(I)=DABS(DA(I))
  0019            14 FL=(AA(1)+AA(2)+AA(3))**2+AA(4)*AA(4)
  0020               IF (FL .GE. 1.D0) RETURN
  0021               D=0.D0
  0022               J=0
  0023               X=10.D0
  0024            15 D=D+1.D0/X
  0025               J=J+1
  0026               IF (D .GT. 1.D0) RETURN
  0027               IF (J  .GT. 100) RETURN
  0028               DO 20 I=1,4
  0029            20 B(I)=DABS(A(I)+D*DA(I))
  0030               F=      (B(1)+B(2)+B(3))**2+B(4)*B(4)
  0031               IF (F -1.D0) 30,35,40
  0032            30 IF (DABS(F-1.) .LE. 0.0004D0) GO TO 35
  0033               FL=F
  0034               GO TO 15
  0035            35 CONTINUE
  0036               RETURN
  0037            40 IF (DABS(F-1.) .LE. 0.0004D0) GO TO 35
  0038               D=D-1.D0/X
  0039               X=X*10.D0
  0040               GO TO 15
  0041            70 RETURN
  0042               END
   *OPTIONS IN EFFECT*  ID,EBCDIC,SOURCE,LIST,NODECK,LOAD,NOMAP
   *OPTIONS IN EFFECT*  NAME = SCFS1   , LINECNT =       57
   *STATISTICS*    SOURCE STATEMENTS =       42,PROGRAM SIZE =      1480
   *STATISTICS*  NO DIAGNOSTICS GENERATED
NO ERRORS IN SCFS1
```

```
0001           SUBROUTINE OUTP(K,IELM,RK,DISK,RNKP1,SW,SCF,SCF1,SCFA,IPS,NUMP,NUB
              1 ,FK1,FRKP)
         C      PRINT OUT THE RESULTS  .
0002           IMPLICIT REAL *8(A-H,P-Z)
0003           INTEGER SW
0004           DIMENSION IELM(14,1),RK(1),DISK(1),RNKP1(20,1),SW(20,1),SCF(20,1),
              2  SCF1(20,1),R(6),U(6),D(6),DISP(20,2)
0005           DIMENSION FK1(20,1),FRKP(20,1)
0006           COMMON/COMC/AMR,FR,ALR
0007           WRITE(6,1) K,SCFA
0008           WRITE(6,2)(J,J=1,6)
0009           M1=NUMP-1
0010           DO 11 I=1,NUMP
0011           WRITE(6,3) I
0012           IS=(I-1)*6
0013           IE=IS+3
0014           DO 10 M=1,3
0015           R(M)=RK(IS+M)*FR
0016           R(M+3)=RK(IE+M)*AMR
0017           U(M)=DISK(IS+M)*ALR
0018        10 U(M+3)=DISK(IE+M)
0019           WRITE(6,4) (R(M),M=1,6)
0020        11 WRITE(6,5)(U(M),M=1,6)
0021           WRITE (6,7)
0022           LB=0
0023           DO 100 I=1,M1
0024           L=I+1
0025           DO 100 J=L,NUMP
0026           IF (IELM(I,J) .EQ. 0) GO TO 100
0027           LB=LB+1
0028           DO 15 N=1,2
0029        15 DISP(LB,N)=SCF1(LB,N)*AMR
0030           DO 20 M=1,3
0031           M3=M+3
0032           M6=M+6
0033           M9=M+9
0034           R(M)=RNKP1(LB,M)*FR
0035           R(M3)=RNKP1(LB,M3)*AMR
0036           D(M)=RNKP1(LB,M6)*FR
0037        20 D(M3)=RNKP1(LB,M9)*AMR
0038           WRITE(6,6) LB,I,(R(M),M=1,6),SW(LB,1),SCF(LB,1),DISP(LB,1)
0039           WRITE(6,6) LB,J,(D(M),M=1,6),SW(LB,2),SCF(LB,2),DISP(LB,2)
0040       100 CONTINUE
0041           IF (IPS .EQ. 0) GO TO 1000
0042           IF (IPS .EQ.2) GO TO 500
0043           WRITE (6,101) K
0044           DO 200 I=1,NUB
0045       200 WRITE (6,102) I,FK1(I,1),FK1(I,2)
0046           GO TO 1000
0047       500 WRITE (6,103) K
0048           DO 300 I=1,NUB
0049           WRITE (6,102) I,FK1(I,1),FK1(I,2)
0050           DO 290 M=1,3
0051           M3=M+3
0052           M6=M+6
```

```
MICHIGAN TERMINAL SYSTEM FORTRAN G(41336 TEST)        OUTP         08-29-73        19:05.12        PAGE P002
          M9=M+9
          R(M)=FRKP(I,M)*FR
          R(M3)=FRKP(I,M3)*AMR
          D(M)=FRKP(I,M6)*FR
      290 D(M3)=FRKP(I,M9)*AMR
      300 WRITE (6,104) I,(R(J),J=1,6),(D(J),J=1,6)
        1 FORMAT (1H1,'K=',I3,' SCFA=',F8.5 )
        2 FORMAT (3X,6(14X,I1),10X,'SW',4X,'SCFP',5X,'DISSP')
        3 FORMAT (2X,'MASS',I3)
        4 FORMAT (3X,'FORCE',2X,6D15.5)
        5 FORMAT (3X,'COORD',2X,6D15.5/)
        6 FORMAT (3X,'BM',I2,'@',I2,6D15.5,3X,I2,1F10.5,D15.5)
        7 FORMAT (//13X,'FORCE & MOMENT ON EACH BEAM ENDS'//)
      101 FORMAT (1H1,'K=',I3,2X,'YIELD FUNCTION AT EACH BEAM END'/)
      102 FORMAT ('YF @ MB',I3,2D15.5)
      103 FORMAT (1H1,'K=',I3,2X,'YIELD FUNCTION & LOCAL FORCES AT EACH BEAM
         1 END'/)
      104 FORMAT ('LF@BM',I3,1X,6D10.3,1X,6D10.3)
     1000 RETURN
          END
  *OPTIONS IN EFFECT*  ID,EBCDIC,SOURCE,LIST,NODECK,LOAD,NOMAP
  *OPTIONS IN EFFECT*  NAME = OUTP    , LINECNT =       57
  *STATISTICS*    SOURCE STATEMENTS =       71,PROGRAM SIZE =     3396
  *STATISTICS*  NO DIAGNOSTICS GENERATED
NO ERRORS IN OUTP
```

```
MICHIGAN TERMINAL SYSTEM FORTRAN G(41336 TEST)        INCRE        08-29-73        19:05.18        PAGE P001

              SUBROUTINE INCRE(M,DU,DR,K)
              REAL*8 DU,DR
              DIMENSION DU(1),DR(1)
              M6=M*6
              DO 10 I=1,M6
              DR(I)=0.D0
           10 DU(I)=100.D0
              DO 16 I=1,6
           16 DU(I)=0.D0
              DU(2)=0.002D0
              DU(5)=0.01D0
              DO 15 I=19,M6
           15 DU(I)=0.D0
              RETURN
              END
  *OPTIONS IN EFFECT*  ID,EBCDIC,SOURCE,LIST,NODECK,LOAD,NOMAP
  *OPTIONS IN EFFECT*  NAME = INCRE    , LINECNT =       57
  *STATISTICS*    SOURCE STATEMENTS =       15,PROGRAM SIZE =       586
  *STATISTICS*  NO DIAGNOSTICS GENERATED
NO ERRORS IN INCRE

NO STATEMENTS FLAGGED IN THE ABOVE COMPILATIONS.
```